Volume 14, Number 1, 2020

Technical University of Cluj-Napoca
North University Centre of Baia Mare
Faculty of Engineering
Electrical, Electronic and Computer Engineering Department

Volume 14, Number 1, 2020

Carpathian Journal of Electrical Engineering

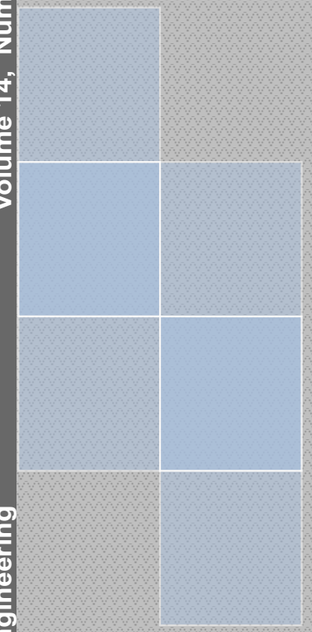

# Carpathian Journal of Electrical Engineering

ISSN 1843 - 7583

UTPRESS PUBLISHER

TECHNICAL UNIVERSITY
OF CLUJ-NAPOCA

NORTH UNIVERSITY CENTRE OF BAIA MARE
FACULTY of ENGINEERING

ELECTRICAL, ELECTRONIC AND
COMPUTER ENGINEERING DEPARTMENT

# Carpathian Journal of Electrical Engineering

Volume 14, Number 1, 2020

**ISSN 1843 – 7583**
http://cee.ubm.ro/cjee.html

## CONTENTS

# PREDICTIVE CAPABILITIES OF A NARX-BASED FORECASTER USED TO PREDICT THE PV PANEL OUTPUT POWER

Toufik **SEBBAGH**[1], Ridha **KELAIAIA**[1], Abderrezak **METATLA**[1] and Abdelouahab **ZAATRI**[2],

[1] *LGMM Loratory, University of 20 Août 1955 – Skikda, Algeria,* [2] *University of Constantine 1 – Constantine, Algeria*

*t.sebbagh@univ-skikda.dz*

**Keywords: PV power output, forecasting, NARX, prediction**

**Abstract***: This paper deals with the predictive capabilities of a NARX-based forecaster used to predict the output power converted with a PV panel in isolated conditions. A timeseries based NARX model is proposed and the influence of the meteorological data such as irradiance, ambient temperature and wind speed, and the impact of the training algorithm on the performance of the NARX based forecaster model is studied. The results show that for the studied area, the NARX model trained by three meteorological data as inputs, the output power as output using Bayesian Regularization algorithm gives best performance with a mean squared error of 2.10414e-2.*

## *NOMENCLATURE:*

PV: Photovoltaic
ANN: Artificial Neural Network
NARX: Nonlinear autoregressive exogenous
$x_{normalized}$: The normalized value,
$x$: The actual value
$x_{min}$: The minimum value of each timeseries dataset
$x_{max}$: The maximum value from each dataset
$T_C$: the cell temperature (°C)
$T_a$: the ambient temperature (°C)
$NOCT$: the nominal operating cell temperature (°C)

$G_{g,t}$: the global irradiance on tilted surface (W/m²)
$P_{PV}$: is the output power from the PV panel (W)
$\eta_{PV,STC}$: the efficiency of the panel at STC conditions (%)
$\mu$: the temperature coefficient (%/°C)
$v$ : the wind speed (m/s)
$A_{PV}$: the area of the PV panel (m²)
$P_{max}$: The maximum power converted by the panel (W),
$V_{OC}$: The open circuit voltage (V)
$I_{SC}$: The short circuit current (A)
MSE: Mean Squared Error (W)
$P_{forcasted_i}$: the power forecasted by the NARX model (W)
$P_i$: the target power (W)
$f$ : a nonlinear function
$P(t)$ and $(t)$ : Input and output of the network at time $t$, respectively;
$n_P$ and $n_y$ : the order of the imput and output, respectively.

## 1. INTRODUCTION

Energy is a key factor for the development of humanity. Electrical energy is the most useful form of energy, it was generated mainly from fossil fuels, and is currently mainly related to them. However, this issue has a harmful environmental effect.

Renewable energy is an alternative solution to this issue mainly in isolated areas where it is hard or impossible to connect to the grid. Among the large variety of renewable energy sources, solar energy is the most promising and the more acceptable source. Therefore, solar energy is gaining the attention of scientist, industrials and governments. However, the installation of any new project requires to know its reliability and its economic feasibility.

Since the generation of PV power is fully dependent on uncertain and uncontrollable meteorological factors, the output power of PV system changes dynamically. Therefore, a pinpoint prediction of PV power conversion is greatly difficult. The accurate forecasting of PV power production is a great challenge, that can improve the reliability of installed systems and maintain the power quality [1].

Several papers have been conducted to propose methods and techniques to forecast the energy produced PV panels. These techniques can be classified as direct and indirect forecasting techniques [1].

Nowadays the most popular techniques in direct forecasting the output power of PV installations, are the soft computing techniques based on Artificial Neural Networks (ANN) [2].

Mellit and Kalogirou outlined in [3] a comprehensive review of the use of ANNs to forecast solar energy.

Ding et all. proposed an approach based on ANN to forecast the output power of a PV system [4]. In this approach the improved back propagation learning Algorithm was adopted to overcome the shortcomings of the standard back propagation learning algorithm.

Lo Brano et all. [5] presented an approach based on different topologies of ANN to forecast the output power of PV modules. The proposed approach investigated the influence of some meteorological data without taking into account the influence of the training algorithm.

In [6], Shi et all. proposed algorithms to predict the output power of a PV system based on weather classification and support vector machine. This research investigated the influence of the weather conditions but not the training algorithm and applied to a grid connected system.

Xiao et all. [7] introduced an ANN forecaster of the output power of three technologies of PV cells. The authors of this research studied the influence of the number of hidden neurons on the prediction of the power.

The current work investigates the use of ANN for a medium-term direct forecasting of PV output power based on timeseries historical data. The main contribution in this study is to present the influence of the type of inputs and the training algorithm on the performance of the nonlinear autoregressive exogenous (NARX) model.

## 2. METHODOLOGY

A Multivariate times series model, based on a NARX model is proposed, to forecast the power generated by the PV panel, using three sets of meteorological data.

The different phases carried out for the current procedure are presented in *fig. 1*.

After collecting the time series dataset, a pre-processing is applied to these data. The dataset is decomposed into three sets, the first one used for the training and represent 70% of the total data, the other sets composed of 15% each are used for the test and the validation of the proposed NN.

To study the influence of the inputs on the performance of the model, different sets of data are used to train the NN.

To study the influence of the learning method on the performance of the network, three different algorithms are used for each set of the input data.

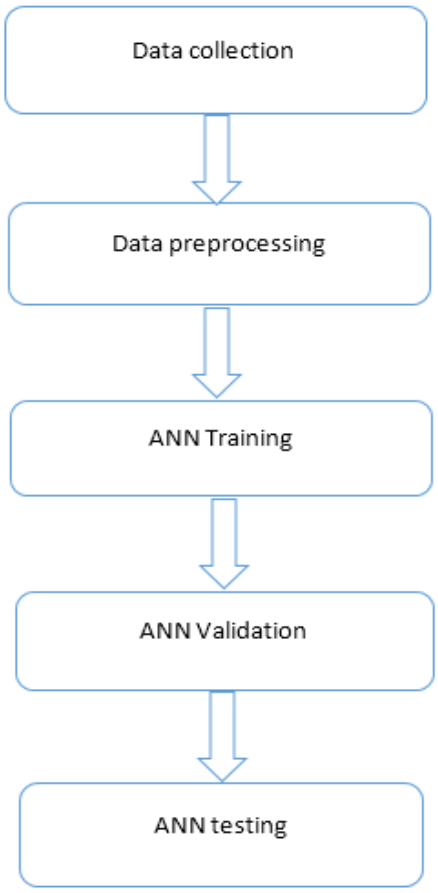


*Fig. 1. Different phases of the proposed model.*

### 2.1. Data collection

It is aimed to use the measured values of the global irradiance, the ambient temperature and the wind speed to the NN as the input data, and the values of the power converted by the PV panel as the target data, during the three phases cited above.

This data concerns one of the panels installed at the laboratory of renewable energy at the university of Skikda (Latitude= 36.848739, Longitude=6.889475).

### 2.2. Data pre-processing

The selected data are pre-processed as the following:

- ✓ Firstly, all the input data that leads to a target equal to zero, are deleted from the dataset.
- ✓ The other data are normalized between 0 and 1 using the following formula:

$$x_{normalized} = \frac{x - x_{min}}{x_{max} - x_{min}} \quad (1)$$

where: $x_{normalized}$is the normalized value, $x$ is the actual value, $x_{min}$ is the minimum value of each timeseries dataset, and $x_{max}$is the maximum value from each dataset.

*2.2.1. Irradiance level*

The irradiance is defined as the density of the solar radiation power received on a given surface [8]. For the present work, a 32° inclined and south oriented pyranometer is used for in-situ measurements.

The normalized data of the hourly irradiance values, for the period of the data acquisition, are presented in *fig. 2*.

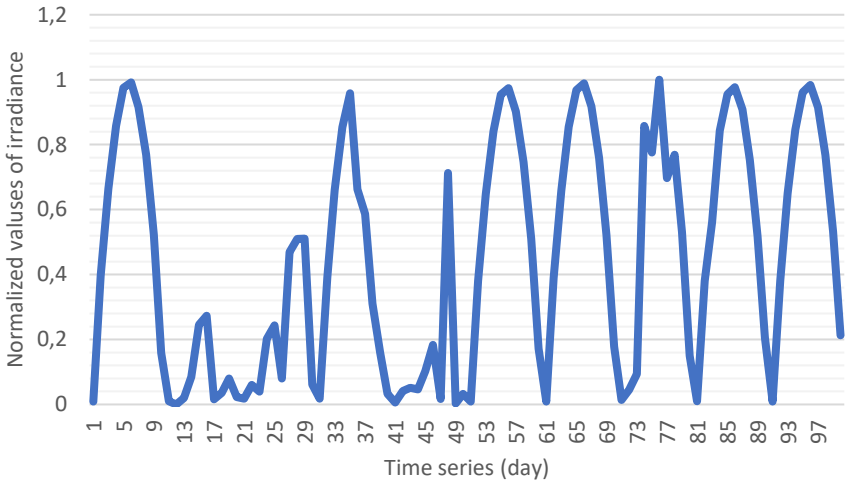


*Fig. 2. Normalized irradiance values, for the period of 2 months.*

*2.2.2. Ambient temperature*

The surface temperature of the panel has a negative impact on the PV panel performance. The power converted by the panel is reduced since the surface temperature increases. The ambient temperature has a direct impact to the panel, it is related to the PV panel surface temperature with the following equation [9]:

$$T_C = T_a + \frac{NOCT-20}{800} G_{g,t} \quad (2)$$

where: $T_C$ is the cell temperature (°C); $T_a$ is the ambient temperature (°C); $NOCT$ is the nominal operating cell temperature (°C) and $G_{g,t}$ is the global irradiance on tilted surface (W/m²).

The normalized data of the hourly ambient temperature values, for the period of the data acquisition, are presented in *fig. 3*.

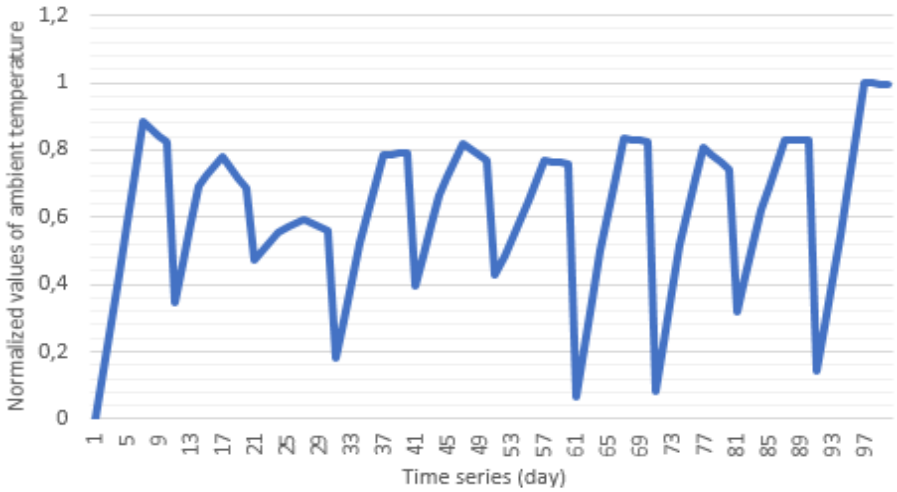


*Fig. 3. Normalized ambient temperature values, for the period of 2 months*

*2.2.3. Wind speed*

The impact of wind speed on the output power of the PV system was given by the following equation modified from [10]:

$$P_{PV} = \eta_{PV,STC}\left[\frac{\mu}{\eta_{PV,STC}}\frac{1+\frac{\mu}{\eta_{PV,STC}}(T_a - T_{STC}) + \frac{9.5}{5.7+3.8v}\frac{(NOCT-20)}{800}\left(1-\eta_{PV,STC}\right)G_{g,t}}{}\right]A_{PV}G_{g,t} \quad (3)$$

where: $P_{PV}$ is the output power from the PV panel (W); $\eta_{PV,STC}$is the efficiency of the panel at STC conditions (%); $\mu$ is the temperature coefficient (%/°C); $v$ is the wind speed (m/s); $A_{PV}$is the area of the PV panel (m²)

The values of wind speed used in the current study were measured for the specified area at the height of 10 m

The normalized data of the hourly wind speed values, for the period of the data acquisition, are presented in *fig. 4*.

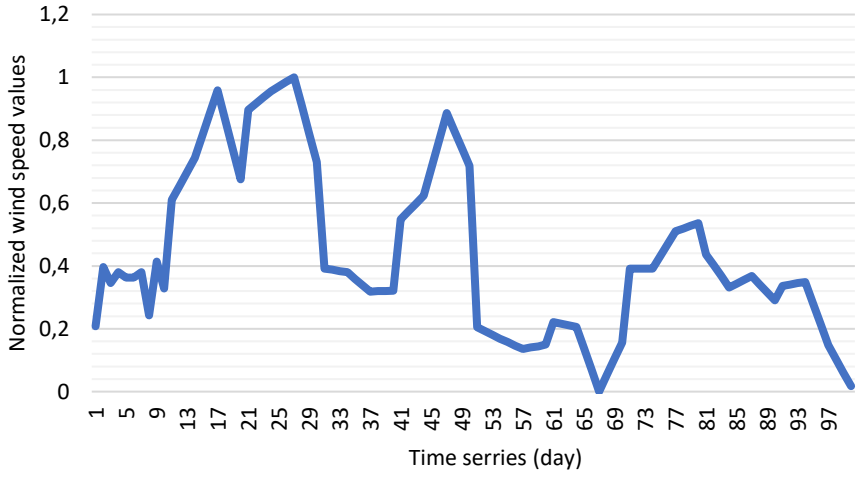


*Fig. 4. Normalized wind speed values, for the period of 2 months.*

*2.2.4. PV panel output power*

The energy converted by the PV panel is measured for a south oriented, 32° tilted monocrystalline panel ($P_{max}$= 235 W, $V_{OC}$= 30.2 V, $I_{SC}$=7.8 A).

The normalized data of the hourly output power values, for the period of the data acquisition, are presented in *fig. 5*.

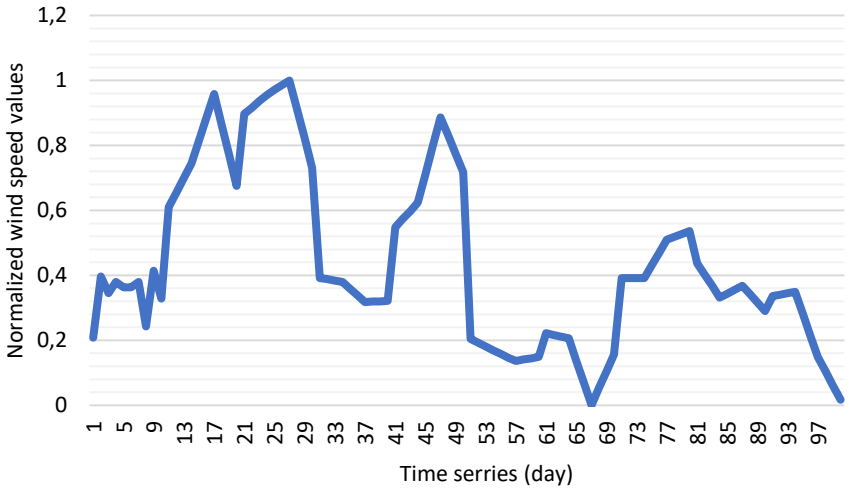


*Fig.5. Normalized PV panel power output values, for the period of 2 months*

## 2.3. ANN Architecture

For the proposed approach, we use the nonlinear autoregressive network with exogenous inputs (NARX) model to predict the output power converted by the PV panel. NARX is a recurrent dynamic NN with feedback connecting to several layers of the NN [11].

The simplest structure of the NARX model is presented in *fig. 6.*

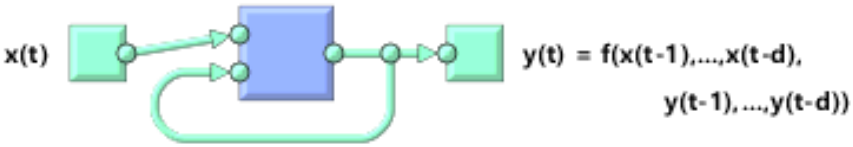


*Fig. 6. General structure of NARX Network*

The NARX model is mathematically formalized as [12]:

$$y(t) = f(P(t-n_P), \dots, P(t-1), P(t), y(t-n_y), \dots, y(t-1)) \quad (4)$$

where: $f$ is a nonlinear function; $P(t)$ and $y(t)$ are, respectively, the input and output of the network at time $t$; $n_P$ and $n_y$ are the order of the imput and output, respectively.

The NARX model used is composed of input layer, one hidden layer and the output layer. The number of neurons in the hidden layer is optimized to be 10 neurons, and the number of delays is set to be 2. *Fig. 7* illustrates the NARX model proposed.

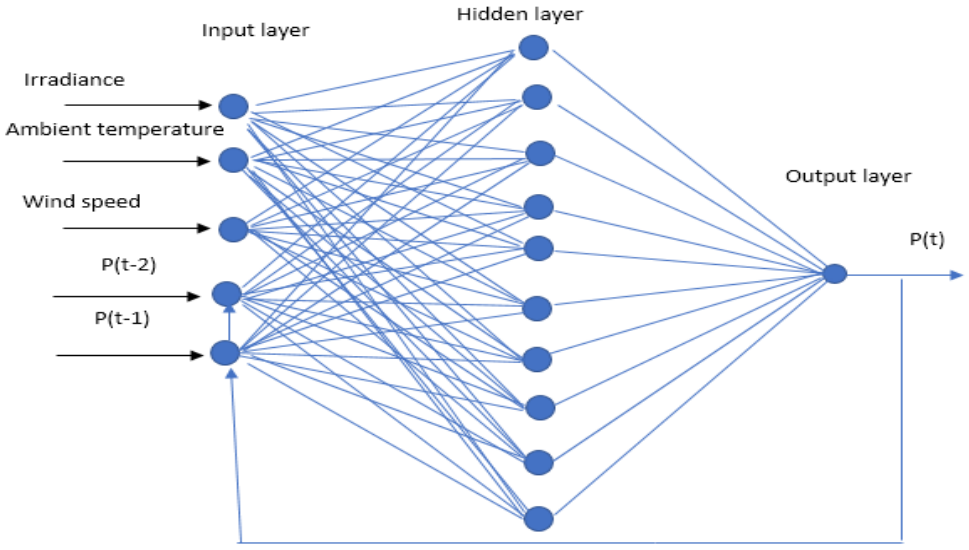


*Fig. 7. Proposed NARX model structure*

*2.3.1. Inputs and outputs*

For the present study four different sets of data are used as inputs data, where the objective is to illustrate the impact of the data on the performance of the neural network model chosen. These sets are defined as:

1. Irradiance.
2. Irradiance + ambient temperature.
3. Irradiance + wind speed.
4. Irradiance + ambient temperature + wind speed.
5. The target data is the hourly values of the PV panel output power.

*2.3.2. ANN Training:*

To study the influence of the training technique on the performance of the NARX model, three training algorithms are applied to each of the four cases. These are the Levenberg-Marquardt (LM), the Bayesian Regularization (BR) and the Scaled Conjugate Gradient (SCG).

*2.3.3. Evaluation Criteria:*

After the training and validation of the forecasting model, the accuracy of the prediction is measured by calculating the difference between the forecasted values and the target.

In this paper, the Mean Squared Error (MSE) is used to quantitatively evaluate the performance of the proposed forecasting model.

The MSE is defined as the average squared difference between the outputs of the forecasting model and the targets. It can be calculated using (5):

$$MSE = \frac{1}{N}\sum_{i=1}^{N}(P_{forcasted_i} - P_i)^2 \quad (5)$$

where: $P_{forcasted_i}$, is the power forecasted by the NARX model (W); $P_i$ is the target power (W).

## III. RESULTS AND DISCUSSIONS

The prediction model is defined and trained, to obtain the best forecasting results. The time series meteorological data consist of irradiance on inclined surface (X1), ambient temperature (X2) and wind speed (X3), taken with an hourly interval, regrouped in four datasets and used in four NARX models as follows: (Model 1 (M1): X1); (Model2 (M2): X1 + X2); (Model 3 (M3): X1 + X3); (Model 4(M4): X1 + X2 + X3). Each of the four models constructed using the previews datasets is trained by three training algorithms.

*Fig. 8* presents a comparative illustration of the values of MSE calculated by the four NARX models during the testing phase.

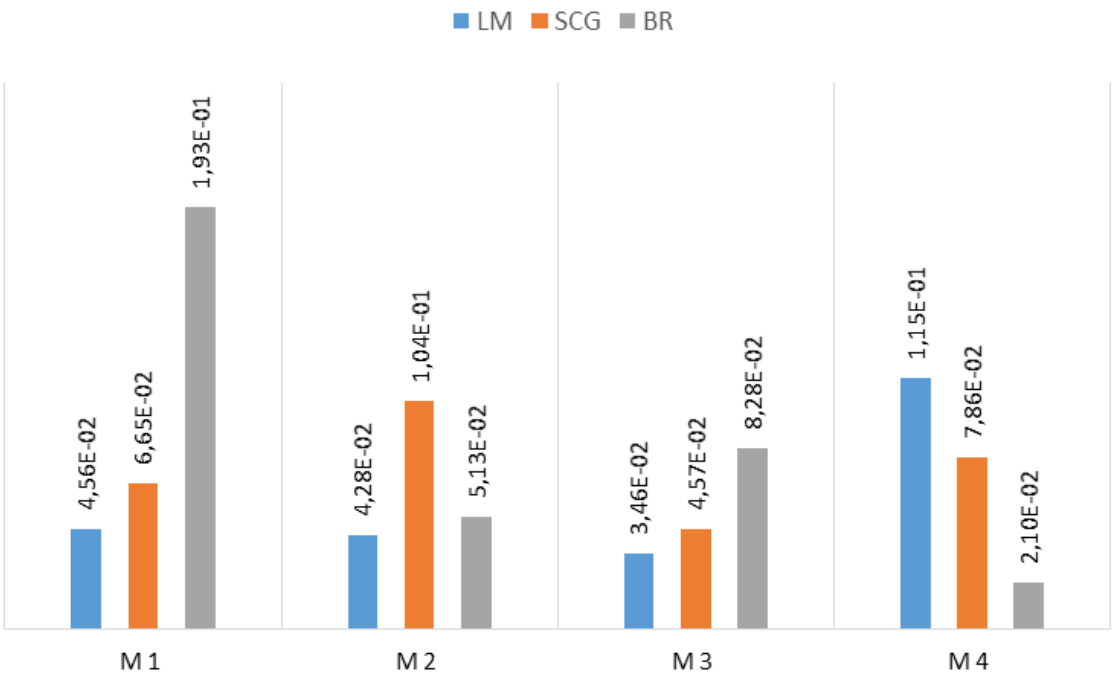


*Fig. 8. Comparison between MSE for the different NARX models*

From these histograms, it can be seen that the NARX model M3 gives best performance when trained using LM algorithm, and the MSE calculated with this model has the lowest value compared with other models. The model M3 presents also the best performance compared with the other models, when trained using SCG. However, the model M4 gives the best performance, when trained using BR. The MSE calculated with M4 in this case, equal to 2.10414e-2 W. It has the lowest value compared with the MSE calculated with the other models trained with the three training algorithms.

From f*ig. 8*, it can be summarized that the best forecasting of the output power converted by a PV panel, is obtained with the model M4 trained by the BR Algorithm.

## IV. CONCLUSION AND PERSPECTIVES

The solar PV energy is an alternative to the traditional sources of energy, especially in remote areas. Having informative idea about the behavior of PV systems, before the installation of such system is important. An accurate prediction of the output power of a PV panel is a complicated task due to its dependence on uncertain variables. In this paper four NARX models were developed to predict the output power of a PV panel, and the performance of the models is compared in terms of the MSE values. The model used the irradiance, the ambient temperature and the wind speed, and trained using the Bayesian Regulation algorithm outperforms other models.

The future development of this work will take into consideration the following points:

- The use of more meteorological data as humidity.
- The classification of the timeseries data into several classes as clear time data, cloudy time data …
- The use of other model and techniques as the convolutional neural network.

## *REFERENCES*

[1] U. K. Das, K. S. Tey, M. Seyedmahmoudian, S. Mekhilef, M. Y. I. Idris, W. Van Deventer, B. Horan, and A. Stojcevski, *Forecasting of photovoltaic power generation and model optimization: A review*, Renewable and Sustainable Energy Reviews, vol. 81, pp. 912-928, 2018.

[2] S. Leva, A. Dolara, F. Grimaccia, M. Mussetta, and E. Ogliari, *Analysis and validation of 24 hours ahead neural network forecasting of photovoltaic output power*, Mathematics and computers in simulation, vol. 131, pp. 88-100, 2017.

[3] A. Mellit and S. A. Kalogirou, *Artificial intelligence techniques for photovoltaic applications: A review*, Progress in energy and combustion science, vol. 34, pp. 574-632, 2008.

[4] M. Ding, L. Wang, and R. Bi, *An ANN-based approach for forecasting the power output of*

*photovoltaic system*, Procedia Environmental Sciences, vol. 11, pp. 1308-1315, 2011.

[5] V. Lo Brano, G. Ciulla, and M. Di Falco, *Artificial neural networks to predict the power output of a PV panel*, International Journal of Photoenergy, vol. 2014, 2014.

[6] J. Shi, W.-J. Lee, Y. Liu, Y. Yang, and P. Wang, *Forecasting power output of photovoltaic systems based on weather classification and support vector machines*, IEEE Transactions on Industry Applications, vol. 48, pp. 1064-1069, 2012.

[7] W. Xiao, G. Nazario, H. Wu, H. Zhang, and F. Cheng, *A neural network based computational model to predict the output power of different types of photovoltaic cells*, PLoS ONE, vol. 12, p. e0184561, 2017.

[8] K. Jazayeri, M. Jazayeri, and S. Uysal, *Comparative analysis of Levenberg-Marquardt and Bayesian regularization backpropagation algorithms in photovoltaic power estimation using artificial neural network*, in Industrial Conference on Data Mining, 2016, pp. 80-95.

[9] A. Luque and S. Hegedus, *Handbook of photovoltaic science and engineering*: John Wiley & Sons, 2011.

[10] J. A. Duffie and W. A. Beckman, *Solar engineering of thermal processes*: John Wiley & Sons, 2013.

[11] T. Lin, B. G. Horne, P. Tino, and C. L. Giles, *Learning long-term dependencies in NARX recurrent neural networks*, IEEE Transactions on Neural Networks, vol. 7, pp. 1329-1338, 1996.

[12] Siegelmann, H.T.; Horne, B.G.; Giles, C.L., *Computational capabilities of recurrent NARX neural networks*, Systems, Man, and Cybernetics, Part B: Cybernetics, IEEE Transactions, vol.27, no.2, pp.208-215, 1997.

# CREATING DCP WORKFLOW FOR DIGITAL CINEMA SYSTEM

Andreja **SAMČOVIĆ**
*University of Belgrade, Faculty of Transport and Traffic Engineering, Belgrade, Serbia*
*andrej@sf.bg.ac.rs*

**Keywords: Digital cinema, compression, Digital Cinema Package, Digital Cinema Distribution Master, JPEG 2000**

**Abstract***: This paper describes in details analysis of Digital Cinema Package (DCP) file format structure, which is today widely used for distribution of digital movies for digital cinema. The whole process from creating source files, following by intermediate steps, to the final form of this format, is presented as well. Security principles are covered by Key Delivery Message (KDM). Some free software for creation DCP are mentioned at the end of this paper.*

## 1. INTRODUCTION

The cinema is the last entertainment industry to be embraced by the digital revolution. Until recently, movies were filmed and reproduced only on celluloid film for more than 100 years [1]. More or less, movies have been filmed in the same way after the launching of cinematography in the late 19$^{th}$ century. Even today, in some movie theaters, old machines rotate wheels of 35mm films, which is actually a century old media.

Over the last few decades, digital technology has transformed the music and home video industries, and has already a huge effect in the motion picture industry. It can be said that a new era has emerged for cinema. The transition to digital cinema has already changed cinema industry and will, undoubtedly continue to change, since its impact has just started being sensed.

Digital cinema refers to digital technology used in the production, post-production, distribution and projection of motion pictures on screen. However, this description does not include all aspects of digital cinema. Cinema can be defined as the art of presenting pictures on a “big screen” with a visual and audio quality not usually found in other media, e.g. television.

It should be pointed out that cinema includes visual and audio quality. By designated cinema as “digital”, it is implied that its quality is at least that of a 35mm celluloid film.

Until last few years, digital films could not achieve the level of quality similar to that of 35mm film. However, recent developments in areas such as digital projection, high-resolution film scanners, and advanced image compression techniques have enabled high quality digital cinema projection.

In digital cinema, motion pictures and sound are recorded digitally. Computers are used to process movies or even construct entire scenes from scratch to enhance color and to create visual effects, subtitles and titles.

The final movie version is compressed, encrypted and distributed on Digital Versatile Discs (DVD), smart phones, USB memories, via internet, or satellite communications to movie theaters. For movie projection, instead of using a conventional movie film projector, digital projectors with high luminosity, transfer rate, resolution and color quality can be used.

Digital cinema has many advantages in processing, transmitting and projecting cinematographic materials comparing to the old system. Digital information is much more suitable for processing than analog information. A computer can handle digital images easily, but cannot process an analog audio-visual stream in a simple way. Presentation quality is one of the main characteristics of digital cinema. It offers high quality image resolution and sharpness, excellent audio quality and visual effects that render viewer’s experience unique and exciting [2]. Digital data allow faster, easier and more economic digital movie distribution methods, such as internet, cable or satellite distribution. Digital technology makes motion picture distribution more robust against piracy, by allowing digital file encryption and subsequent decryption in the movie theater only by legitimate users, who have the appropriate decoding keys.

These technological advances were recognized by the movie industry. It was also recognized that these technological advances into commercially digital cinema use, industry-wide standards would need to be created. To establish such standards, Digital Cinema Initiatives (DCI) consortium was created in March 2002 [3]. DCI is a joint venture of seven the most important major Hollywood studios (Disney, Fox, MGM, Paramount, Universal, Sony Pictures Entertainment, and Warner Bros. Studios). The goal of DCI was to establish a standard with an open architecture for digital cinema. Such a standard would ensure the players in the movie industry that their final products and services will be compatible and interoperable with other industry members. The final version of the DCI specification was published online in July 2005 [3].

This paper is organized as follows. After description of the digital cinema system, including video, audio and subtitles, JPEG 2000 as a standards for image compression for digital cinema, is considered. The next section describes digital cinema package as a file format for the digital film. Some free software for digital cinema illustrate the process of DCP creation.

## 2. DIGITAL CINEMA SYSTEM

DCI has defined very detailed and comprehensive digital cinema standards as early as of 2005 and has updated those standards since then. DCI specifications are internationally used as digital cinema standards. Basic DCI standards cover image compression, audio, text, transmission and encryption.

The block-diagram of a digital cinema flow is illustrated in *figure 1*. As shown in the figure, a digital cinema system can be divided into four stages: Mastering, Transport, Storage and Playback, and Projection. At the mastering phase, the movie is compressed, encrypted and packaged for delivery to the movie theatres. The data is then transported to the projection site, where it is decrypted, uncompressed, and played back. The DCI standards discuss each of these stages.

Concerning transmission, the final composition is compressed, encrypted and packaged to form the Digital Cinema Package (DCP), using Material Exchange Format (MXF) and the Extensible Markup Language (XML). MXF is a container format, which supports separate information streams, encoded by a variety of codes [4]. Encryption is carried out by Advanced Encryption Standard (AES) 128 bits standard, which receives an 128 bit text for encoding and makes 128 bits encrypted text. AES 128 encoding uses a secret key. Keys are distributed by Key Delivery Message (KDM). The decoding algorithm is similar to encoding.

Creation of DCP format is carried out by using specific form of source files, which depends very much on the format of the stored data and the quality of the recording techniques. In fact, a normal user is not able to use of all the advantages of the DCP file format with available technical equipment. Today, images are used with four times higher resolution than the most widespread HD 1080p resolution, and double sampling rate and audio bit depth, which can be achieved with professional microphones.

In practice, the entire process of creating a complex package of files is controlled by experts for mastering or distribution companies. Resulting form of DCP depends on whether the files come from commercial or amateur production. Differences can be found in the input data, professional or amateur hardware and software in output files. This format is primarily used for movie projection in the cinema for commercial use, as well as for advertisements, trailers and spots that are designed for screening in digital cinemas [3].

## 3. DIGITAL CINEMA DISTRIBUTION MASTER

The DCP creation process consists of the following three basic steps:

- Digital Source Master (DSM);

- Digital Cinema Distribution Master (DCDM);
- Digital Cinema Package (DCP).

### 3.1 Digital Source Master (DSM)

A prerequisite for creating a digital cinema format is the existence of a data set, created in post-production. Post-production is the phase after filming, when the film is being edited to the final form. The format of these data and record parameters is not fixed. It depends on the provider, but also on the distributor and whether will be able to process this data format. The data format has an influence on the quality of the provided number of recording tracks, and the recording medium on which the data is stored. Input data can be in digital and analog form and it is edited to final forms of film. Today, the digital form of recording and storing data is used without exception [3].

DSM consists of:

- Video recording - video in analog or digital form;
- Audio tracks - audio in analogue or digital form;
- Subtitles - text usually in electronic form.

### 3.2 Digital Source Master (DSM)

The DCDM format was launched by DCI and its data formats are fixed and regulated by standards. Standardized format structure of DCDM was created by mastering companies from any of the DSM sources. It is important to ensure sufficient control of the output quality of the DCDM data. Also, the quality control of individual structures for both standalone playback and synchronization with other structures should be kept. Furthermore, it is also of importance to check the stored data for the presence of errors caused by transfer. For this purpose, DCDM files must be played on the device (projector, speaker set) for which they are designed. However, this is not possible on digital cinema systems. This is because the data is still uncompressed at this point and all data tracks have a very high bit rate. Therefore, there are high demands on the capabilities of the playback device, in particular the computing capability of a processor.

DCI computer assemblies were created for this verification and testing and they are capable for playing back these data structures. DCDM is not intended for distribution for two main reasons. First, it contains uncompressed data with too high bit rate and above all, data is not at all protected by encryption against tampering. To reduce the amount of data and playback device requirements they must be compressed. The compression rate is chosen so that the quality of signal is not significantly reduced. Ordinary viewers must not notice errors on projection due to compression [3].

The DCDM workflow is shown in *figure 2*. DCDM contains all digital material required

for playback and includes image and audio information, subtitles, comments, animation, optical and sound effects, etc. Audio, image and text conform to the DCI standards. DCDM files can be directly played by the media playback equipment (e.g. projector and sound system) for projection quality control, or for synchronization and composition integration. Composition refers to all content and metadata required for a movie, trailer or advertisement projection

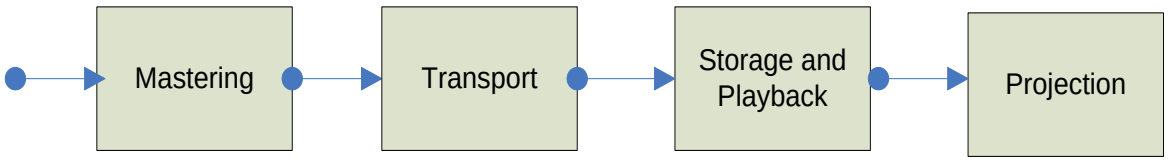


*Fig. 1. Digital cinema system*

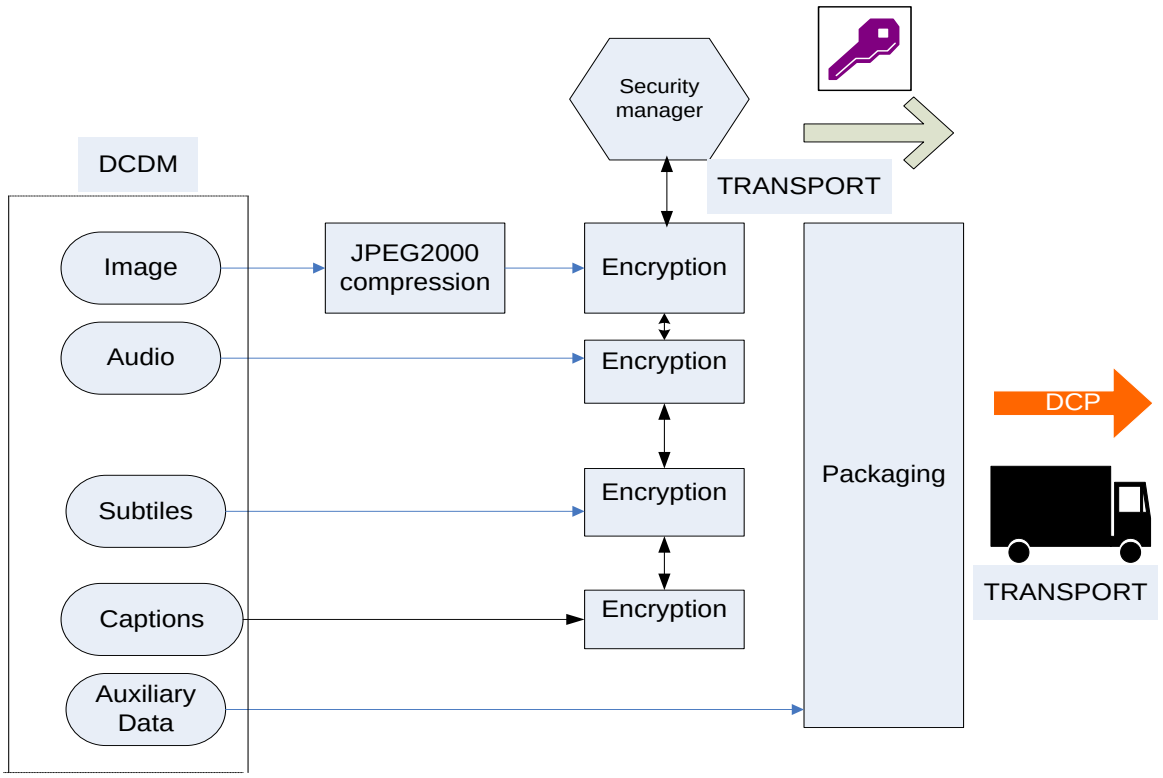


*Fig. 2. Digital cinema mastering*

DSM consists of:

- Image structure – J2C format;
- Sound structure - WAV format;
- Title structure - PNG or XML format;

### 3.3 Video

It is possible today to meet analog recording films that were shot before process of film digitization. At the start of digitization, the film strip is shot frame by frame by high-resolution

special film scanner and saved in TIFF (Tagged Image File Format) format. Furthermore, images are edited in graphics editors for color adjustment and removal of image defects. This is often caused by scanning errors, time degradation of the recording or incorrect handling of the film record.

Compared to the previous procedure, the processing of digital image recording is substantially simpler and the resulting image is much better. The recording quality depends very much on the used hardware and software, and the chosen file format chosen where the data is stored. It is understood that the best results can be achieved by use quality recording techniques, saving the file without using compression and with the highest possible quality. The sequence of TIFF images has a data volume of approximately 8TB for 4K resolution (for a film length of 200k frames).

### 3.4 Audio

As a video recording, audio has been recorded in analog form historically and stored on different carriers. Therefore, there is a need to digitize the audio. Various defects can exist on the recorded audio, caused very often by the aging of the recording medium or by mechanical means damage. For instance, tape cassettes were very often damaged in the sensing head or player mechanism. The tapes were not resistant to high temperatures nor exposure to dust. This can be reflected in the signal-to-noise ratio (SNR) or in a sound recording that negatively affects on its fidelity Resulting quality will also greatly affect on the quality of used analogue–digital (A/D) audio converters. Film studios use unquestionably high-quality digital converters and storing without the use of compression into a 96 kHz WAV file and a bit depth of 24 bits/sample [5]. Each sequence of images is always accompanied with a multi-channel audio track that physically represents one or more record carriers. Each audio track can contain a maximum of 18 channels for surround sound. Every sound channel contains different audio information and as many channels as possible must be present for perfect preservation of spatial information [3].

### 3.4 Subtitles

Subtitles are the last feature to be edited in a movie. Today, computer programs are used to create and edit subtitles. A template that is based on a scenario is available for a subtitle structure pattern. This template is formed by DCP - data format for digital cinemas. The corresponding software contains everything for creating subtitles in all languages. The template contains text and audio information in text form. The translations and scene notes for easy translation and orientation in subtitle timing are available. Final control, however, is still dependent on a person, and the native speaker of the language in which the subtitles are made. It is necessary to control a lot of aspects that the software is unable to do, such as accurate

timing, comfortable reading speed, or correct placement of subtitles in the image. Only a native speaker can make headlines to perfection so that every viewer can fully understand the story of the film in his language [3].

## 4. JPEG 2000 CODING FOR DIGITAL CINEMA

The recommended image compression standard for digital cinema is JPEG 2000 and the maximal data rate is 250 Mb/s [7]. JPEG 2000 has been standardized by the Joint photographic Expert Group (JPEG) of the International Organization for Standardization (ISO) and has been published as ISO 15444-1 standard [8]. JPEG 2000 uses a wavelet based image compression technique, which does not require image division in blocks, as the popular JPEG does. Therefore, it yields fewer blocking artifacts. Additionally, it conveys 20% better image compression, at significantly higher image quality. The main benefits of JPEG 2000 are the following:

- Support of lossless and lossy compression in a single codec;
- Multiple aspect ratios and resolutions;
- Intra-frame coding, which does not require motion estimation and compensation;
- Scalable image reproduction; a low resolution image version can be shown after the reception of a small part of the image file and can be enhanced progressively, after receiving more data. The first layer which can be transmitted and displayed, corresponds to the image background, which is, usually, its least important part.

With three color components, high bit-depth of 12 bits per pixel (bpp) and per color component, and 24 f/s, the total size of a three-hour feature film exceeds 9 TB. Such large sizes make the distribution of uncompressed digital movies impractical. Thus, the DCI specification includes data compression technique to decrease the size of the image data for economical storage and delivery. The compression technology chosen for digital cinema is JPEG 2000 [8]. It should be noted that JPEG 2000 was selected because of its tremendous flexibility, as well as its ability to deliver excellent picture quality. One important feature is its ability to compress both 2K and 4K pixel resolutions with one pass of 4096x2160 down the network. A second feature is that the JPEG 2000 compression engine is primary-set independent [7].

Another advantage is that separate signals simultaneously passing through can be selectively compressed or ignored and seamlessly passed along together. For example, accompanying metadata in MXF track files are not compressed, but are sent along in the output code streams, in sync with the compressed image representations. Among other features, JPEG 2000 has also the ability to extract sub-frame objects within full frames without any loss of quality [6].

In order to meet all the requirements, as well as those of using only standardized and non-proprietary formats, the standard JPEG 2000 was chosen for both lossless and lossy

compression, while MXF can be selected as a wrapper to package together all data streams and metadata in the *Master Archive Package* and *Intermediate Archive Package* [9]. DCI required a compression algorithm to be an open standard, so that multiple hardware manufactures would be able to build digital cinema systems. Significantly, the compression algorithm needed to support both 2K and 4K resolution projectors from the same file. JPEG 2000 satisfies these requirements and more [10].

The particular set of parameters (that will be used in digital cinema applications) is defined in JPEG 2000 profiles. A JPEG 2000 profile is a set of parameters that are designed to best serve the needs of a particular application. Currently, there are three profiles, defined as part of the JPEG 2000 standard. Two of these profiles, described a restricted set of parameters for use in particular applications, while the third profile is unrestricted. Two additional profiles are being developed for use in digital cinema applications by the JPEG 2000 committee.

The DCI specifications require a 4K decoder to decode all data for every frame in a 4K distribution. Similarly, a 2K decoder is required to decode all data in a 2K distribution. A 2K decoder is allowed to discard the highest resolution level of a 4K distribution [11]. No other data can be discarded. In other words, discarding data to keep up with peak decoding rates is not allowed.

## 5. DIGITAL CINEMA PACKAGE

This digital data format is referred to the classic film format wheels. The individual video and audio structures are packaged in separate files in MXF format and saved separately [12]. This is because subtitle tracks in the individual language could be separated to allow separate projection. MXF is the carrier format of all structures (tracks) together, intended for distribution, which is formed from DCDM. There is no change in the appearance of the tracks. The subtitles are saved in XML or PNG format and descriptive files in XML. Descriptive files include: Composition Playlist - CPL (list of all files in DCP), and Volume index file - VOLINDEX (volume information). The DCP designation includes all these files. The packing list is only added at the end of the process and can be used to verify that the DCP did not lose any stored data after decryption and whether all data is read properly and errors are eliminated [3]. The whole package is encrypted at the end against unauthorized playback, copying and further copyright infringement by KDM. Complete DCP includes also lot of trailers and advertisements. The exact structure of the DCP depends on the used software and may vary slightly in some respects (e.g. in directory structure). *Figure 3* shows the process of DCP delivering to a movie theater.

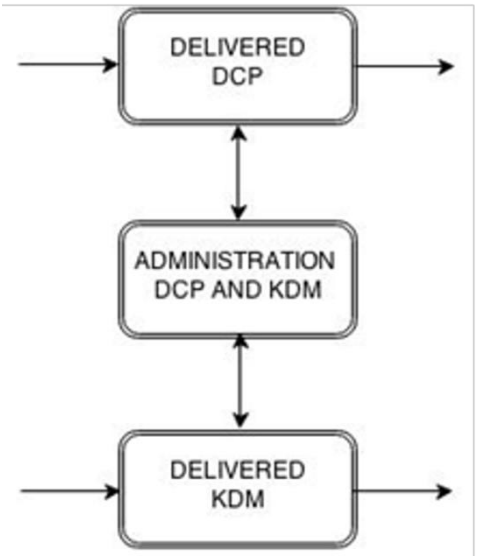


*Fig. 3. Digital cinema package delivering*

### 5.1 Key delivery message

This is a security mechanism that is used to prevent unauthorized access to DCP data [13]. When creating a DCP from DCDM, the video and audio tracks are encrypted with unique keys that allow the owner to decrypt encrypted data. These decryption keys must be securely delivered to all end customers, such
as cinemas, distributors or editorial companies. Each key is unique and it is used to decrypt only certain traces for which it is intended. It is not possible to have a key that decrypts all tracks on data medium [13].

KDM has three levels of security:

- 128-bit AES key for video and audio track security;
- RSA (*Rivest–Shamir–Adleman*) key used to encode content to level 1;
- RSA key for the final encryption of the content to level 2 by another type of key of the same kind.

KDM specifies the following [13]:

- Closer rights to CPL;
- Access rights to individual tracks;
- Key validity period - time of day, time interval;
- List of trusted devices - public key.

KDM takes the form of a very small digital XML file that the distributor sends to the cinema stored on a USB stick or simply as an electronic attachment. Usually an external company handles the issue of these keys. They can only decrypt the data devices that own a unique private key associated with a public key contained in KDM. The first decryption option is using a private key. This is a device description issued by a manufacturer or supplier. A model, serial number, device role in the distribution chain (mastering, playback…), as well as

proof that the private key comes from a trusted source, are shown. If an invalid (pirated) certificate is included in the database of certificates, it would mean financial losses for film production and mastering company. For this reason, when issuing certificates, greater attention is paid to credibility of the applicant.

The second option is to decrypt the data using the internet. If the device is certified for this server, it is capable of using protected data and it allows access to content. Device certification information for the server is listed in the CPL. If the device is certified for another generation of certificates KDM must be able to decrypt and extract the necessary data. The device creates its own KDM, for which it is certified and fully supported. This happens in practice very often, as a large number of KDM and playback systems are widely used throughout the world. The key issuer must anticipate this option in advance. A typical certificate database consists of a relatively small number of root and signed certificates, but with a large number of device certificates. Managing a certification database is a tough task. This is mainly because servers can move to repair or replace with newer models. Cinema server operators are therefore forced to constantly communicate with key distributors and provide them with up-to-date information, to receive the correct KDM for projection [3].

### 5.2 Projection

Within the DCI specification, the projection system converts the digital picture information into light which is projected on a screen. The DCI specification defines several aspects of the projection system including colorimetry, performance specifications and requirements, as well as physical connections to and from a projector.

A projection system can support many interfaces and various digital cinema architectures. In addition to the main image, a projection system may also project text and still images on a screen. This requires additional interfaces. Two major technologies are used in digital cinema projectors, namely Digital Light Processing (DLP) and Digital Image Light Amplifier (DILA).

DLP has three basic benefits, compared to alternative existing projection technologies:

- It allows high quality color or monochrome image projection without noise;
- It is more efficient than other alternatives (e.g. LCD technology), because it doesn’t require polarized light;
- The dense location of micromirrors produces images at the highest perceivable image resolution.

DILA technology has other benefits:

- It allows maximal pixel density and supports high image resolution;
- It allows powerful light emission, even at high resolution;
- It provides high image contrast.

Digital content can be stored on a local or central cinema server hard disk. The local disk is located right next to the cinema server. The central disk is common to the entire multiplex and is located at a central site that is connected via 1 Gb/s Ethernet projector. In practice, the best combination of both solutions is where the central disk is used for retention of all data and only digital content needed for the nearest is transferred to the local disk projection.

### 5.2 Transport

The DCI specification does not specify a particular mode of transport. It is envisioned that the transport can be via physical media or over a network. It is required that the content owners' encryption is not removed during transport. All of the data of the original movie files must be intact upon completion of the transport.

## 5. NON-COMMERCIAL SOFTWARE PRODUCTS

Creating DCP format using non-commercial products from source files is not a simple matter if legally free available programs are used. Still several years ago, no commercial software was available for this purpose. A large number of software companies, computer programmers and enthusiasts made a big step forward in developing software products that make this possible.

Nowadays, ordinary users interested in DCP encoding also have a choice from several available programs. However, the complete flawlessness of this software has yet to be discussed. The reason for this is largely the limited number of experts involved in their development.

Non-commercial software products can be used free of charge, where only registration on the product website is required. Main software requirements include:

- Freeware;
- Simple installation and operation;
- Encoding speed;
- No restrictions: time of coded recording, adding text or logo to the image;
- Possibility of basic output settings;
- A wide range of supported codecs.

Although these products are very specific, they are available for use in large amount. The main drawback of all programs is their unfinished and unverified development. It is occurred very often that while using applications instead of responding to a command or

execution it happens either an inadequate response, an incorrect execution of the command, or in worse case, unexpected crash or freezing of the application.

### 5.1 DCP Builder

This software makes use of multiple free available libraries. According to the appropriate page, the program is designed to be used by film professionals and not by an occasional user because of large number of options compared to other programs of the style. DCP Builder is a good alternative to commercial OpenDCP software.

The electronic application must be relatively detailed compared to other similar registrations; it must contain a detailed purpose for the use of the program, institution, etc. A shoot screen of this program is shown in *figure 4*. However, the use of the program has one drawback. Internet registration requires a detailed electronic application for serial issue keys to be completed on the web site of this program. Moreover, there is a request on the allocation of a key for study reasons. To unlock the necessary features of this program the serial key is necessary and therefore the alternative software should be found. A watermark should be embedded, but there is a free code to disable it.

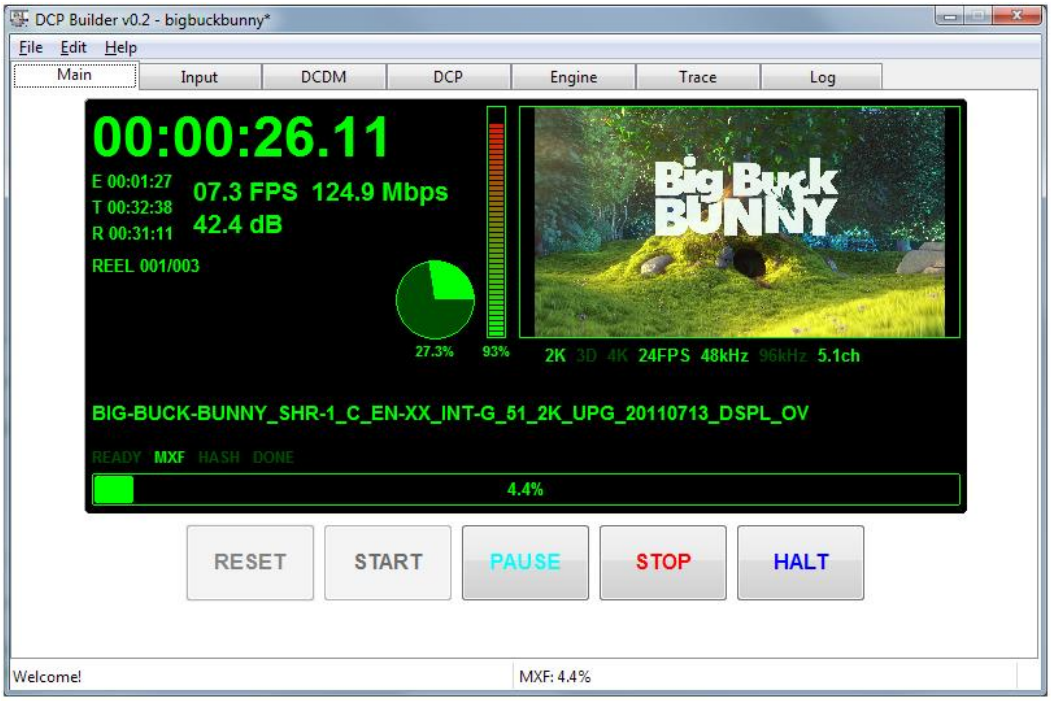


*Fig. 4. DCP Builder*

### 5.2 Digital Cinema Package Editor (DCPC)

This is a program that is available only on the platform Microsoft Windows. A shot screen of this program is presented in *figure 5*. It is available in non-commercial and

commercial versions. The price includes only the encoding program itself that is identical to the non-commercial version. To store multiple tracks into one DCP file, multiple audio channels at maximum, plug-ins are required for support encoding.

Program features include:

- 2D and 3D image tracks;
- 2K and 4K image resolution;
- 6-channel 24 bit/48 kHz audio.

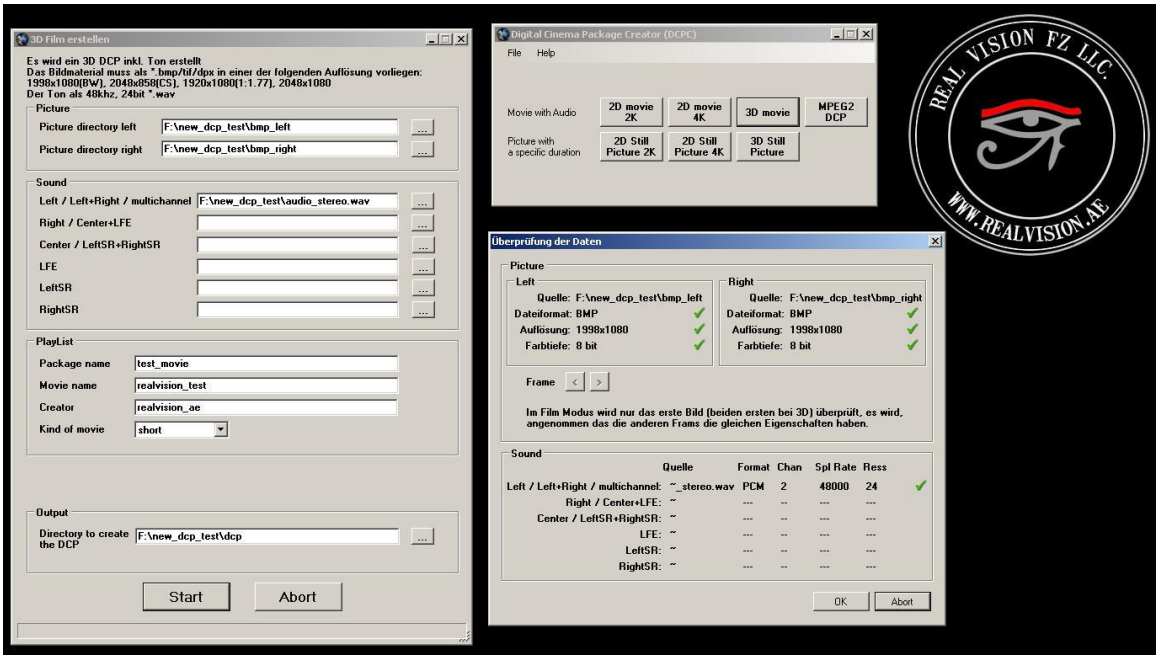


*Fig. 5. Digital Cinema Package Editor*

### 5.3 DVD-o-matic

It is a free and open source program and supports files in very different formats, including DVDs, Blu-ray, MP4, AVI, and many more. The last updated version includes a professional option such as sending the DCP to the Theater Management System. It includes a guide for the correct use of the software.

The program can use codecs that already exist in the installed system. The input file format can be any common type of video file formats, DCP data format, or still image. Software operation is very simple. Required time for encoding depends on the input file for codec.

The drawback is that it is a copy of another program and does not include enough new options that make us opt for this new program. Also, this software doesn't have a version for Mac OS system.

*Figure 6* shows a simple initial form for setting conversion parameters. It is always performed before starting the transfer by filling the basic output parameters. It is essential to specify the address of the space on the input disk and output file, output file name, crop, and

default image frame. Other parameters that can be set are, for example, video image filters or audio sync with video using delay settings. The shortcoming of this program is that some file formats of the program don't recognize the frame rate and encoding would not be well performed.

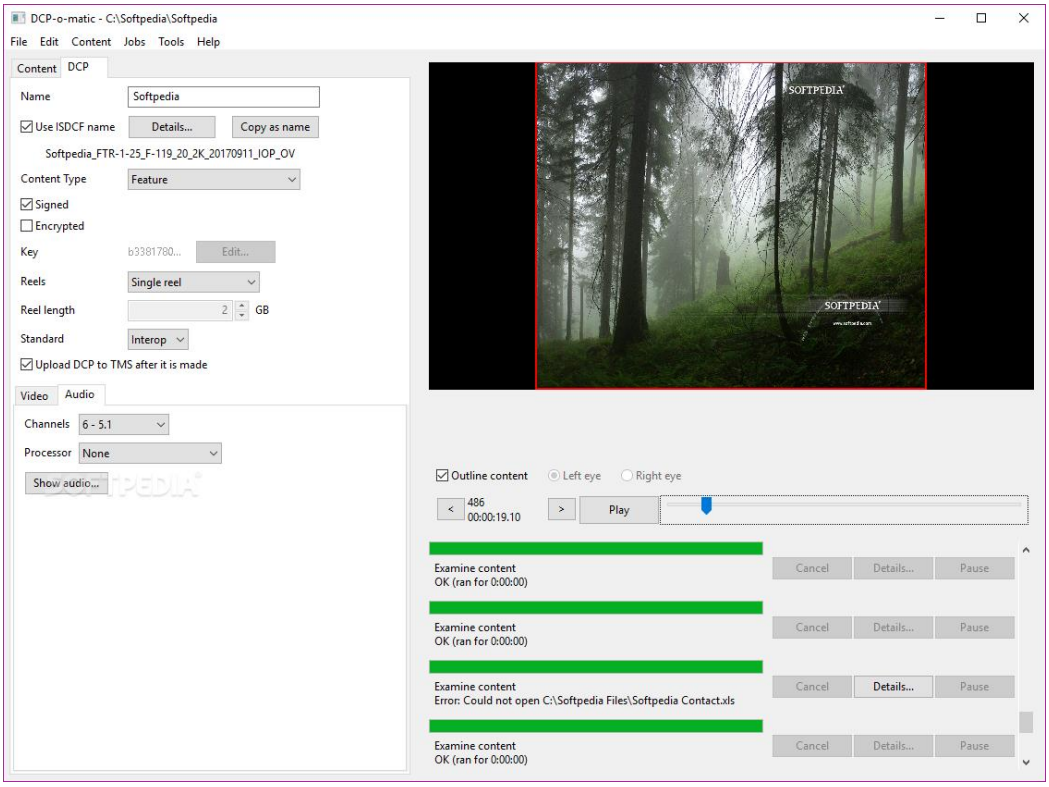


*Fig. 6. DVD-o-matic*

The main features of free software for digital cinema are presented in Table 1.

Table 1. Main properties of free software for digital cinema

| **Software** | **Source file format** | **Output file format** | **Operating system** | **Licence** |
|---|---|---|---|---|
| DCP Builder | Image sequences, video with extern FFmpeg codec | JPEG 2000, MXF, XML, 3D | Windows, Mac OS X, Linux | Freeware, registration necessary |
| DCPC | Image and audio sequences | JPEG 2000, MXF, XML, 3D | Windows | Freeware |
| DVD-o-matic | Video | JPEG 2000, MXF, XML | Windows, Linux | GNU |

## 6. CONCLUSION

Digital cinema became possible thanks to the major Hollywood film studios. We have presented the necessary information about the digital cinema technology and the steps to be followed to create the digital cinema package, from production to distribution. At first glance it may be somewhat complicated, but it is far from reality. To achieve a DCP a few simple steps should be followed, though, paying special attention is necessary in order to obtain the final result is as expected.

We emphasized the role of digital source master in DPCM development. When producing the DCP signal processing methods are necessary. The DCI System Specification represents an important step towards establishing an interoperable, secure digital cinema production and exhibition environment. It makes a broad use of the existing, well accepted cryptographic standards. As digital cinema has been built and deployed worldwide, standard organizations will further refine the functionality and interoperability requirements of various digital cinema components.

After seeing the pros and cons of each free program for creating DCP, choosing software depends on some variables. However, there are certain guidelines to be followed.

ACKNOWLEDGMENT

The author would like to express sincere thanks to the Ministry of the Education and Science of the Republic of Serbia, project TR 32015.

*REFERENCES*

[1] A. Maltz, *How do you store a digital movie for 100 years?*, IEEE Spectrum, 51(3), pp 40-44. 2014.

[2] M. Bertalmio, *Image processing for cinema*. CRC Press, 2014.

[3] http://www.dcimovies.com.

[4] 377M-2004. *Television - Material Exchange Format (MXF)*. File Format Specification, 2014.

[5] P. Fornaro, D. Gubler, *DCP/A: discussion of an archival digital cinema package for AV-media*, Proceedings of the Archiving Conference, Society for Imaging Science and Technology, pp 5-8, 2014.

[6] A. Bilgin, M.W. Marcellin, *JPEG2000 for digital cinema*, Proc. International Symposium on Circuits and Systems ISCAS 2006, Island of Kos, Greece, pp 3878-3881, May 2006.

[7] ISO/IEC 15444-1. *JPEG2000 Image Coding System*, 2000.

[8] S. Fossel, G. Fottinger, J. Mohr, *Motion JPEG 2000 for high quality video systems*, IEEE Transactions on Consumer Electronics, 49(4), pp 787-791, 2003.

[9] Z. Bojković, A. Samčović, *Film archives as a future enhancement of digital cinema technology*, Proceedings of the 9th International conference on telecommunications in modern satellite, cable and broadcasting services TELSIKS 2009, Vol. 1, pp 273-276, 2009.

[10] Z. Lischer-Katz, *Considering JPEG 2000 for video preservation: A battle for epistemic ground*, Proceedings of the iConference 2014, pp 1056-1065, 2014.

[11] A. Samčović, *A review of the digital cinema chain – from production to distribution*, Chapter 12 in Emerging research on networked multimedia communication systems, IGI Global, pp 366-394, 2016.

[12] N. Mazzanti, A. Nowak, P. Read, *Preservation and access solutions for moving image archives in the digital cinema era*, Axmedis, pp 131-137, 2008.

[13] J. Bloom, *Digital cinema content security and the DCI*, Proceedings of the 40th Annual Conference on Information Sciences and Systems, 2006.

# OPTIMAL CONTROL OF AIR CONDITIONING SYSTEM

Asma **REBAI**, Salim **HADDAD**, Ridha **KELAIAIA**
*LGMM Laboratory, Université 20 Août 1955 - Skikda, Algeria*
*{a.rebai, s.haddad, r.kelaiaia}@univ-skikda.dz*

**Keywords: Air conditioning, Optimization, Thermal comfort, Optimal control strategy.**

**Abstract***: This paper presents an optimal method for control the functioning time of an air condi- tioning system that allows reducing the electrical consumption by maintaining thermal comforts. In this work, the minimizing of the electrical consumption of a house is adop- ted as objective function, and thermal comfort is taken as a primary constraint, thus the mathematical model of air conditioning is formulated. Then an optimal control method based on reducing the electrical consumption of a house equipped with air conditioning system by optimizing the operating time of the air conditioner is proposed. Subsequently, the simulation results show a significant reduction of the total consumption at the same time maintaining thermal comfort. The proposed optimal control strategy of air condi- tioning system is carried out in MATLAB/Simulink with satisfactory results for a house. The rest of the load (washing-machine, refrigerator, freezer, etc.) is assumed as a constant complementary charge. Simulation results show a significant reduction of the electrical consumption.*

## 1. INTRODUCTION

The sharp rise in the electricity demand is a direct consequence of the change in consumption habits, especially because of the use of more and more prevalent of air conditioning. This is evident to create peak consumption in the summer. Peak energy demand refers to the time of day when loads on the electricity distribution infrastructure reach a maximum. During the summer months this tends to happen between 16:00 and 20:00 when high outdoor temperatures coincide with people returning home from work, resulting in high residential air-conditioner use. Reducing these loads is becoming increasingly important, because of an emerging shortage of electricity as a result of rapid population growth.

The air conditioning process is a controllable load which takes an important part in the tertiary and residential buildings. Therefore its management has an important potential to reduce the peaks of consumption.

In the literature, many control methods have been developed or proposed for air conditioning systems [1], this work focuses on a study of control methods for heating, ventilation and air-conditioning (HVAC) systems and the emphasis is on the predictive control approach model. Other studies have shown that pre-cooling thermal mass can reduce the cooling load of commercial buildings or shift the cooling load away from peak demand periods [1–9].

However, reductions in peak cooling demand have been demonstrated in theory and through field tests by either increasing the amount of thermal insulation used within a wall [10], or by increasing the thermal mass of the wall [11–13]. Automatic control for air conditioning systems On/Off control, PID control, time control (On/Off switch, fixed time, boosted start and optimum start and stop) were reviewed in [14].Al-Sanea and Zedan [15] showed that peak cooling loads in Riyadh could be reduced by up to 26% by optimizing summertime thermostat temperatures. [16] In this project we addresses the problem of designing a new control algorithm for HVAC systems that improves the comfort level of the occupants in buildings and at the same time consumes less energy to reach this goal. Callaway [17] considered the manipulation of 60,000 air conditioner thermostat set points to follow the dynamic output of a wind farm at a resolution of one minute. The air conditioning models were based on resistance-capacitance (RC) models. Callaway and others [18–21] have considered the dynamics associated with controlling a large number of thermostatically controlled loads or electric vehicles to achieve short-term grid benefits. Because they consider shorter-term periods, weather is held constant for the simulations and on this model [22], a discrete-time inverse optimal control strategy was developed and implemented to an experimental air conditioning system for simultaneously controlling indoor air temperature and humidity.To meet the energy demands while maintaining human thermal comfort,this paper [23] established a comfortable space air conditioning system of environmental parameters on extent of comfort index through the simulation analysis of the air conditioning thermal comfort equation.

However, this section analyzes the main references on optimization methods applied to the load management.

The first group [24] optimal load management in a building includes the methods of cost minimization. This cost is a combination of electricity and the cost penalty expressed as human comfort. The principle of these methods is to identify the key strategies of shedding and issue recommendations for building operators to offoad the load properly.

The second group consists of the realization of extensive simulations with different combinations of parameters; comparison means between these simulations the optimal point, which is a sub-optimal solution. For example, [25] developed a simulation environment to

study a range of key parameters that influence the cost of operating the system. The optimal control strategy which consists in minimizing all costs of electricity has been validated by simulations.

The objective of this research is to minimize the electrical consumption of a house without sacrifice human comfort by control functioning time of the air conditioning system.

The paper is organized as follows: Section 2 presents case study for our air conditioning system where its presents a brief presentation of the loads in the house and illustrate a mathematical model for the air conditioning and the modal implemented in matlab/Simulink and Section 3 describes the optimization problem with the objectives function and constrains and the problem formulation after the results and discussion of optimization.

## 2. CASE STUDY

In this research, we used the data from Nevada, USA, in July 6, 2016 (*Figure 2*) for a house (300 $m^2$) with required temperature inside the rooms given by the limits: $T^{min}$ = 20°C and $T^{max}$ = 22°$C$.

The appliances considered are:

- 5.5 kW Air Conditioning Unit (varies with compressor power demand)
- 3.5 kW Air Conditioning Unit (varies with compressor power demand)
- Refrigerator (700 W) - variable
- Pool pump (1 kW) - works 8 hours/day in summer (morning and afternoon)
- One electric oven (3 kW) used occasionally
- Dishwasher (500 W) used occasionally
- Cloth-washer (750 W) used occasionally
- Cloth-dryer (2.5 kW) used occasionally
- Numerous light fixtures (used mainly at night)
- Two flat screen TV sets (usually one the two is used in the afternoon and evening hours)
- 4 ceiling fans (100 W each usually 2 out of 4 are used on a continuous basis.
- Electronic loads (laptops, clocks, alarm system, etc.)

The differential equation system is obtained [26]:

$$\frac{dT_m}{dt} = \frac{I_s}{C_m} + \frac{T_{int}}{R_m C_m} + \frac{T_{ext}}{R_m C_m} - \frac{2T_m}{R_m C_m} \tag{1}$$

$$\frac{dT_{inst}}{dt} = \frac{I_{inst}}{C_0} - \frac{I_{ac} S(t)}{C_0} + \frac{T_{ext}}{R_f C_0} + \frac{T_m}{R_m C_0} - \frac{T_{int}}{C_0}\left(\frac{1}{R_m} + \frac{1}{R_f}\right) \tag{2}$$

where:

$E$: The electrical consumption of the air conditioner [$KW\,h$]

$X(t)$: The switching function (1 when the compressor motor is ON and 0 when is OFF)

$T^{min}$: Minimum temperature inside the room [$^{\circ}C$]

$T^{max}$: Maximum temperature inside the room [$^{\circ}C$]

$T_m$: The wall temperature [$^{\circ}C$]

$T_{ext}$: Exterior temperature [$^{\circ}C$]

$R_m$, $C_m$: The equivalent thermal conduction resistance [$^{\circ}C/W$] and thermal storage capacity of the room (wall, base and roof) [J/°C]

$R_F$, $C_0$: The equivalent thermal conduction resistance of the average air infiltration [°C/W] and thermal capacity the air inside the room [$J/^{\circ}C$]

$I_s$: The current source of two components (solar radiation and the portion of in- ternal heat sources involved in this indirect heating of air) [$W$]

$I_{inst}$: The current source of heat source produced by lamp, computer, nobody, etc. [W]

$I_{ac}$: The heat removed by the air conditioner [$W$]

The values of model parameters are listed:

| | |
|---|---|
| $C_m$ | 6000000 J/°C |
| $C_0$ | 118235.4 J/K° |
| $R_f$ | 0.01 °C/W |
| $R_m$ | 0.004 °C/W |

*Figure 1* shows the conditioning room model in MATLAB/Simulink that is built from this differential equation system.

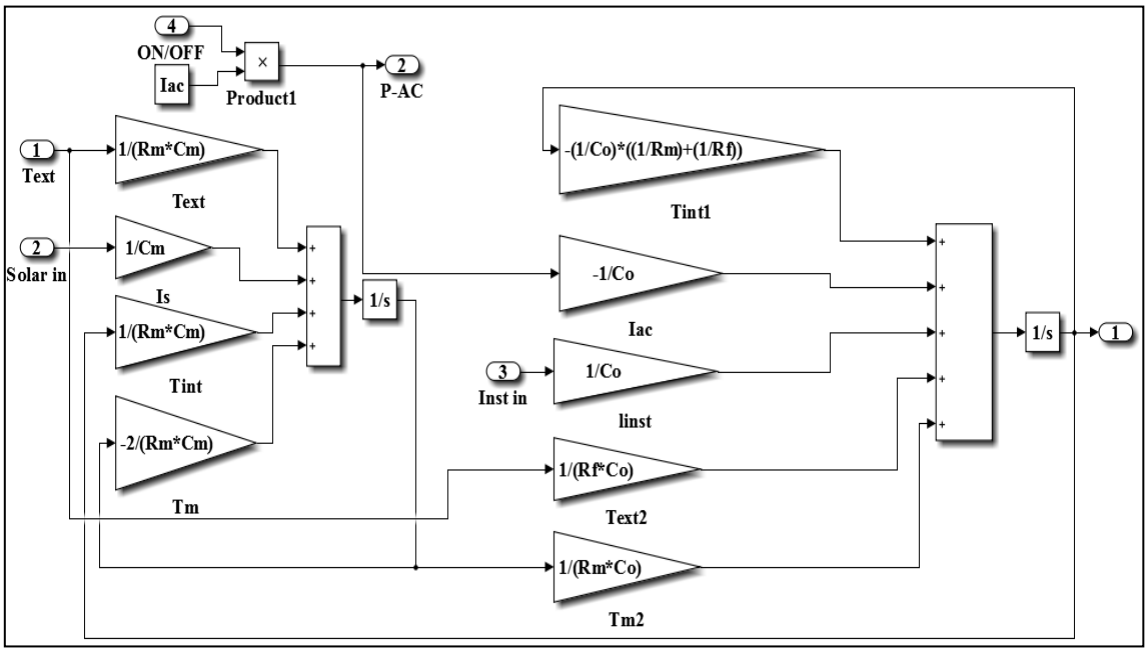


*Fig.1. Air conditioning room model*

Table 1. Exterior temperature of 6 July 2016

| Time | 00:00 | 01:00 | 02:00 | 03:00 | 04:00 | 05:00 | 06:00 | 07:00 | 08:00 | 09:00 | 10:00 | 11:00 |
|---|---|---|---|---|---|---|---|---|---|---|---|---|
| $T_{ext}$ (°C) | 28 | 27 | 26 | 25 | 25 | 24 | 25 | 28 | 29 | 31 | 32 | 34 |

| Time | 12:00 | 13:00 | 14:00 | 15:00 | 16:00 | 17:00 | 18:00 | 19:00 | 20:00 | 21:00 | 22:00 | 23:00 |
|---|---|---|---|---|---|---|---|---|---|---|---|---|
| $T_{ext}$ (°C) | 35 | 36 | 37 | 37 | 37 | 37 | 35 | 34 | 32 | 31 | 30 | 29 |

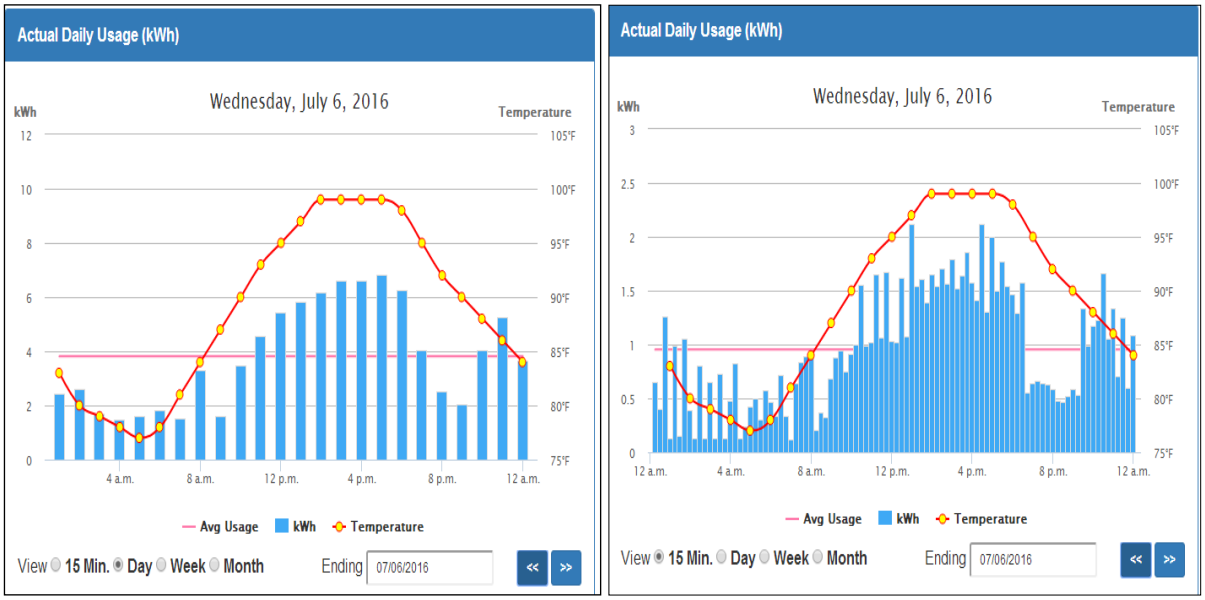


*Fig.2. Exterior temperature and the power demand curve for July 6, 2016*

## 3. OPTIMIZATION PROBLEM

The objective of the problem is to reduce the electrical consumption of a house equipped with air conditioner of 5.5 kW by optimizing the operating time of the air conditioner.

### 3.1. Definition of the objective function

The objective of the problem is to reduce the electrical consumption of a house equipped with air conditioner of 5.5 kW by optimizing the operating time of the air conditioner. Consequently, the objective function can be summarized, as follows:

$$\underbrace{Min}_{x_i \in \{0,1\}} [E] = \sum_{i=1}^{D} E x_i \ , \ i = 1 \ldots \mathrm{D} \tag{3}$$

*D* being the simulation time.

### 3.2. Definition of the constraints

In the following, our interest is focused on the comfort*:*

Since human thermal comfort is strongly related to the building, the requirement of thermal comfort is generally considered as a primary constraint of the optimization of the building problem

$$T^{min} \leq T^{int} = f(E\ x_i) \leq T^{max} \tag{4}$$

$T^{int} = f(Ex_i)$ *:* Interior temperature of the room, it can be obtained from resolution of the following differential equations [26]:

$$\frac{dT_m}{dt} = \frac{I_s}{C_m} + \frac{T_{int}}{R_m C_m} + \frac{T_{ext}}{R_m C_m} - \frac{2T_m}{R_m C_m} \tag{5}$$

$$\frac{dT_{inst}}{dt} = \frac{I_{inst}}{C_0} - \frac{I_{ac} S(t)}{C_0} + \frac{T_{ext}}{R_f C_0} + \frac{T_m}{R_m C_0} - \frac{T_{int}}{C_0}\left(\frac{1}{R_m} + \frac{1}{R_f}\right) \tag{6}$$

### 3.3. Problem formulation

Mathematically, the problem of the optimization is formulated as follows:

$$\underbrace{Min}_{x_i \in \{0,1\}} [E] = \sum_{i=1}^{D} E\ x_i \text{ , i=1...D} \tag{7}$$

Such that the constraint:

$$20°C \leq T_{int} \leq 22°C \tag{8}$$

is satisfied.

### 3.4. Optimization results

The dsolve matlab function was used to solve the differential equations system (constraint of comfort).

*3.4.1. Before Optimization*

Total consumption of the house in the day of July 6, 2016 reaches to 94.11 KWh.

*3.4.1. After Optimization*

The operating time of the air conditioner: 2 h and 17 mn.

The electrical consumption of other loads: 55.611 KWh

The electrical consumption of the air conditioner: 11.935 KWh Total consumption of the house: 67.546 KWh

By this optimization, we were able to reduce the energy consumed from 94.11KWh to 67.546 KWh by saving 28% of the energy consumed during 24h.

## 4. CONCLUSION

From the discussion above, it can be concluded that the optimal control method for the air conditioning system can reduce the total electrical consumption

The presented method is based on efficiently reducing the total electrical consumption without sacrificing the thermal comfort of occupants.

Optimal control method to minimize functioning time of air conditioning was planned using optimization method .From the results, it was concluded that it is possible to save around 28 % from the total consumption in 24 hours.

The results of simulation show that air conditioning system can substantially save energy and also maintain thermal comfort. This method can adapted for all the house or building.

## *REFERENCES*

[1] A. Abdul, J. S. Farrokh, *Theory and applications of HVAC control systems- A review of model predictive control*, Building and Environment, vol. 72, 343-355, 2014.

[2] A.Rabi, L.K. Norfod, *Peak load reduction by preconditioning buildings at night*, International Journal Energy Ressource, 15:781-798, 1991.

[3] J.E. Braun, *Load control using building thermal mass*, J Sol Energy Eng, 125:292, 2003.

[4] P. Xu, P. Haves, M. Piette, J.E Braun, *Peak demand reduction from pre-cooling with zone temperature reset in an office building*, (LBNL-55800), 2004.

[5] K. Le, J.E. Braun, *Model-based demand-limiting control of building thermal mass*, Build Environ, j.buildenv, 43:1633-1646, 2008.

[6] R. Yin, P. Xu, M.A. Piette, S. Kiliccote, *Study on auto-DR and pre-cooling of commercial buildings with thermal mass in California*, Energy Build, 42: 967-975, 2010.

[7] S.P. Corgnati, A. Kindinis, Thermal *mass activation by hollow core slab coupled with night ventilation to reduce summer cooling loads*, Build Environ, 42:3285-3297, 2007.

[8] D.O. Rijksen, C.J. Wisse, AWM. Van Schijndel, *Reducing peak requirements for cooling by using thermally activated building systems, Energy* Build, 42: 298-304, 2010.

[9] SA. Al-Sanea, M. Zedan, *Improving thermal performance of building walls by optimizing insulation layer distribution and thickness for same thermal mass*, Appl Energy, 88: 3113-3124, 2011.

[10] M.E. Dexter, *Energy conservation design guidelines: including mass and insulation in building*

*walls*, ASHRAE J, 22:35-48, 1980.

[11] D.M. Burch, W.E. Remmert, D.F. Krintz, C.S. Barnes, Laboaratory ORN, *Field study of the effect of wall mass on the heating and cooling loads of residential buildings*. (Log home report.). Build Therm Mass Semin, 265-312, 1982.

[12] SA. Al-Sanea, M. Zedan, SN. Al-Hussain, *Effect of thermal mass on performance of insulated building walls and the concept of energy savings potential*. Appl Energy, 89:430442, 2012.

[13] M.V. Harrold, D.M. Lush, *Automatic controls in building services*. IEE Proc B Electr Power Appl, 135:105-133, 1988.

[14] SA. Al-Sanea, M. Zedan, *Optimized monthly-fixed thermostat-setting scheme for maximum energy-savings and thermal comfort in air-conditioned spaces*. Appl Energy, 85:326-346, 2008.

[15] P. Prahlad, *Modeling and optimal control algorithm design for HVAC systems in energy efficient buildings*. International Research journal for engineering science, Technology Innovation (IRJEST), ISSN-2315-5663 vol2 (2), pp.29-39, Feb2013.

[16] D.S. Callaway, *Tapping the energy storage potential in electric loads to deliver load following and regulation with application to wind energy*. Energy Convers Manage, 50(5):1389–1400, 2009.

[17] S. Bashash, H.K. Fathy, *Modeling and control of aggregate air conditioning loads for robust renewable power management*. IEEE Trans Control Syst Technol, 21(4):1318–1327, 2013.

[18] N.A. Sinitsyn, S. Kundu, S. Backhaus. *Safe protocols for generating power pulses with heterogeneous populations of thermostatically controlled loads*. Energy Convers Manage, 67:297–308, 2013.

[19] N. Lu. *An evaluation of the HVAC loads potential for providing load balancing service.* IEEE Trans Smart Grid, 3(3):1263–1270, 2012.

[20] C.Y. Chang, W. Zhang, J. Lian, K. Kalsi . *Modeling and control of aggregated air conditioning loads under realistic conditions*. Innovative smart grid technologies (ISGT), IEEE PES, 2013.

[21] C. Perfumo, E. Kofman, J.H. Braslavsky, J.K. Ward. *Load management: model-based control of aggregate power for populations of thermostatically controlled loads*. Energy Convers Manage, 55:36–48, 2012.

[22] T. Broeer, J. Fuller, F. Tuffner, D. Chassin, N. Djilali. *Modeling framework and validation of a smart grid and demand response system for wind power integration.* Appl Energy, 113:199–207, 2014.

[23] M. Flavio, N.S. Edgar, X. Yudong, D. Shiming. *Real time neural inverse optimal control for indoor air temperature and humidity in a direct expansion air conditioning system*. International journal of refrigeration.S0140-7007(17)30147, 2017.

[24] K. Keenery, J. Braun. *Simplified method for determining optimal cooling control strategies for thermal storage in building mass, Intl. J. of HVAC&R Research*, Vol.2, No.1, 59-78, 1996.

[25] G. Henze, R. Dodier, M.Krarti. *Development of a predictive optimal controller for thermal energy storage systems*, Intl. J. of HVAC&R Research, Vol.3, No.3, 233-264, 1997.

[26] K. Le, T. Tran-Quoc, Jean-Claude Sabonnadière, and Ch. Kieny, and N. Hadjsaid, *Peak load reduction by using air-conditioning regulators*. Electrotechnical Conference. MELECON, The 14th IEEE Mediterranean, pp. 713-718, 2008.

# WAVELET ANALYSIS AND NEURAL NETWORK TECHNIQUE FOR PREDICTING TRANSIENT STABILITY STATUS

Emmanuel Asuming **FRIMPONG**[1], Philip Yaw **OKYERE**[1], Johnson **ASUMADU**[2]
[1]*Kwame Nkrumah University of Science and Technology, Kumasi, Ghana,* [2]*Western Michigan University, Kalamazoo, Michigan, USA*
*eafrimpong.soe@knust.edu.gh*

**Keywords: Neural network, Out-of-step, Power system stability, Stability prediction, Transient stability**.

**Abstract***: This paper presents a method based on wavelet analysis (WA) and Multilayer perceptron neural network (MLPNN) to predict transient stability status (TSS) after a disturbance. It uses as input data, generator terminal frequency deviations extracted at a rate of thirty-two samples per cycle. Only the first eight frequency deviation samples per machine are needed. The eight samples are sub-divided into two sets, one set consisting of the first four samples and the other set consisting of the last four samples. Each set of samples is decomposed into 2 levels using the Daubechies 8 mother wavelet and the absolute peak value of detail coefficients obtained. The absolute peaks of detail coefficients of the first sample sets of all generators are added and so are the absolute peaks of detail coefficients of the second sample sets. The two summed values are then used as inputs to a trained MLPNN which predicts the TSS. The method was evaluated using dynamic simulations carried out on the New England test system. The method was found to be accurate and can be implemented in real-world systems to provide system operators advance information on system stability, following disturbances, to aid the deployment of needed emergency control measures.*

## 1. INTRODUCTION

Power grids are subjected to a wide range of abnormal conditions due to faults. Severe abnormal conditions can cause rotor angle separations that may also lead to out-of-step (OS) conditions between generators (groups or individual) or interlinked systems. OS conditions can cause torsional resonance and pulsating torques that are destructive to machine shafts [1]. When OS conditions arise, generator or system separation is needed to avoid flashovers,

damage to system equipment and wide-scale outages [2]. For example, in 2003, there were several major outages in USA, Canada and some European countries due to OS conditions [3]. Furthermore, in 2006, disturbances that occurred in the Union for the Co-ordination of Transmission of Electricity system caused it to uncontrollably separate into three islands [3]. A possible solution to OS problems is the use of schemes that analyse transient disturbances to determine critical clearing times, predict possible transient instability, and offer techniques for improvement of transient stability [4]. To this end, there is on-going research and a number of schemes for determining critical clearing times [5], detecting transient instability [2,6], predicting transient stability or otherwise [4], [7-12], and improving transient stability [13,14] have been put forth. These techniques have tackled the problem using various input parameters, signal processing and decision-making tools, with varying degrees of accuracy and easy of practical implementation.

An OS scheme must operate on-line, act speedily and accurately. It must also be robust and simple to implement. All these desired features are yet to be completely addressed in a single scheme. For example, the technique in [8] needs samples from ten to twelve different data types for each generator leading to a huge volume of required data for large systems which delays the technique's response. That in [9] takes close to two and half seconds after fault clearance to decide on the stability or otherwise of a system. The methods in [10] and [11] employ templates that are pre-determined. Thus, system conditions other than those used to develop the templates will cause the techniques to maloperate. Furthermore, the method in [12] uses pre-determined stability boundaries for each machine and its application in a practical system with a large number of generators will require extensive simulation to realize those boundaries.

To address the deficiencies in TSS prediction, this paper proposes a wavelet analysis and multilayer perceptron-based method. The scheme uses as input data, generator bus frequency deviations obtained after fault clearance. The frequency deviation samples are taken at a rate of thirty-two samples per cycle. Only the first eight samples of each machine bus frequency deviation are required. The eight samples are sub-divided into two sets, one set consisting of the first four samples and the other set consisting of the last four samples. Each set of samples is decomposed into 2 levels using the Daubechies 8 mother wavelet and the absolute peak value of detail coefficients obtained. The absolute peaks of detail coefficients of the first sample sets of all generators are added and so are the absolute peaks of detail coefficients of the second sample sets. The two summed values are then used as inputs to a trained MLPNN which predicts the stability status. The strengths of the proposed method are highlighted as follows:

(a) The technique makes use of data sampled in a very short time window.
(b) Minimal data is needed to train the MLPNN decision tool used.
(c) No predetermined templates are used.
(d) The working of the technique does not require complex computations.

(e) It can detect instability status early to aid the maintainance of synchronism.

The remaining sections of the paper are organized as follows: Section 2 explains the input parameter used while Section 3 describes the signal processing tool employed. In Section 4, the decision tool used is explained. Section 5 highlights the proposed technique. The study system used is described in Section 6. Results obtained and analysis done are captured in Section 7. Finally, conclusions drawn are elucidated in Section 8.

## 2. FREQUENCY DEVIATION AS INPUT PARAMETER

Like rotor angles, machine bus frequencies swing during disturbances [8,15]. For a system that becomes stable, although the bus frequencies of all machines may initially increase or decrease, they will ultimately settle at a synchronous value. The rates of change of the bus frequencies are all reduced. Conversely, for a system that becomes unstable, frequency of one or more machines will rise or decay with higher amplitudes [15].

*Figures 1* and *2* show plots of frequency deviations of the ten machines of the New England test system (described in section 6) obtained through dynamic simulation of a three-phase line fault between buses sixteen and twenty-one. The simulation was done by means of the Power System Simulator for Engineers (PSS®E) software [16]. In *fig. 1*, the fault duration was 100 ms and the system was stable.

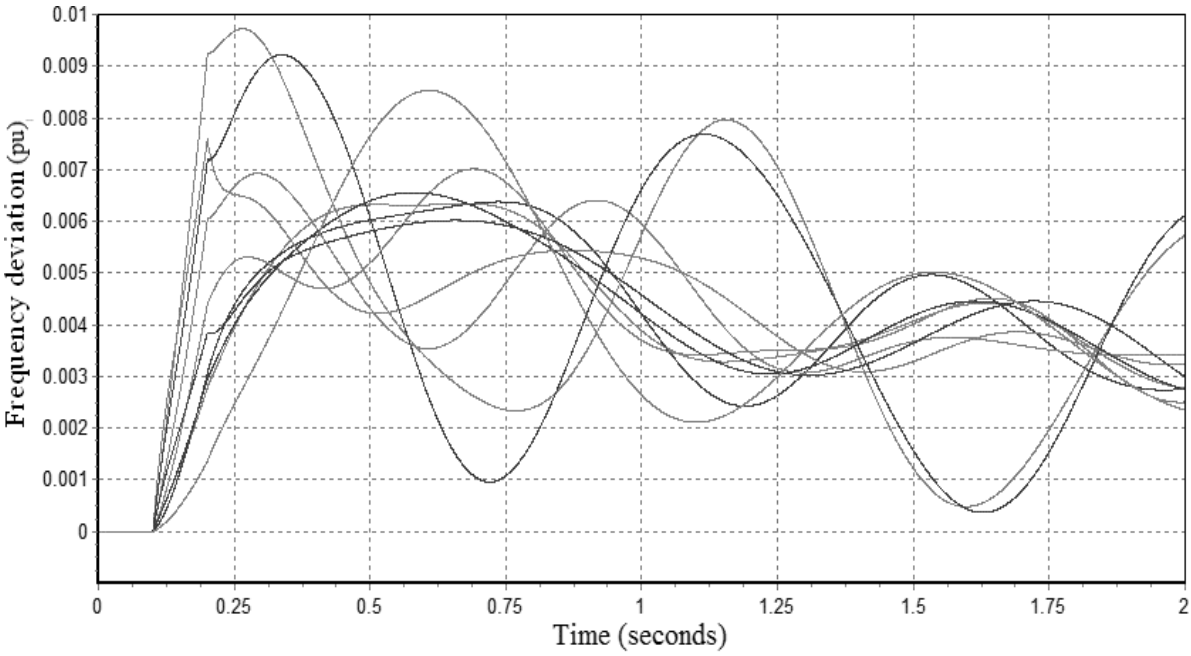


*Fig. 1. Frequency deviations for a stable system.*

On the other hand, when the fault duration was increased to 400 ms, the system became unstable as depictured in *fig. 2*. It is noted that in *fig. 1*, the bus frequencies initially increased

but later stabilized. On the other hand, the bus frequencies of some of the generators in *fig. 2* grew progressively. The clear variations in the curves in the two figures illustrate the possibility of using the trajectories of bus frequencies to predict TSS [15]. However, the success or otherwise depends on the effectiveness of the methodology used for data processing.

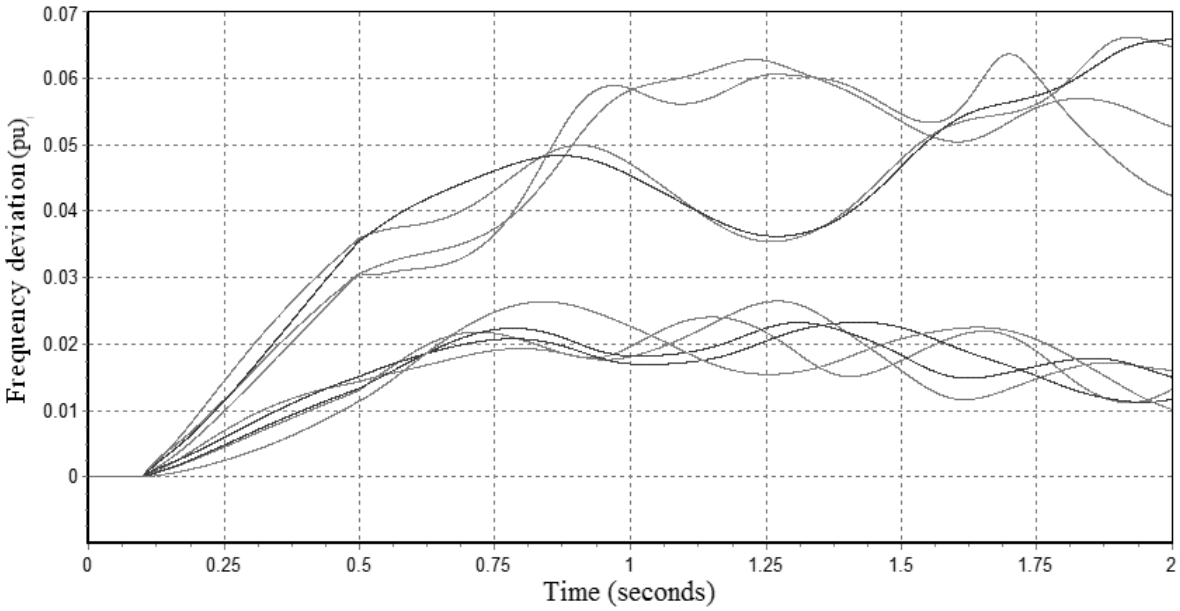


*Fig. 2. Frequency deviations for an unstable system.*

## 3. WAVELET TRANSFORM

Wavelet transform (WT) is a commonly used tool for analyzing localized variations of variables. It decomposes a time series into time–frequency space, allowing the realization of the pronounced modes of variability and how they vary in time. In power system studies, the widely used form of wavelet transform is discrete wavelet transform (DWT). This is so because the time series in power systems are discrete [17-19]. DWT is done using mother wavelets. Daubechies 4 and Daubechies 8 mother wavelets are commonly used to analyze transients in power systems [17, 18]. This work used Daubechies 8 wavelet. The choice was informed by the superiority of Daubechies 8 wavelet. Daubechies 8 wavelet has the following advantages over Daubechies 4 [18, 19]: (a) It closely matches a signal to be processed, which is of utmost importance in wavelet applications. (b) Daubechies 8 wavelet is more localized, that is, it is compactly supported in time and is better suited for short and fast transient analysis compared to Daubechies 4 wavelet. (c) It provides almost perfect reconstruction. (d) Daubechies 8 wavelet is found to be more suitable in representing transient signals because it is smoother and more oscillatory in nature which is also the nature of transient signals.

A *l*-level transformation of an input parameter like frequency deviations, $f(x)$, can be

done using (1) [17]:

$$f(x)=\sum_{k} a_{l+1,k}\varphi_{l+1,k}(x)+\sum_{l=0}^{l} d_{l+1,k}\psi_{l+1,k}(x) \tag{1}$$

where $l=0,1,2,...,N$, $\varphi(x)$, is a scaling function, and $\psi(x)$ is the mother wavelet.

Approximate coefficients, $a_{l+1,n}$, and detail coefficients, $d_{l+1,n}$ at scale $l+1$ can be obtained if coefficients at scale *l* are available using (2) and (3):

$$a_{l+1,n}=\sum a_{l,k}h(k-2n) \tag{2}$$

$$d_{l+1,n}=\sum a_{l,k}g(k-2n) \tag{3}$$

where *h* and *g* are seen as filter coefficients of half band low-pass and high-pass filters respectively.

Wavelet transformation of a variable gives rise to one approximate coefficient (this is constant) and two or more detail coefficients (this equals the levels decomposed). Valuable information is contained only in the detail coefficients. One such valuable information is the absolute peak value [17]. It is expected that, the absolute peak values of detail coefficients of machine terminal frequency deviations for stable swings will be much lower than those for unstable swings. This forms the basis of the proposed scheme.

## 4. MULTILAYER PERCEPTRON NEURAL NETWORK

Multilayer perceptron neural network (MLPNN) is a commonly used form of artificial neural networks which imitate the human brain. Other types of neural networks include radial basis function networks, Kohonen networks and recurrent networks [20]. Two commonly used neural networks are radial basis function neural network (RBFNN) and multilayer perceptron neural network (MLPNN) [20]. A comparative study of the performances of RBFNN and MLPNN in stability prediction shows that MLPNN performance better than RBFNN [21].

MLPNNs can extract meaning from intricate or vague data and detect complicated trends [22, 23]. MLPNNs are composed of highly interconnected processing elements named neurons. A neuron may or may not have a bias. A bias has a fixed input value of 1. The output, $O_j$, of a neuron, *j*, with a bias, can be mathematical expressed as [15]:

$$O_j = f_j\left[\sum_{n=1}^{N} x_n w_{nj} + w_{0j}\right] \quad n=1,2,3,...,N \tag{4}$$

where, $j$ is the neuron number, $x_n$ is input signal, $w_{nj}$ is connection weight between $x_n$ and neuron $j$, $w_{0j}$ is the bias weight, and $f_j$ is the activation (transfer) function of neuron $j$.

Linear (*purelin*), log-sigmoid (*logsig*), and hyperbolic tangent sigmoid (t*ansig*) are widely used neuron activation functions [24]. The values of connecting weights are determined in the training phase using a training algorithm. MLPNNs are generally trained using the Levenberg-Marquardt back-propagation algorithm. The MLPNN is optimized by varying the number of layers as well as the number of neurons in the hidden layer(s) through a trial and error approach.

The architecture of the MLPNN used, which is optimal, is shown in Fig. 3. It had two neurons in the input layer because the input data set has two distinct values. Also, one neuron was used in the output layer since only one state (that is stable or unstable) has to be determined. The hidden layer had three neurons. In Fig. 3, $s^1$ and $s^2$ are the required inputs (explained in section 5). The neurons in the input and output layers had *purelin* transfer functions while those in the hidden layer had *tansig* transfer functions. *Purelin* and tansig functions are expressed as (5) and (6) respectively,

$$f(x) = x \tag{5}$$

$$f(x) = \frac{e^{2x} - 1}{e^{2x} + 1} \tag{6}$$

Letting $y_n$ be the output of neuron $n$, the final output 'O' of the MLPNN is mathematically determined as follows:

$$y_1 = f\left(s^1 w_{11} + s^2 w_{21} + w_{01}\right) = s^1 w_{11} + s^2 w_{21} + w_{01} \tag{7}$$

$$y_2 = f\left(s^2 w_{22} + s^1 w_{12} + w_{02}\right) = s^2 w_{22} + s^1 w_{12} + w_{02} \tag{8}$$

$$y_3 = f\left(y_1 w_{13} + y_2 w_{23} + w_{03}\right) = \frac{e^{2(y_1 w_{13} + y_2 w_{23} + w_{03})} - 1}{e^{2(y_1 w_{13} + y_2 w_{23} + w_{03})} + 1} \tag{9}$$

$$y_4 = f\left(y_1 w_{14} + y_2 w_{24} + w_{04}\right) = \frac{e^{2(y_1 w_{14} + y_2 w_{24} + w_{04})} - 1}{e^{2(y_1 w_{14} + y_2 w_{24} + w_{04})} + 1} \tag{10}$$

$$y_5 = f\left(y_1 w_{15} + y_2 w_{25} + w_{05}\right) = \frac{e^{2(y_1 w_{15} + y_2 w_{25} + w_{05})} - 1}{e^{2(y_1 w_{15} + y_2 w_{25} + w_{05})} + 1} \tag{11}$$

$$O = y_6 = f\left(y_3 w_{36} + y_4 w_{46} + y_5 w_{56} + w_{06}\right) = \frac{e^{2\left(y_3 w_{36} + y_4 w_{46} + y_5 w_{56} + w_{06}\right)} - 1}{e^{2\left(y_3 w_{36} + y_4 w_{46} + y_5 w_{56} + w_{06}\right)} + 1} \tag{12}$$

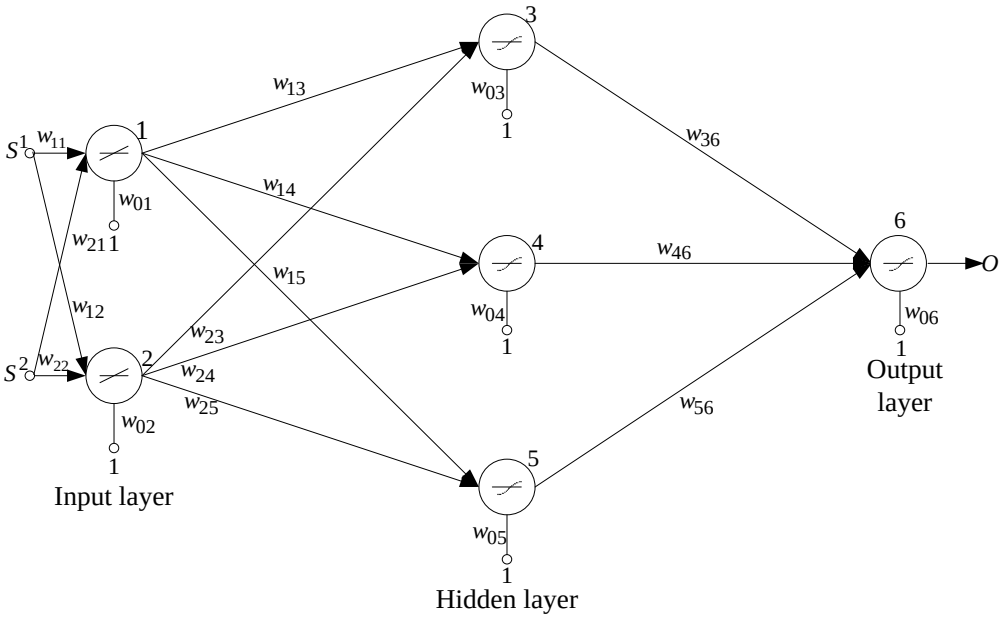


*Fig. 3. Architecture of used MLPNN*

## 5. PROPOSED METHOD

*Figure 4* depicts a flowchart of the method proposed. It is triggered when a line, bus, generator, or transformer is tripped. The method is outlined as follows:

1. Capture the first eight samples of each generator's bus frequency deviation at a rate of thirty-two samples each cycle and divide each eight samples equally into two sets $f_n^{\,1}$ and $f_n^{\,2}$ as follows:

$$f_n^{\,1} = \left\{ f_{1n}, f_{2n}, f_{3n}, f_{4n} \right\},\ n = 1, 2, 3, ..., N \tag{13}$$

$$f_n^{\,2} = \left\{ f_{5n}, f_{6n}, f_{7n}, f_{8n} \right\},\ n = 1, 2, 3, ..., N \tag{14}$$

where *N* is the number of system machines and superscripts 1 and 2 indicate first sample and second sample respectively.

2. Decompose each set ( $f_n^{\,1}$ and $f_n^{\,2}$ ) into one approximate coefficient (*a*) and two detail coefficients ($d_1$ and $d_2$) using the Daubechies 8 (db8) mother wavelet. The useful outputs of $f_n^{\,1}$ and $f_n^{\,2}$ after the transformation are mathematically represented as follows:

$$dwt\left(f_n^{\,1}\right)=\left\{d_{1n}^{\,1},d_{2n}^{\,1}\right\} \tag{15}$$

$$dwt\left(f_n^{\,2}\right)=\left\{d_{1n}^{\,2},d_{2n}^{\,2}\right\} \tag{16}$$

where $d_{1n}, d_{2n}$ are detail 1 and 2 coefficients respectively of machine *n*. It must be noted that each detail coefficient $d_{1n}$ or $d_{2n}$ is a set of numerical values.

3. Extract the absolute peak value of each detail coefficient:

$$d_{1n\ \max}^{\ 1}=\left|Max\left(d_{1n}^{\,1}\right)\right| \tag{17}$$

$$d_{2n\ \max}^{\ 1}=\left|Max\left(d_{2n}^{\,1}\right)\right| \tag{18}$$

$$d_{1n\ \max}^{\ 2}=\left|Max\left(d_{1n}^{\,2}\right)\right| \tag{19}$$

$$d_{2n\ \max}^{\ 2}=\left|Max\left(d_{2n}^{\,2}\right)\right| \tag{20}$$

4. Obtain the sum of absolute peaks of detail coefficients of each sample namely $D_n^{\,1}$ and $D_n^{\,2}$ $D_n^{\,1}$ and $D_n^{\,2}$ are given by:

$$D_n^{\,1}=d_{1n\ \max}^{\ 1}+d_{2n\ \max}^{\ 1} \tag{21}$$

$$D_n^{\,2}=d_{1n\ \max}^{\ 2}+d_{2n\ \max}^{\ 2} \tag{22}$$

5. Sum $D_n^{\,1}$ values of all generators and $D_n^{\,2}$ values of all generators separately to obtain two composite values, $S^1$ and $S^2$ respectively:

$$S^1=\sum_{n=1}^{N}D_n^{\,1} \tag{23}$$

$$S^2=\sum_{n=1}^{N}D_n^{\,2} \tag{24}$$

6. Feed $S^1$ and $S^2$ values as inputs to the trained MLPNN to predict the TSS.

The MLPNN was trained to output ‘0’ and ‘1’ for conditions leading to stability and instability respectively. The training was done using input-output data pairs.

MLPNNs like other networks rarely give outputs that are precisely ‘0’ or ‘1’. Consequently, in this method, (23) and (24) are utilized to achieve the desired output of ‘0’ or ‘1’.

$$O \geq 0.5 \quad \Rightarrow \quad O = 1 \tag{25}$$

$$O < 0.5 \quad \Rightarrow \quad O = 0 \tag{26}$$

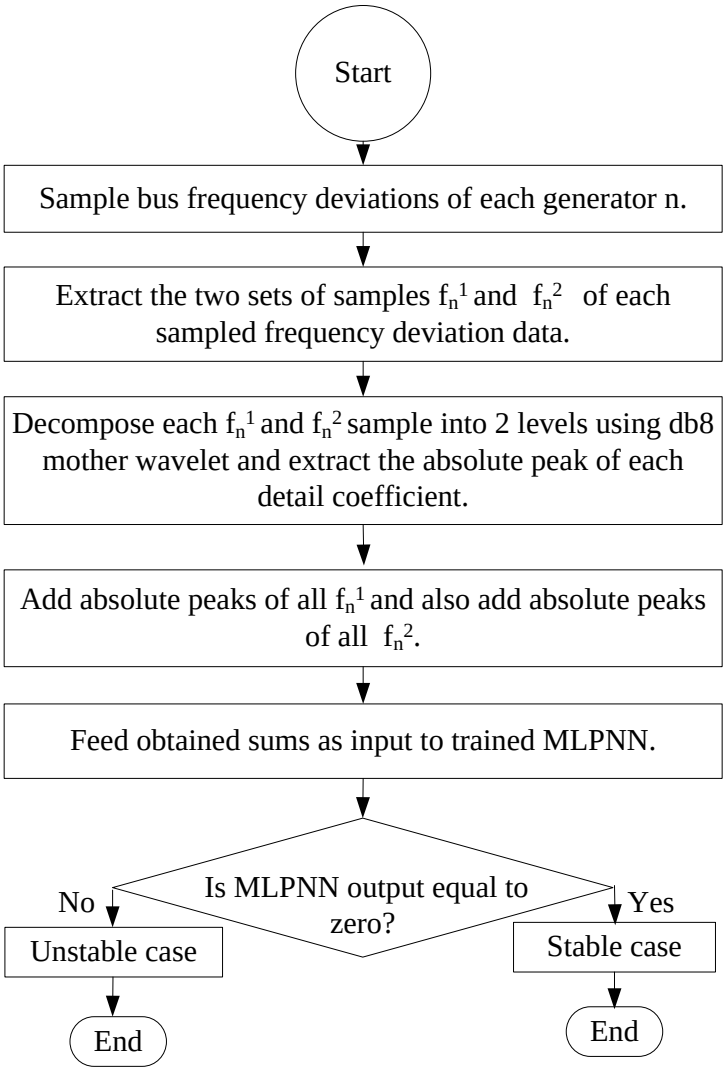


*Fig. 4. Flowchart of method*

The performance of the proposed technique was evaluated using a mean absolute percentage error (MAPE) index. The index is given as follows:

$$MAPE = \frac{1}{N} \sum_{k=1}^{N} |T(k) - O(k)| \times 100 \tag{27}$$

where $T(k)$ is the target value of the MLPNN for test case number *k*, $O(k)$ is the obtained output of the MLPNN and N is the total number of test cases.

## 6. STUDY SYSTEM

Testing of the method was done using the New England test system (also known as IEEE 39-bus system). It is a standard test system universally used for steady state and transient stability studies [4,10,11]. It is shown as *fig. 5*. It comprises ten generators, with one (G1) representing a large system.

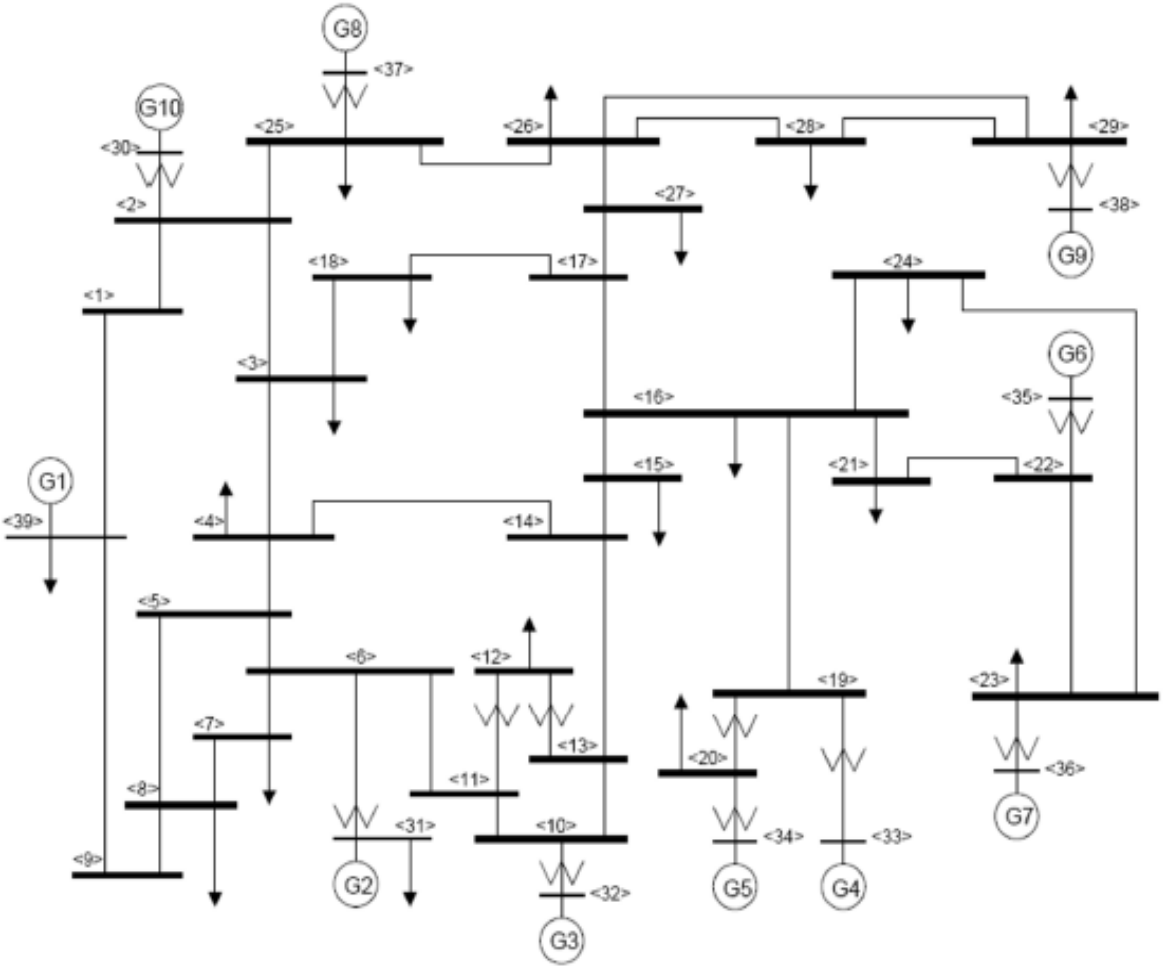


*Fig. 5. IEEE 39-bus test system*

Simulations of the study system was done using the PSS®E software. A comprehensive model capturing the dynamics of prime mover and excitation system was employed. Numerous fault conditions were simulated by changing fault location, fault duration, system loading, network topology and generator availability. In all, one hundred and sixty faults were simulated. The simulations were done such that stability was maintained for fifty percent of the cases while

transient instability occurred for fifty percent of the cases. This was achieved by varying the fault duration. Frequency deviation data was obtained from the simulations for the development and testing of the proposed scheme. The percentages of data used for training and testing are 5% and 95% respectively.

## 7. RESULTS AND ANALYSIS

*Figure 6* shows the architecture of the MLPNN after training. Results for two test cases (one stable case and one unstable case) are presented to demonstrate the scheme's operation. The fault for both cases is a three-phase line fault between bus sixteen and bus twenty-one at base load. Waveforms for this condition have been shown in *figures 1* and *2*. The fault duration for which stability was maintained was 100 *ms* whiles that for which stability was lost was 400 *ms*. The inputs $S^1$ and $S^2$ to the MLPNN are obtained as shown in Table 1 using (21), (22), (23) and (24).

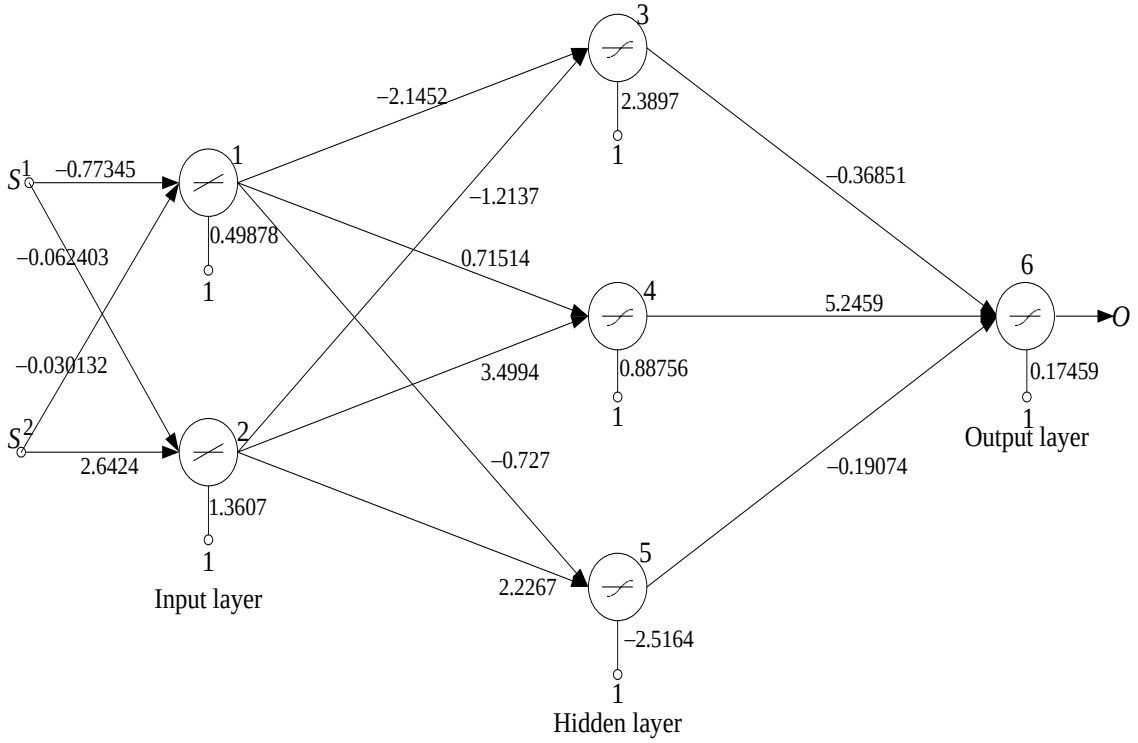


*Fig. 6. Architecture of trained MLPNN.*

Table 1. Sum of absolute peak values of detail coefficients

| Machine no. | Stable | | Unstable | |
|---|---|---|---|---|
| | $D_n^1 \times 10^{-3}$ | $D_n^2 \times 10^{-3}$ | $D_n^1 \times 10^{-3}$ | $D_n^2 \times 10^{-3}$ |
| 1 | 0.02017 | 0.00630 | 0.03639 | 0.03633 |

| Machine no. | Stable | | Unstable | |
|---|---|---|---|---|
| | $D_n^1 \times 10^{-3}$ | $D_n^2 \times 10^{-3}$ | $D_n^1 \times 10^{-3}$ | $D_n^2 \times 10^{-3}$ |
| 2 | 0.03098 | 0.02607 | 0.07401 | 0.07335 |
| 3 | 0.04181 | 0.03947 | 0.03945 | 0.03935 |
| 4 | 0.04243 | 0.02744 | 0.03130 | 0.03055 |
| 5 | 0.05960 | 0.07440 | 0.06423 | 0.04372 |
| 6 | 0.04490 | 0.00764 | 0.03245 | 0.03348 |
| 7 | 0.05897 | 0.00176 | 0.03508 | 0.03402 |
| 8 | 0.04542 | 0.00145 | 0.05325 | 0.05514 |
| 9 | 0.03219 | 0.02529 | 0.04886 | 0.04880 |
| 10 | 0.01669 | 0.01706 | 0.09134 | 0.08944 |
| | $S^1 = 0.39316 \cdot 10^{-3}$ | $S^2 = 0.22688 \cdot 10^{-3}$ | $S^1 = 0.50636 \cdot 10^{-3}$ | $S^2 = 0.48418 \cdot 10^{-3}$ |

Applying the above inputs to the MLPNN using (7)-(12), (25) and (26) yields the following results:

*Stable case*:

$O(s^1 = 0.39316 \times 10^{-3}, s^2 = 0.22688 \times 10^{-3}) = 0$, implying transient stable.

*Unstable case*:

$O(s^1 = 0.50636 \times 10^{-3}, s^2 = 0.48418 \times 10^{-3}) = 1$, implying transient unstable.

A summary of results for other fault cases are shown in Table 2. Overall, the method accurately predicted the TSS of 143 out of the 152 test cases. The MAPE, after testing, was 5.9%, which is low. The prediction accuracy of the scheme is thus 94.1%.

Table 2. Test results for some fault cases

| Fault | Stable | | | Unstable | | |
|---|---|---|---|---|---|---|
| | $s^1$ | $s^2$ | $O$ | $s^1$ | $s^2$ | $O$ |
| Bus11 | 0.2828 | 0.1047 | 0 | 1.0194 | 1.0007 | 1 |
| Bus14 | 0.2646 | 0.1048 | 0 | 0.9741 | 0.9356 | 1 |
| Bus28 | 0.1283 | 0.1297 | 0 | 0.4809 | 0.4800 | 1 |
| Bus11-Bus12 | 0.2634 | 0.1664 | 0 | 0.6569 | 0.6493 | 1 |
| Bus13-Bus14 | 0.2634 | 0.1664 | 0 | 0.4954 | 0.4736 | 1 |
| Bus16-Bus21 | 0.39316 | 0.22688 | 0 | 0.50636 | 0.48418 | 1 |

The MLPNN produced these results having been trained with only 5% of total simulation data. This percentage of training data set is extremely low compared with the 85% training data set used in [25]. The low percentage of training data set was realised because the used input data and the data processing approach employed, resulted in the processed data for transient stable cases being distinct from processed data relating to transient unstable cases.

Such distinctiveness of processed data makes is easy for the decision tool used (MLPNN) to distinguish between conditions that will lead to transient instabilty and those for which a system will remain stable. On the contrary, the use of large volumes of training data, such as was the case in [25], depict a difficulty of the decision tool to make out differences in data sets for stable and unstable conditions. The advantage of realisng a low volume of training data set in a technique is that, it becomes easy to deploy such a scheme in large real world systems.

The proposed technique uses only one data variable (or component feature), which is generator frequency deviation. The data set required for processing and final decision making is also minimal. These avoid potential processing delays associated with large data variables and datasets. The lower the volume of data to be processed, the faster the processing. Furthermore, the approach to data processing and final decision is simple and will not present any computational delays. Consequently, the proposed technique will offer a quick response to provide system operators or emergency control softwares ample time to deploy the needed control measures.

Frequency deviation data can be captured by phasor measurement units which have seen increasing deployment in power systems, in recent times. Phasor measurement units are capable of capturing frequency data in real-time. Aided by phasor data concentrators (PDCs) and super phasor data concentrators (super PDCs), which are all integral parts of Wide Area Monitoring Systems (WAMS), frequency deviation data from generator buses can be collected at a control center for processing by the proposed technique, for utilization by system operators and the activation of emergency control softwares.

## 8. CONCLUSION

A method for predicting TSS has been presented. It employs bus frequency deviations as input data, wavelet analysis for signal processing and MLPNN for final decision making. The input data can be obtained from phasor measurement units (PMUs) which have seen active deployment in power systems. A low volume of input data, captured in a short time window, is required. Minimal training data is needed to train the decision tool. This will allow for easy application in large real-world systems. The method does not use any predetermined templates or stability boundaries that could adversely affect its application in real world systems. It can be easily implemented on-line aided by phasor measurement units capable of capturing real-time frequency data and transmitting them to a centralized point. The analytical and decision-making tools employed are also simple, reliable, and easy to implement. Also, the short time window (1/4 of a cycle) of input data capture will make the scheme respond speedily.

Consequently, systems operators will have ample notice to deploy the needed emergency control measures. The simulation results indicate that the proposed method has high accuracy.

## *REFERENCES*


[1] K.N. Al-Tallaq and E.A. Feilat, *Online Detection of Out-of-Step Operation Based on Prony Analysis-Impedance Relaying,* Proceedings of 5th WSEAS International Conference on Power Systems and Electromagnetic Compatibility, pp. 55-60, 2005.

[2] E.A. Frimpong, J. Asumadu and P.Y. Okyere, *Neural Network and Speed Deviation based Generator Out-of-Step Prediction Scheme*, Journal of Electrical Engineering, vol. 15, no. 2, pp. 1-8, 2015.

[3] P.A. Trodden, W. A. Bukhsh, A. Grothey and K.I.M. McKinnon. *MILP Islanding of Power Networks by Bus Splitting*, IEEE Power and Energy Society General Meeting, 2012.

[4] N. Amjady and S. F. Majedi. *Transient Stability Prediction by a Hybrid Intelligent System*, IEEE Transaction on Power Systems, vol. 22, no. 3, pp. 1275 -1283, 2007.

[5] H.E. Brown, H.H. Happ, C.E. Person and, C.C. Young. *Transient stability solution by an impedance matrix method*, IEEE Transactions on Power Apparatus and Systems, vol. 84, no. 12, pp. 1204-1214, 2009.

[6] H.-Z. Guo, H. Xie, B.-H. Zhang, G.-L Yu, P. Li, Z.-Q Bo and A. Klimek. *Study on Power System Transient Instability Detection Based on Wide Area Measurement System*, European Transactions on Electrical Power, vol. 20, pp. 84–205, 2010.

[7] E.A. Frimpong, J. Asumadu, and P.Y. Okyere. *Speed Deviation and Multilayer Perceptron Neural Network Based Transient Stability Status Prediction Scheme*, Journal of Electrical Engineering, vol. 15, no. 2, pp. 9-16, 2015.

[8] J. Hazra, R. K. Reddi, K. Das, D. P. Seetharam and A. K. Sinha. *Power Grid Transient Stability Prediction using Wide Area Synchrophasor Measurements*, Proceeding of 3rd IEEE PES Innovative Smart Grid Technologies Europe (ISGT Europe), Berlin, China, pp. 1-8, 2012.

[9] T. Guo, and J. V. Milanović: On-line Prediction of Transient Stability Using Decision Tree Method — Sensitivity of Accuracy of Prediction to Different Uncertainties, Proceedings of the IEEE Grenoble PowerTech, Grenoble, 2013.

[10] A. D. Rajapakse, F. Gomez, O. M. K. K. Nanayakkara, P. A. Crossley and V. V. Terzija: Rotor angle stability prediction using post-disturbance voltage trajectory patterns, IEEE Transactions on Power Systems, vol. 25, no. 2, pp. 945-956, 2010.

[11] F. Gomez, Rajapakse A., U. Annakkage and I. Fernando. *Support Vector Machine-Based Algorithm for Post-Fault Transient Stability Status Prediction Using Synchronized Measurements*, IEEE Transactions on Power Systems, vol. 26, no. 3, pp. 1474-1483, 2011.

[12] D. R. Gurusinghe, and A. D. Rajapakse. *Post-Disturbance Transient Stability Status Prediction Using Synchrophasor Measurements*, IEEE Transactions on Power Systems, vol. 31, no. 5, pp. 3656-3664, 2016.

[13] E.A. Frimpong, P.Y. Okyere and E.K. Anto. *Adaptive Single-Pole Autoreclosure Scheme Based on Wavelet Transform and Multilayer Perceptron*, Journal of Science and Technology, vol. 30,

no. 1, pp. 102-110, 2010.

[14] E.A. Frimpong, P.Y. Okyere and E.K. Anto. *Adaptive Single-Pole Autoreclosure Scheme Based on Standard Deviation and Wave Energy*, Journal of Electrical Engineering, vol. 9, no. 4, pp. 61-68, 2009.

[15] E.A. Frimpong, P.Y. Okyere and J.A. Asumadu. *On-line Determination of Transient Stability Status Using Multilayer Perceptron Neural Network, Journal of Electrical Engineering*, vol. 69, no. 1, pp. 1-7, 2018.

[16] Power System Simulator for Engineers, PSS®E University Edition, 2016.

[17] M. Uyar, S. Yildirim. and M.T. Gencoglu. *An Effective Wavelet-Based Feature Extraction Method for Classification of Power Quality Disturbance Signals*, Electric Power Systems Research, vol. 78, pp. 1747–1755, 2008.

[18] S. Pittner and S. V. Kamarthi. *Feature Extraction from Wavelet Coefficients for Pattern Recognition Tasks,* IEEE Transactions on Pattern Analysis and Machine Intelligence, vol. 21, no. 1, pp. 83-88, 1999.

[19] D. Chanda, N.K. Kishore and A.K. Sinha. *Application of Wavelet Multiresolution Analysis for Classification of Faults on Transmission lines*, Proceedings of IEEE Conference on Convergent Technologies for the Asia-Pacific Region, pp. 1464-1469, 2003.

[20] K. J. McGarry, S. Wermter, and J. MacIntyre. Knowledge Extraction from Radial Basis Function Networks and Multi-layer Perceptrons. Proceedings of International Joint Conference on Neural Networks, Washington D.C., pp. 1-4, 1999.

[21] E.A. Frimpong, J. Asumadu, and P.Y. Okyere. *Real-Time Transient Stability Status Prediction Scheme and Comparative Analysis of the Performance of SVM, MLPNN and RBFNN*, Carpathian Journal of Electrical Engineering, vol. 12, no. 1, pp. 22-38, 2018.

[22] A.D. Angel, M. Glavic, and L. Wehenkel. *Using Artificial Neural Networks to Estimate Rotor Angles and Speeds from Phasor Measurements*. Neurocomputing, vol. 70, no. 16-18, pp. 2668-2678, 2007.

[23] A.N. Fathian and M.R. Gholamian. *Using MLP and RBF Neural Networks to Improve the Prediction of Exchange Rate Time Series with ARIMA*, International Journal of Information and Electronics Engineering, vol. 2, no. 4, pp. 543-546, 2012.

[24] M.H. Beale, M.T. Hagan and H.B. Demuth. *Neural Network Toolbox™*, User Guide, MATLAB, R2016b, pp. 3-4 – 3-5, 2016.

[25] Z. Shi, W. Yao⋆, L. Zeng, J. Wen, J. Fang, X. Ai and J. Wen. *Convolutional neural network-based power system transient stability assessment and instability mode prediction*, Applied Energy vol. 263, pp. 1-13, 2020.

# TRACTION MOTOR SELECTION BASED ON THE PERFORMANCE ANALYSIS OF PURE ELECTRIC VEHICLE UNDER DIFFERENT DRIVING SCENARIOS

Khaled **ATAMNIA**, Abdesselam **LEBAROUD,** Messaoud **MAKHLOUF**
*National Polytechnic School of Constantine, Algeria (ENPC),*
*Department of Electronics, Electrical engineering and Automatic Control*
*Laboratory of Polytechnic Engineering of Constantine*
*khaled.atamnia@enp-constantine.dz*

**Keywords: Electric vehicle, Driving Cycle, PMSM, Induction Motor.**

**Abstract:** *Selecting the appropriate powertrain components for electric vehicles, in terms of size and efficiency became a challenging task, especially the traction motor that requires special care. Since it is the only source of traction power, its selection may affect the performance of the electric vehicle. Therefore, an analysis of the vehicle performance with various motors types and design is necessary to outline its importance and to verify the impact of its selection on the entire vehicle system. The Permanent Magnet Synchronous Motor (PMSM) and the Induction Motor (IM) were tested during different driving cycles using the ADVISOR tool, designed based on Matlab/Simulink, for rapid analysis of the performance and fuel consumption of conventional hybrid and electric vehicles. The 2WD GM EV1 model from General Motors Company has been selected to investigate the electric vehicle performance during different driving scenarios, such as dealing with high aggressive acceleration, or several stops and start situations*.

## 1. INTRODUCTION

The electric vehicle is the result of combining several engineering fields such as electrical, mechanical, automation, chemical, and electronics. The major components of this technology are the storage system, power electronics converters, the electric motor and its controller, and the transmission system. These parts connect to form the electric vehicle powertrain where the electric motor represents its heart, since it is the only source of traction that delivers torque to the wheel. The vehicle performance determined by the Torque-Speed or

Power-Speed characteristic of the traction motor [1]. While designing an electric vehicle, the first and foremost component to be selected is an electric motor [2] that has some specific characteristics which required for traction purpose. The desired options of an electric motor drive for traction application (electric and hybrid vehicles) are high torque at the low speed region for fast acceleration, hill climbing and obstacle negotiation, and low torque at high speed for cruising. Also, the electric motor drive is required to have a long constant power range to meet the torque and speed demand [3]. We cannot compare the traction motor to drives used in industrial plants or manufacturing processes because an EV motor drive needs to face different circumstances such as frequent start/stop, or operating under many environmental conditions [4]. The electric motor drive must have high torque generating capacity and high acceleration.

As the vehicle needs to run on any terrain and in harsh environments, it must have a high torque when operating at slow speeds with high efficiency as well [4]. The process of selecting the appropriate electric propulsion systems should be performed at the system level [5]. Different types of motor exhibit many characteristics which makes it necessary to evaluate motors under different driving cycles to choose a particular motor type for EVs. It should have some features such as simple design, high specific power, and low maintenance cost [6]. However, the selection of traction motors for the EV propulsion systems is an important step that requires special attention. The automotive industry is still seeking the most appropriate electric propulsion system [7].

In literature, the selection of the motor started from the comparison between electric traction motors regarding certain factors like the energy efficiency, power to weight ratio, Torque-Speed characteristics, the maturity of the technology, reliability and the cost for both motor and controller [4][6][8]. Others made the selection based on several factors related to the driver expectation, power source, and the vehicle constraints [7]. In this paper, a comparison between AC induction motor (IM) and Permanent Magnet Synchronous Motor (PMSM) has been made based on the Torque-Speed characteristic, effect on battery SOC (State Of Charge), the overall system performance, and motor/controller efficiency for generating and motoring mode. Acceleration and grade-ability tests considered as well.

For the sake of this paper, ADVISOR (ADvanced VehIcle SimulatOR) tool as an open and free simulation tool developed by NREL (National Renewable Energy Laboratory) for vehicle design used to make this comparison done. ADVISOR tests the impact of variations in electric components or other changes that might affect the vehicle performance parameters. By selecting components types and sizes the user can alter simulation results. It is flexible enough to model specific components and vehicle performance configurations for the needs of users [9].

## 2. VEHICLE DYNAMIC MODEL

In this paper, the GM EV1 model has been selected from ADVISOR vehicle configuration menu to study the vehicle performance with different motor characteristics and types. In this study, we only focused on the longitudinal model, and a simplifying hypothesis developed when we did not consider the displacement on the transversal, vertical direction, rotation, rolling and pitching.

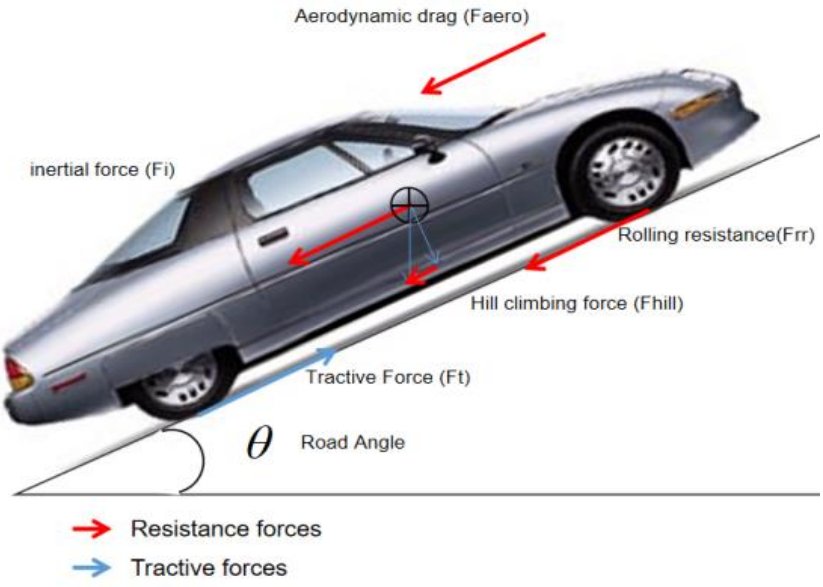


*Fig. 1. Electric vehicle longitudinal model*

### 2.1. Rolling resistance Force

Rolling resistance is the force that resists vehicle movement on a surface. It is approximately constant and it barely depends on vehicle speed.

$$F_{rr} = C_{rr} mg \cos(\theta) \tag{1}$$

In (1), $C_{rr}$ is the rolling resistance coefficient, its typical value being from 0.015 down to 0.005 for electric vehicle tires [13], $g$ is acceleration of gravity and $m$ is vehicle weight.

### 2.2. Aerodynamic drag

Aerodynamic drag caused by the friction of the vehicle body moving through the air, we can notice from the equation (2) that force $F_{aero}$ is a function of vehicle shape and size

defined by drag coefficient and weight respectively. Drag coefficient $C_d$ typical value is between 0.25 and 0.3, but some electric vehicle designs have achieved values as low as 0.19 [13] like GM EV1.The later is directly affected by the shape of the vehicle.

$$F_{aero} = \frac{1}{2}\rho A C_d v^2 \tag{2}$$

where $\rho$ is density of the air and 1.25 kg/m$^3$ is a reasonable value to use in most cases [13], $A$ is the frontal area, $v$ is the vehicle velocity.

### 2.3. Grade or hill climbing force

Grade force $F_{hill}$ or hill climbing, sometimes called gravitational force is required force to drive a vehicle uphill, and it is proportional to vehicle mass and grade angle.

$$F_{hill} = mg\sin(\theta) \tag{3}$$

### 2.4. Inertial force

If the velocity of the vehicle $v$ is changing, then clearly a force $F_i$ will need to be applied in addition to previous force. This force will provide the *linear and angular acceleration* of the vehicle, and is given by well-known equation derived by Newton's second law [11]. The angular acceleration force $F_{wa}$ will be slightly smaller than the linear acceleration force $F_{la}$, in this case the $F_{wa}$ will be ignored, and the vehicle mass will be increased by 5% as a reasonable approximation [11].

$$F_{la} = ma \tag{4}$$

$$F_{wa} = I\frac{G^2}{\eta_g r^2}a \tag{5}$$

where $I$ is moment of inertia, $G$ *is* gear ratio, $r$ is wheel radius and $\eta_g$ is gear system efficiency.

$$F_i = F_{la} + F_{wa} = m_i a \tag{6}$$

where $m_i$ is the vehicle inertial mass, and $m_i = m{\cdot}1.05$.

### 2.5. Tractive effort

Is a total traction force, or a summation of all the previous resistive forces (inertial force ($F_i$), hill climbing force ($F_{hill}$), aerodynamic drag ($F_{aero}$) and rolling resistance force ($F_{rr}$) needed to move a vehicle forward or backward.

$$F_t = F_i + F_{hill} + F_{aero} + F_{rr} \tag{7}$$

## 3. ADVISOR AS A VEHICLE PERFORMANCE ANALYSIS TOOL

ADVISOR has been developed by the National Renewable Energy Laboratory for the US DOE. It is a tool that can be used to evaluate and quantify the vehicle level impacts of advanced technologies applied to vehicles. It is written in the Matlab/Simulink environment (see *figure 3*) and is freely distributed on the Internet [11].

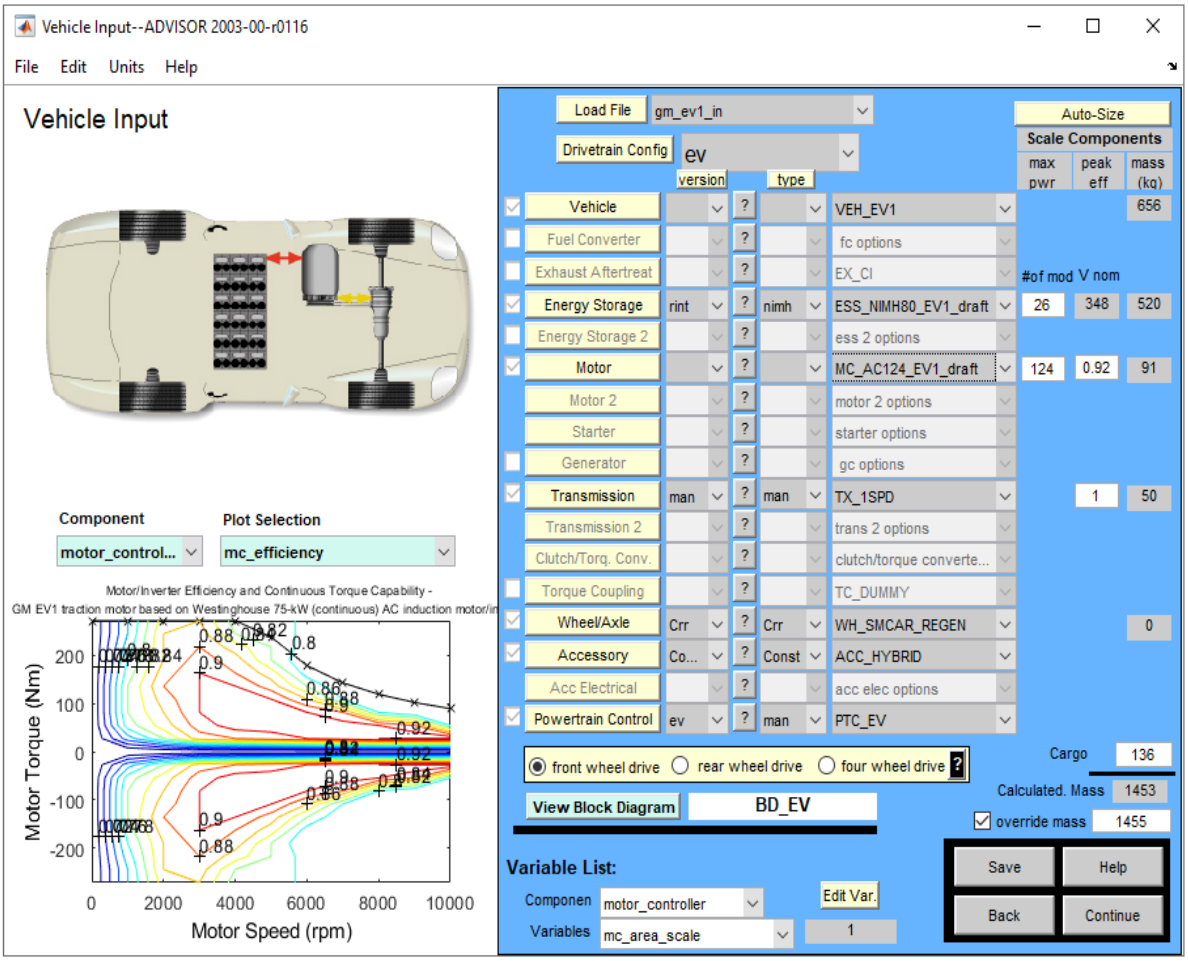


*Fig. 2. ADVISOR main interface*

It provides the vehicle engineering community with an easy to use, flexible, yet robust and supported analysis package for advanced vehicle modelling [11]. We can see from the *figure 2* that shows the flexibility of this tool when the user can build a vehicle of interest by selecting its configuration (electric, hybrid, or conventional), and drive-line components from pull-down menus. It primarily used to quantify the fuel economy, the performance, and the emissions of vehicles that use alternative technologies including fuel cells, batteries, electric motors, and internal combustion engines in hybrid (i.e. multiple power sources) configurations [11]. ADVISOR supports backward facing and forward facing approaches for vehicle simulation. For the first approach it takes the required/desired speed as an input, it determines what drive-train torque, speed, and power would be to meet that vehicle speed. On the other hand, the forward facing approach includes a model of the driver who senses the required speed, and responds with accelerator and brake position to which the drive responds with torque. This type of simulation is well suited to the design of control systems and implementation [12]. The models in ADVISOR are mostly empirical relying on drive-train components. Input/output relationships measured in the laboratory, and quasi-static using data collected in steady-state (for example the constant torque and speed) tests and correcting them for transient effects such as the rotational inertia of drive-train components [12].

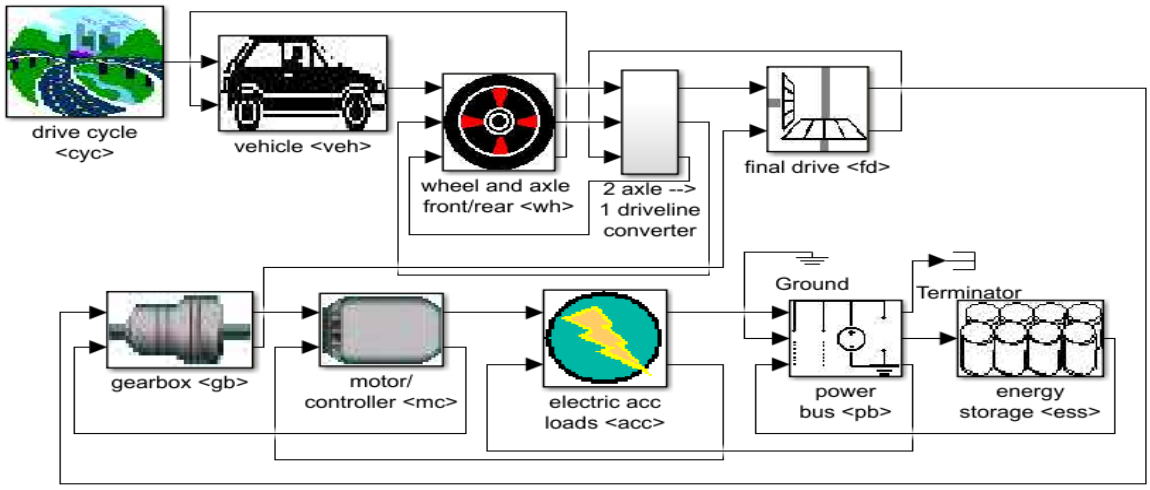


*Fig. 3. Simulink block diagram of ADVISOR for 2WD-Electric vehicle model*

The Limitation of this tool is developed as an analysis tool not originally intended as a detailed design tool. Its component models are quasi-static, and cannot be used to predict phenomena with a time scale of less than a tenth of a second or so. Physical vibrations, electric field oscillations and other dynamics cannot be represented using ADVISOR. However, linkages with other tools such as Saber, Simplorer, and Sinda/Fluent allow a detailed study of these transients in these tools with the vehicle level impacts linked back into ADVISOR [12]. ADVISOR used by researchers at NREL, industry, government, and academia to understand the effect of various technologies on the performance, fuel economy and

emissions of a vehicle. Typical applications include requirements definition, system optimisation, and energy usage assessments [11].

## 4. RESULTS AND DISCUSSIONS

### 4.1. PM/controller and IM/Controller Operating points for motoring and generating modes

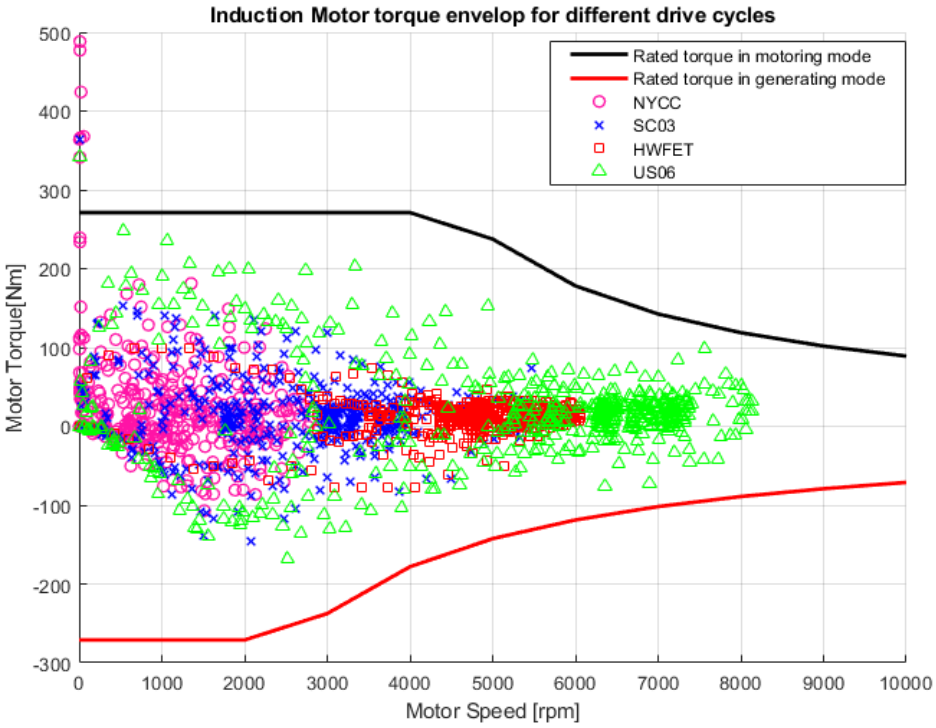


*Fig. 4. Torque-speed envelope for IM during many driving scenarios, and scatter plot of motor operating points*

*Figure 4* and *figure 5* show the envelope of rated torque during motoring and generating modes. They refer to the operating points of PM and IM for different driving cycles. We see from figures that coloured dots in case of IM are entirely within this envelope, and this is a good sign for this motor design (This motor has used by GM EV1 is based on AC75 that has been modified by 'Tony Markel' to better represent the motor in GM EV1). But it is not the case for PM (refer to Appendix for more details) where some operating points are outside of the torque-speed envelope, especially for US06 drive cycle that simulates an aggressive driving behaviour. The high density of points in low torque region or constant power region tells us that this motor is considerably operating in this region during US06 and HWFET drive cycle. The same thing for high dots density in low power region or high torque region during NYCC and SC03. Also, we can notice that the spread of these dots is directly related to the way of driving, or where we intend to drive this car.

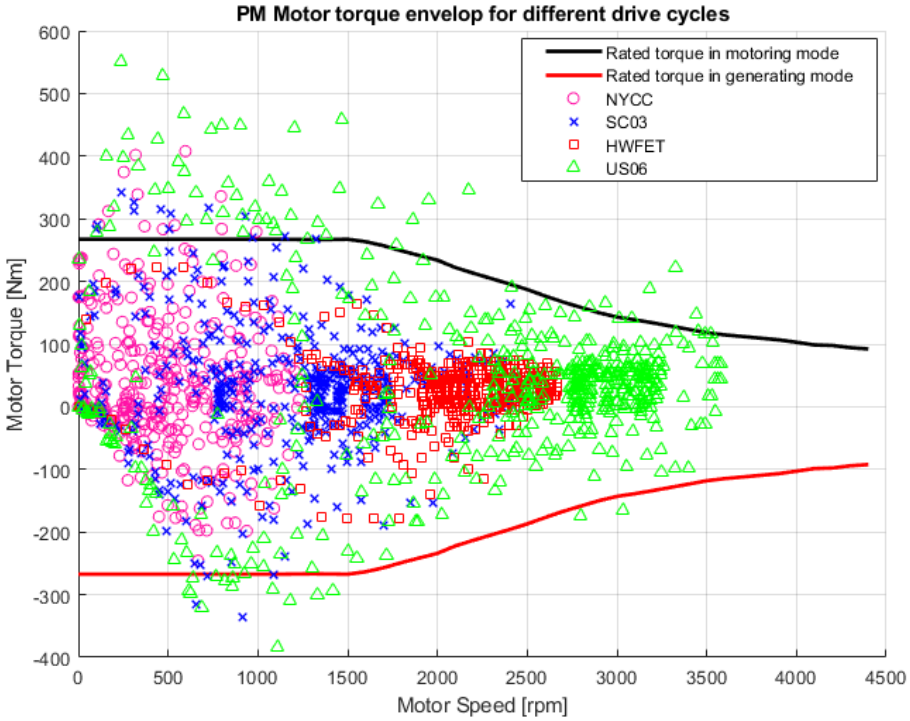


*Fig. 5. Torque-speed envelope for PMSM during many driving scenarios, and scatter plot of motor operating points*

For high speed and high acceleration driving styles like HWFET and US06, the motor needs to rotate at high RPM (from 4000 to 8000 rpm in case of IM and from 2000 to 3500 rpm in case of PM ) to respond to driver demand. It differs from the low-speed driving style like driving a car within a city (NYCC) where the stop-and-go behaviour is needed. We can see also that the regenerative braking system is operating well at the low-speed region from 500 rpm to the base speed for PM, and from 1000 rpm to the base speed as well for IM. We can make a great decision from this kind of information like resize the motor to be larger or smaller to meet the drive cycle that we need. As a result, motor design and selection for electric vehicle application has a strong relationship with the driving styles.

### 4.2. Vehicle grade-ability and acceleration tests

Vehicle performance usually includes acceleration performance evaluated by the time used to accelerate the vehicle from zero speed to a given speed (starting acceleration), or from a low-speed to a given high speed (passing ability). The grade-ability evaluated by the maximum road grade that the vehicle can overcome at a given speed and the maximum speed that the vehicle can reach [1]. The acceleration performance of the vehicle still almost depend on the speed-torque characteristic of the traction motor [3].

In this section, two performance tests have been done for different motor types (PM, IM) to estimate the vehicle performance as showed in Table 1.

Table 1: Acceleration and grade-ability test results for PM and IM

| Acceleration and grade test | PM | IM |
|---|---|---|
| Time in (s) for 0-26.82 m/s | 8.5 | 7.6 |
| Time in (s) for 17.88- 26.82 m/s | 3.5 | 3.5 |
| Time in (s) for 0-37 m/s | 15.8 | 14.6 |
| Maximum acceleration ($m/s^2$) | 4.96 | 4.69 |
| Distance in 5 s (m) | 46.42 | 57.06 |
| Time in (s) for 402.336 m | 16.7 | 16 |
| Vehicle Maximum speed (m/s) | 43.54 | 43.50 |
| Grade ability test (%) | 11.5 | 24.8 |

The first one is the acceleration and maximum speed test. The objective is to measure the vehicle acceleration from 0-26.82 m/s, 17.88-26.82 m/s and 0-37 m/s, and to determine the maximum acceleration and speed which the vehicle can achieve. Also, it included the maximum distance achieved by the car in five seconds.

The second one is the grade-ability test when we measure the high grade that the vehicle can overcome for both motor types, and investigate the effects of motor selection on vehicle performance. We can note from Table 1 the induction motor shows a good performance especially the covered distance in 5s. Another parameter that makes IM the best choice for the tough road is the grade-ability. The test shows a big difference between PM and IM in this area when the IM reaches 24.8% of grade-ability rather than 11.4 % for PM, and this happened because the long constant power region of IM compared to PM that enhanced the vehicle grade-ability.

### 4.3. Motor/controller efficiency comparison under different driving behaviour

Electric motors utilized in the electric vehicle can be used as a generator for capturing braking energy to be stored in the battery. Their effectiveness varies according to their design and type as well as the way of driving a car. For that reason, many tests for different driving scenarios have conducted to investigate the efficiency of IM and PM motors for both modes (motoring and generating). As we can see from Table 2 that the PM motor showed to be a right candidate for the electric vehicle when it kept the efficiency in the range of 84-88% for motoring mode, and from 82-88% for generation mode. This supposed to extend the vehicle range. The same thing happened to IM except for NYCC (simulate low-speed urban drive with many stops) drive cycle when the motor suffers from low efficiency due to stop/go driving cycle.

Table 2. Motor/controller efficiency during several drive cycles as motor and generator

| | PM | | IM | |
|---|---|---|---|---|
| | Motor | Generator | Motor | Generator |
| HWFET | 0.86 | 0.87 | 0.81 | 0.86 |
| NYCC | 0.84 | 0.82 | 0.69 | 0.75 |
| SC03 | 0.88 | 0.86 | 0.84 | 0.82 |
| US06 | 0.88 | 0.88 | 0.88 | 0.86 |

### 4.4. Motor power loss during different driving styles

Comparing motors power loss during all the above drive cycles was necessary to understand the electric motor behaviour for each case. As we can see from the *Figure 6* the performance of the electric motors varied according to the driving style. At high-speed (HWFET, US06). The IM consume less energy than PM unlike the low-speed (NYCC, SC03) where the IM motor performs worse. Generally, the average PM power loss is less than the losses produced by the IM even at high-speed.

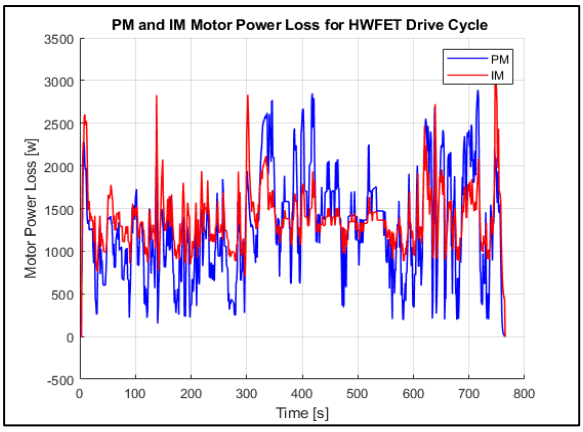


(a) HWFET

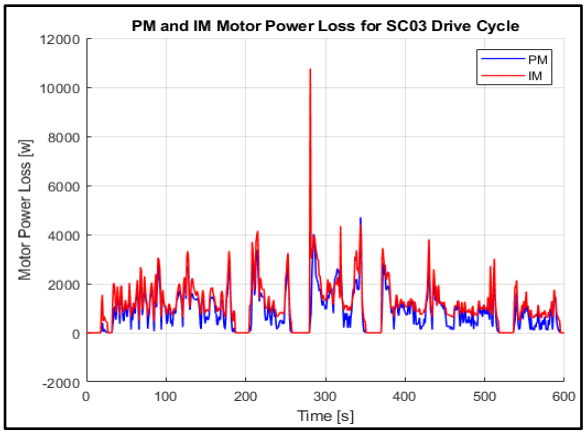


(b) SC03

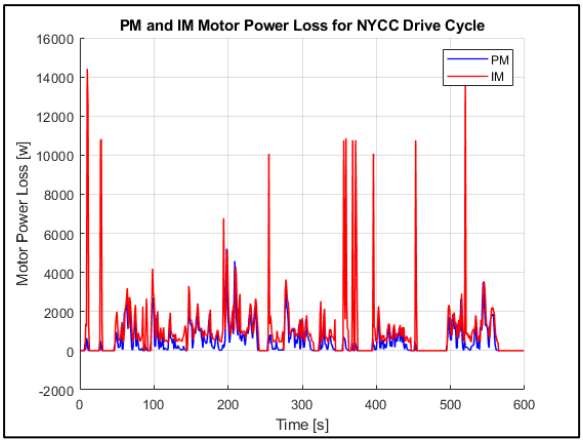


(c) NYCC

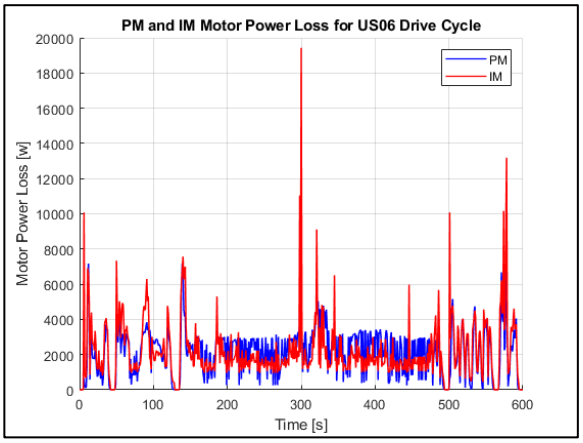


(d) US06

*Fig. 6. Power loss for PM and IM motors*

### 4.5. Battery state of charge (SOC) during many driving scenarios

Battery State-of-charge (SOC) represents an important parameter to evaluate the Electric vehicle performance. Since the electric motor is the heart of the electric car, it was worth to make a comparison between PM and IM to see its characteristics effect on battery SOC as a motor, and as a generator when the vehicle is slowing down. In this test, the initial SOC fixed at 80%. From *Figure 7* we can see that both motors drain more power from the battery in the case of driving at high speeds. On the contrary to driving a car at low speeds, or within the city where the vehicle could recover some of its battery energy through the use of regenerative braking system, and this would help to extend the vehicle range, and it doesn't mean improving vehicle efficiency because driving a car at low speed will hurt the overall system efficiency even with the presence of regenerative braking (refer to table 3).

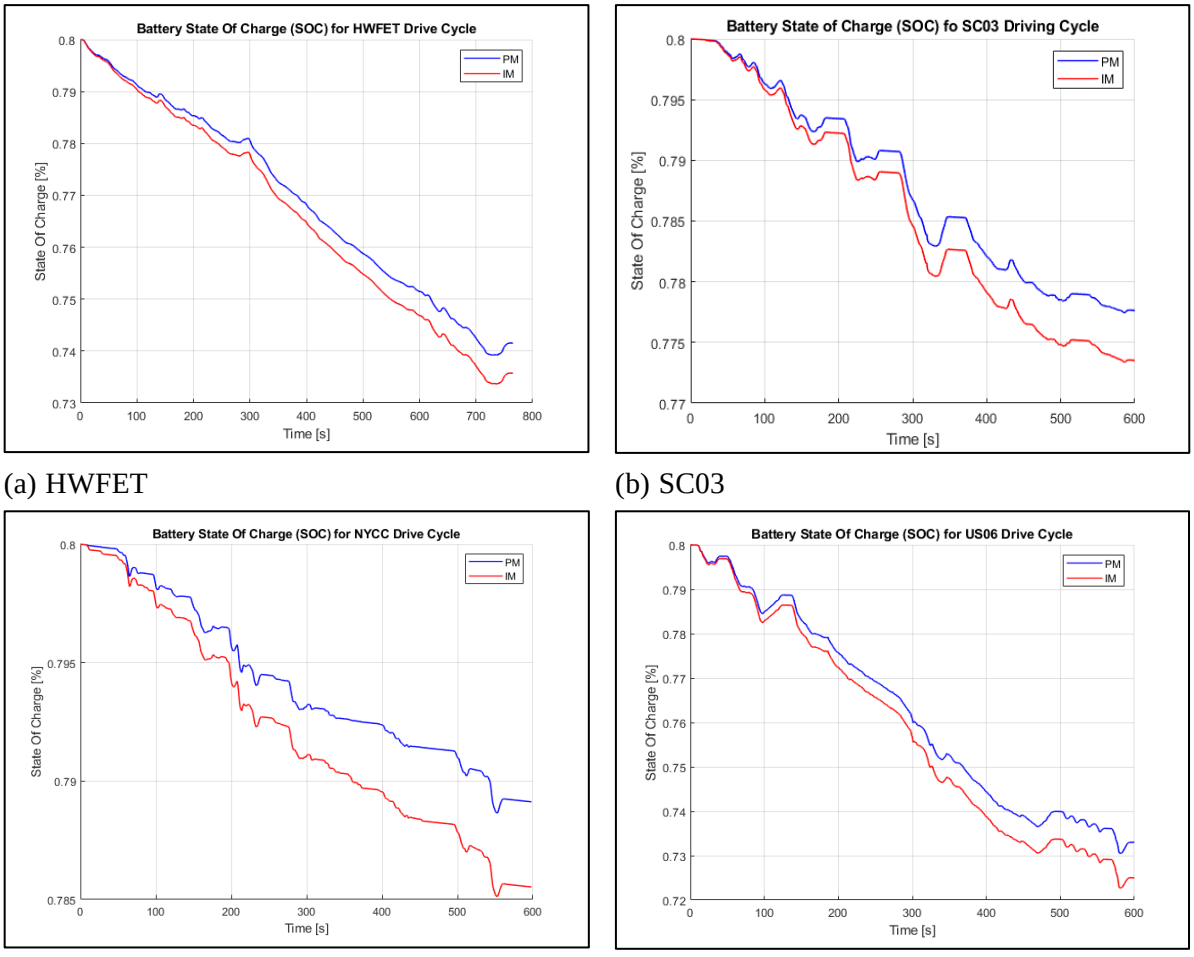


(a) HWFET (b) SC03

(c) NYCC (d) US06

*Fig. 7. Battery State Of Charge (SOC) during different driving cycles for IM and PM motor.*

The comparison results also show that the PM motor performed better at low-speed scenarios when the battery SOC has dropped slowly then the case of IM.

### 4.6. Vehicle efficiency for different motor type under many driving styles

Table 3 shows the overall system efficiency under different driving styles and for two motors. The results for both motors are almost equal. We denote that the PM could be a choice for high way roads like HWFET and US06 cycles when the vehicle reaches a high performance. On the other hand, driving a car in an urban (SC03), or within a city (NYCC) has a profound effect on vehicle performance, especially with the presence of the Induction Motor (IM) when the vehicle suffers from low efficiency (14%). However, Vehicle efficiency not only depends on the power-train components like the case of IM and PM motors, but it strongly depends on the driver behaviour.

Table 3. Electric Vehicle efficiency for different traction motor types

| | Vehicle efficiency [%] | |
|---|---|---|
| Driving cycle | PM | IM |
| HWFET | 0.599 | 0.545 |
| NYCC | 0.189 | 0.142 |
| SC03 | 0.38 | 0.344 |
| US06 | 0.519 | 0.506 |

## 5. WHAT WE CONSIDER WHEN WE SELECT AN ELECTRIC MOTOR FOR EV APPLICATION

Through the performed tests and the published papers, and some expert opinions concerning the topic of selecting the right, or an appropriate electric motor for electric vehicle application. We conclude that the choice is not an easy matter, and it depends on many factors and circumstances stated as follows:

### 5.1. Motor maximum torque and power

The maximum power enables the vehicle to reach and maintain a constant speed under stringent slope and speed conditions. To calculate the maximum-power you need a simulator that takes into account the drag and friction coefficients of the vehicle in addition to the forces required for the climb [14]. As we can see from the Table 4 the induction motor with higher power limit (124 kW) has achieved a grade-ability of 24.8%, and it could maintain a vehicle speed at 50 miles/hour during this road condition. Compared to PM which only achieved 11.4%. For the maximum torque, it enables the vehicle to start at any given slope, and it is possible to calculate the maximum rated torque of the motor based on the maximum-grade

that the car can overcome considering the differential, and gearbox and maximal weight that also have to be taken into consideration [14].

### 5.2. Efficiency

Electrical efficiency of an electric motor gives us the relation between electrical input and useful mechanical output of the motor. Generally, given by the ratio of shaft power output and motor input power [6]. When the electric motor used in an electric vehicle, the electric motor will operate at different loads. Therefore, the efficiency at different loads has to be considered to make the right selection [6].

### 5.3. Driving cycle

The way of driving a vehicle has to be taken into account when choosing a traction motor. The motor performance changed according to driving styles. A drive cycle with many stop/start phases like NYCC would cause much more losses. On contrary to highway experience when the driver supposed to maintain a vehicle at a certain speed. Consequently, knowing where we are going to drive a car could help us to select a battery pack size and other vehicle components.

### 5.4. Torque-speed characteristics

This characteristic could tell us where the motor is operating most at low power region (or high torque) where frequent stop and start is required, or at constant power region (or low torque region) while driving a vehicle at high speed. Based on these characteristics, we can see the spread of motor operating points which will help us to decide if the motor is suited for the suggested drive cycle.

### 5.5. Specific power

Specific power is defined as the power-to-weight ratio and is calculated by dividing the motor peak power by its mass. Selecting a motor that has a high specific power value could be the right choice to improve the vehicle efficiency because the overall vehicle weight will be reduced.

### 5.6. Vehicle maximum speed

Before selecting an electric motor, we have to define a vehicle speed requirement. Based on the vehicle targeted speed and other vehicle parts design like wheel radius and

gearbox specifications which will be helpful to calculate the maximum speed of traction motor.

### 5.7. Torque density

The torque density is an important parameter that should be taken into account when we select a traction motor which indicates the amount of torque per unite volume. It represents the torque capability of the electric motor which has a specific weight and space. However, many other factors to consider when choosing a traction motor for EVs application such as the price if it meets the requirements of the project, and the required power density to fit the reserved volume within a car design.

## 6. CONCLUSION

In this work, a comparison between PM and IM conducted to analyse their performance during different driving scenarios. Electric motors designed for a traction application have some features which supposed to influence the vehicle system performance as a whole in terms of speed, acceleration and grade-ability.

From the conducted tests we found that the PM could be the right candidate for high way roads when the vehicle reaches a high performance. On the other hand, driving a car in city has a profound effect on vehicle performance, especially with the presence of the Induction Motor (IM) when the vehicle suffers from too low efficiency. Generally, the average PM power loss is less than the losses produced by the IM even at high-speed.

The selection of the appropriate motor for EVs depends on many factors including what is related to its design like the specific power, efficiency, and torque density. Factors related to the environment like driving on a highway or driving in cities. However, among the features mentioned above the high torque at starting, and long or extended power region at cruising are the principal features for traction applications to deal with a different situations.

## *REFERENCES*

[1] X.D. Xue, K. W. E. Cheng and N.C. Cheung, *Selection of electric motor drives for electric vehicles.* Proocedings of Australian Universities Power Engineering Conference, NSW, pp. 1-6, 2008.

[2] T. Porselvi, M. K. Srihariharan, J. Ashok, and S. A. Kumar, *Selection of power rating of an electric motor for electric vehicles*, International Journal of Engineering Science and Computing IJESC, vol. 7, issue 4, pp. 6469 -6472, 2017.

[3] M. Ehsani, Y. Gao and S. Gay, *Characterization of electric motor drives for traction applications*, Proocedings of 29th Annual Conference of the IEEE Industrial Electronics Society, IECON'03, vol. 1, pp. 891-896, 2003.

[4] G. Luthra, *Comparison of characteristics of various motor drives currently used in electric vehicle propulsion system*. International Journal of Mechanical and Production Engineering, vol. 5, no.6, 2017.

[5] M. Zeraoulia, M. E. H. Benbouzid, and D. Diallo, *Electric motor drive selection issues for HEV propulsion systems: A comparative study*. IEEE Transactions on Vehicular Technology, vol. 55, no. 6, pp.1756-1764, 2006.

[6] S. R. Jape and A. Thosar, *Comparison of electric motors for electric vehicle application*, International Journal of Research in Engineering and Technology, vol. 6, no.09, p. 12-17, 2017.

[7] B. Tabbache, S. Djebarri, A. Kheloui and M. Benbouzid, *A power presizing methodology for electric vehicle traction motors,* International Review on Modelling and Simulations, vol. 6, no. 1, 2013.

[8] P. Bhatt, H. Mehar and M. Sahajwani, *Electrical Motors for Electric Vehicle a Comparative Study*. Available at SSRN 3364887, 2019.

[9] P. K. Prathibha, E. R. Samuel and A. Unnikrishnan, *Parameter Study of Electric Vehicle (EV), Hybrid EV and Fuel Cell EV Using Advanced Vehicle Simulator (ADVISOR) for Different Driving Cycles.* In Green Buildings and Sustainable Engineering, Springer, Singapore, pp. 491-504, 2020.

[10] C. Gang, W. Long and W. Lei, August. *Redevelopment of ADVISOR for Design and Simulation of Plug-in Hybrid Electric Vehicle*. In 2015 AASRI International Conference on Circuits and Systems, CAS, Atlantis Press, 2015.

[11] J. Larminie and J. Lowry, *Electric vehicle technology explained*. John Wiley & Sons, 2012.

[12] T. Markel, A. Brooker, T. Hendricks, V. Johnson, K. Kelly, B. Kramer, M. O'Keefe, S. Sprik, and K. Wipke, *ADVISOR: a systems analysis tool for advanced vehicle modeling*, Journal of power sources, vol. 110, no. 2, pp.255-266, 2002.

[13] *ADVISOR, NREL's ADvanced VehIcle SimulatOR*, http://adv-vehicle-sim.sourceforge.net/.

[14] C. Pronovost, *10 things to consider when choosing an electric motor*, https://www.danatm4.com/blog/10-things-consider-choosing-electric-motor/, 2016, viewed May 17, 2020.

## Appendix

Battery: voltage = 348V, power = 26kW, mass =520kg.

Motors characteristics used in this paper: PM-UQM100 (manufacturer: UQM) and AC75 (manufacturer: Westinghouse 75 kW (cont))

Table 4. PM and IM characteristics

| Characteristics | PM | IM |
|---|---|---|
| Weight [Kg] | 101.9 | 91 |
| Maximum power [kW] | 100 | 124 |

| | | |
|---|---|---|
| Maximum Rated torque [Nm] | 300.1 | 271.14 |
| Peak torque [Nm] | 550.6 | 488.52 |
| Specific power [kW/Kg] | 0.98 | 1.36 |
| Minimum Voltage [V] | 180 | 120 |
| Maximum speed [rpm] | 4400 | 10000 |
| Peak Efficiency [%] | 94 | 92 |
| Maximum current [A] | 400 | 480 |

# THE WEEE MANAGEMENT AND ITS INFLUENCE ON ENVIRONMENT AND HUMAN HEALTH. CASE STUDY: MARAMUREȘ COUNTY, ROMANIA

Irina **SMICAL**[1], Mariia **ORFANOVA**[2]

[1] *North University Centre of Baia Mare, Technical University of Cluj-Napoca, Engineering of Mineral Resources, Materials and Environment Department, 62A Victor Babes str., 430083, Baia Mare, Romania*

[2] *Ivano-Frankivsk National Technical University of Oil and Gas, Institute of Tourism and Geoscience, Ecology Department, Ivano-Frankivsk, Ukraine*

*irina.smical@cunbm.utcluj.ro*

**Keywords: WEEE, hazardous substances, waste management, contaminants**

**Abstract:** *This paper addresses a number of issues regarding the management of waste electrical and electronic equipment (WEEE) and its influence on environmental and human health factors. The study was conducted for Maramures County to highlight the WEEE management and its threats to tne environment and human health. Worldwide research results show that improper WEEE treatment and recycling is a factor of environmental pollution and the generation of various diseases, especially where rudimentary techniques are used and there is no means of protecting workers. By dismantling mechanical and pyrometallurgical processing of WEEE components result in a series of contaminants that can pollute the soil, surface water, groundwater, the atmosphere and finally can cause a lot of human diseases. Following the investigations, it is found that the management of WEEE in Maramureș County poses a low risk of contamination given the fact that in this county only WEEE collection is made not also their treatment or recycling. Moreover, all collection activities of WEEE are made safe and are authorized by the environmental protection point of view.*

## 1. INTRODUCTION

Studies made on the WEEE treatment in some developing countries showed that the rudimentary treatment technologies pose a risk on the environment and human health by

releasing some toxic pollutants like lead (Pb), polybrominated diphenylethers (PBDEs), polychlorinated dioxins and furans as well as polybrominated dioxins and furans (PCDD/Fs and PBDD/Fs). In China and India high concentrations of these pollutants were found in air, bottom ash, dust, soil, water and sediments especially in WEEE recycling area [1-3].
The most observed health problems related to e-waste processing include diseases, problems of skin, stomach, respiratory tract, tuberculosis, blood diseases, malfunctioning of the kidneys, lung cancer, or congenital ones like birth defects, underdevelopment of the brain of children, damage of nervous and blood systems [4-6].

From places where this waste is dismantled and burned in order to recover useful materials, pollutants and especially fine particle with heavy metals are transported by air currents over large areas. This leads to air pollution and soil and surface water contamination. Soil pollutants can easily pass into plants and from there into the food chain causing a number of diseases [4, 7].

In line with European waste management policy (Directive 2008/98/EC), the legislative provisions on WEEE focus on preventing the occurrence of WEEE and minimizing the toxic substances and elements contained in it, on the recovery and reuse of components, recycling and the energy recovery of non-recoverable components and, last but not least, the disposal of WEEE in conditions that do not create pollution or damage to the environment [8]. Also, in Romania the content of toxic substances in EEE is regulated, being allowed only those EEE that comply with the maximum permitted limits to be placed on the market [9]. Therefore, there are not allowed EEE which contain substances in concentrations exceeding the maximum allowed limits set out in Annex 2 to GD no. 322/2013 [10]. To this end, EEE producers apply the product conformity assessment procedure by carrying out internal control and issuing the declaration of conformity and affixing the CE marking to the finished product, respectively. The purpose of these regulations is to reduce the hazardous properties of the future WEEE [9,10].

The objective of this study is to highlight the WEEE management activity in Maramureș County and the possible risks for the environment and human health.

## 2. MATERIALS AND METHOD

In order to carry out this study, data published in specialized scientific papers were used, respectively statistical data held by environmental protection authorities at European, national and county level.

In order to obtain the statistical evidence regarding the quantities of WEEE collected at the level of Maramureș County, reporting data provided by National Environment Protection Agency (NEPA) for the period 2015-2018 were used. In order to highlight the evolution of WEEE management in the Maramureș county, statistical interpretations and graphical

representations were made for each category of WEEE, in accordance with the provisions of GEO no. 5/2015 [11].

## 3. RESULTS AND DISCUSSIONS

At European level, the statistics of the quantities of WEEE collected from the population, indicate the lowest collection rate for Romania in the period 2012-2016 [12]. Moreover, for the years 2017 and 2018 there are no data reported by Romania for this waste. It can be seen in the graph in *fig. 1* that there is a big discrepancy even compared to Bulgaria, the country that joined at the same stage with Romania to the European Union. Compared to developed European countries such as Denmark or Belgium, the differences are even more obvious.

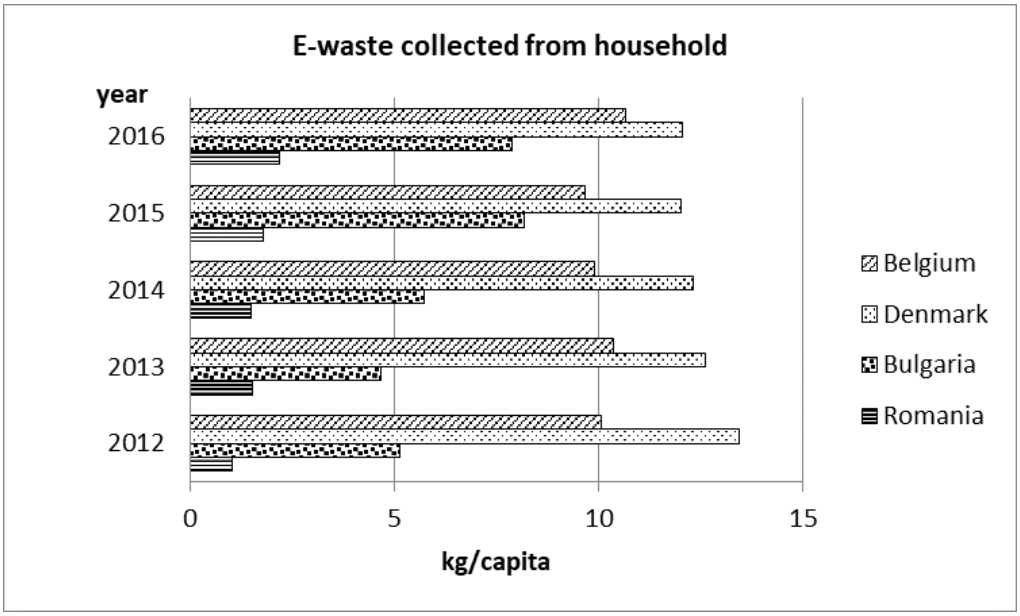


*Fig. 1. Amount of WEEE/capita collected in several European countries in the period 2012-2016 [12]*

The placing on the market of EEE is allowed only by producers who are registered in the "Register of Producers and Importers of EEE" [13, 14]. At national level, at the end of 2019, there were 3431 registered producers of electrical and electronic equipment (EEE) [14] and at the level of Maramureș County, 30 operators [15].

According to Environment Protection Agency of Maramures County (EPA MM)[15], at present, in Maramureș County there are 21 WEEE collection points by economic operators authorized for this type of activity.

The environmental report for 2019 (table 1), prepared by NEPA, shows that Romania has failed to achieve its collection targets set by European and national legislation [8, 11], thus:

- ✓ 4 kg of waste/inhabitant/year in the period 2008 - 2015;

- ✓ at least 40% of the average quantities of EEE placed on the market in the previous 3 years, for 2016 ,;
- ✓ 45% of the average quantities of EEE placed on the market in the previous 3 years, for the period 2017 – 2020

Table 1. Quantities of EEE placed on the market and WEEE collected in 2015-2018 period in Romania [14]

| Crt. no. | EEE/WEEE category / year | Quantities of EEE placed on the market and WEEE collected (tonnes) | | | | | | | |
|---|---|---|---|---|---|---|---|---|---|
| | | 2015 | | 2016 | | 2017 | | 2018 | |
| | | EEE | WEEE | EEE | WEEE | EEE | WEEE | EEE | WEEE |
| 1 | Large household appliances | 103475.36 | 24122.22 | 129548.53 | 29592.17 | 140581.09 | 31175.22 | 146784.12 | 35755.95 |
| 2 | Small household appliances | 14667.61 | 1218.31 | 16224.62 | 1320.07 | 18467.35 | 1303.18 | 22675.82 | 1633.02 |
| 3 | IT and telecommunications equipment | 13469.45 | 6837.44 | 13231.54 | 5645.37 | 15230.91 | 6571.14 | 16042.00 | 9362.28 |
| 4 | Consumer equipment and photovoltaic panels | 15236.29 | 5385.17 | 17594.37 | 7063.19 | 27702.55 | 6545.39 | 26189.23 | 9699.59 |
| 5 | Lighting equipment | 6010.49 | 1781.32 | 7042.15 | 1292.77 | 9084.30 | 2002.53 | 13666.18 | 3171.92 |
| 6 | Electrical and electronic tools (with the exception of large-scale stationary industrial tools) | 9654.61 | 796.00 | 11108.44 | 891.33 | 18030.34 | 903.08 | 23932.63 | 1206.34 |
| 7 | Toys, leisure and sports equipment | 1616.51 | 107.26 | 2150.54 | 115.51 | 3489.87 | 83.39 | 4718.89 | 91.31 |
| 8 | Medical devices (with the exception of all implanted and infected products) | 673.90 | 48.43 | 564.86 | 83.24 | 889.33 | 67.33 | 1430.59 | 114.16 |
| 9 | Monitoring and control instruments | 2566.35 | 383.15 | 2126.21 | 411.01 | 3343.29 | 700.15 | 4538.30 | 2065.84 |
| 10 | Automatic dispensers | 808.83 | 94.84 | 1093.56 | 239.79 | 1225.34 | 337.79 | 1169.18 | 678.47 |
| 11 | Total | 168179.40 | 40774.14 | 200684.82 | 46654.45 | 238044.36 | 49689.20 | 261146.92 | 63778.88 |

In Maramureș County, in the period 2013-2018 there is an increasing trend of the quantities of WEEE collected by authorized economic operators, the highest amount being registered in 2018. Unfortunately, the activity of the associations taking over the responsibility of producers is not fully reflected in centralized and reported data at environmental authority level (Table 2) [15].

Table 2. WEEE collected in Maramures County during 2013-2018 (tonnes) [15]

| Collector name | amount/year (tonnes) | | | | | |
|---|---|---|---|---|---|---|
| | 2013 | 2014 | 2015 | 2016 | 2017 | 2018 |
| Economic operators authorized for collection | 29.84 | 41.86 | 59.79 | 176.46 | 119.69 | 846.36 |
| Ecotic | | | 152.55 | 259.82 | | |
| Asociaţia Română pentru Reciclare – RoRec | | | | 232.35 | | |
| The Green Project (RoRec partner) | | | | | 111.229 | |

The management of WEEE in Maramureș County encounters some difficulties regarding the complete realization of the database because some economic operators that were authorized to collect WEEE stored the waste without sending it for treatment or others went into insolvency and the associations taking responsibility for the producer did not reported to the county environmental protection authority the quantities of WEEE collected from citizens during the collection campaigns.

## 4. WEEE STATISTICS FOR MARAMURES COUNTY

At the level of Maramureș county, the total quantities of WEEE collected are reported differently on the categories of equipment according to the provisions of GEO no. 5/2015 [11]. As can be seen in the graphs below (*fig*. 2-10), except for waste from category 7 (Toys, leisure and sports equipment (*fig.* 8)), there was an increase in the quantities collected. This increase is more accentuated, in the case of the first 5 categories of equipment waste as they are presented in the annex to GEO no. 5/2015 [11].

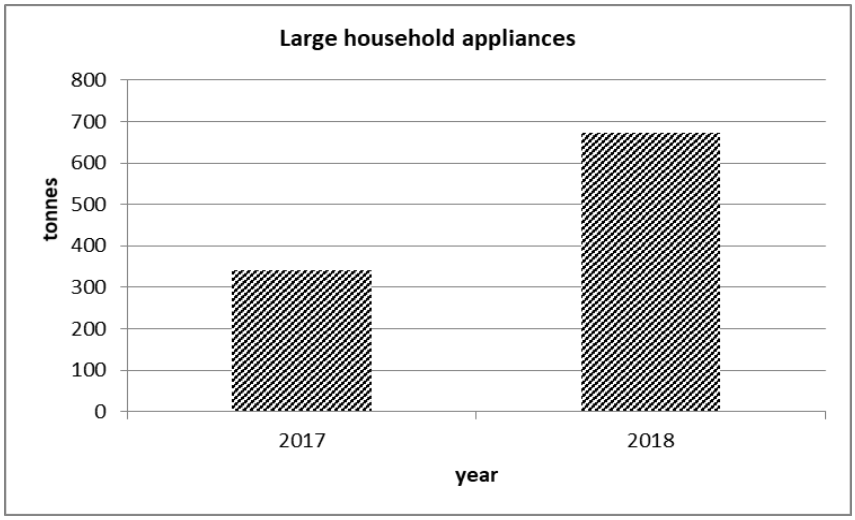


*Fig. 2. Large household appliances collected during 2017-2018 in Maramures County [16]*

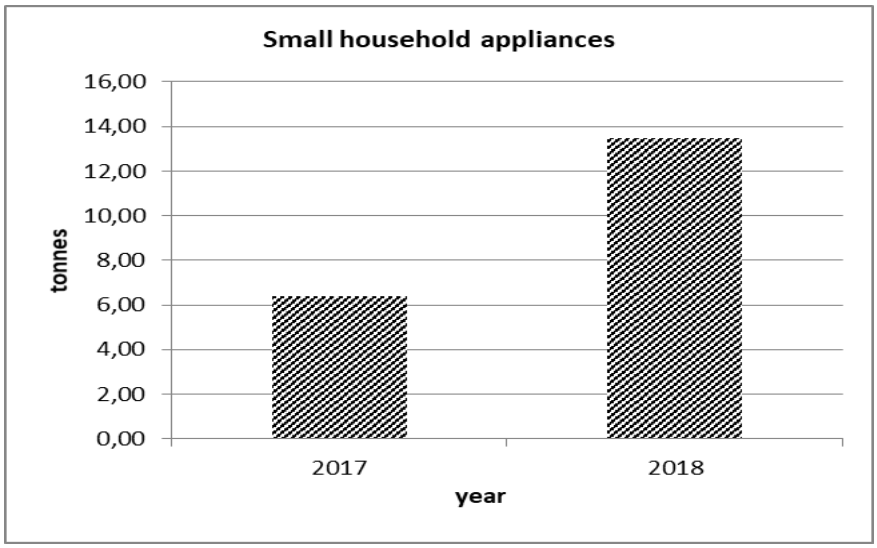


*Fig. 3. Small household appliances collected during 2017-2018 in Maramures County [16]*

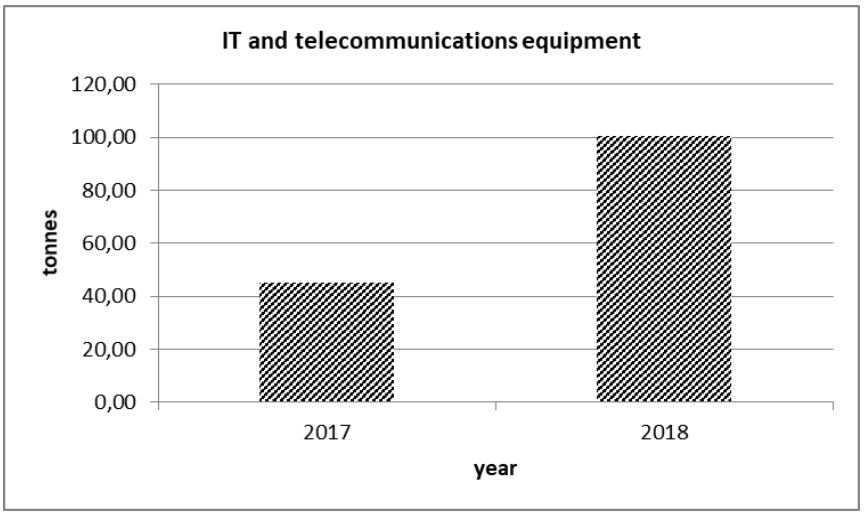


*Fig. 4. IT and telecommunications equipment collected during 2017-2018 in Maramures County [16]*

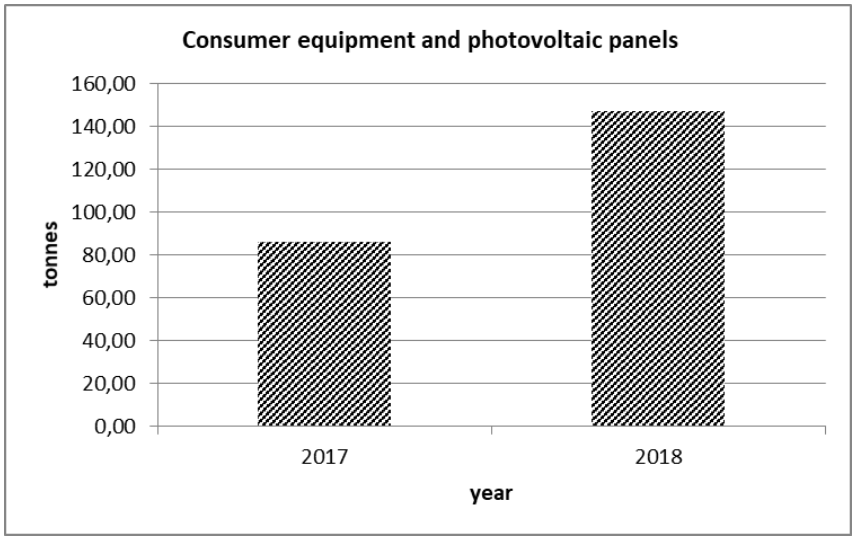


*Fig. 5. Consumer equipment and photovoltaic panels collected during 2017-2018 in Maramures County [16]*

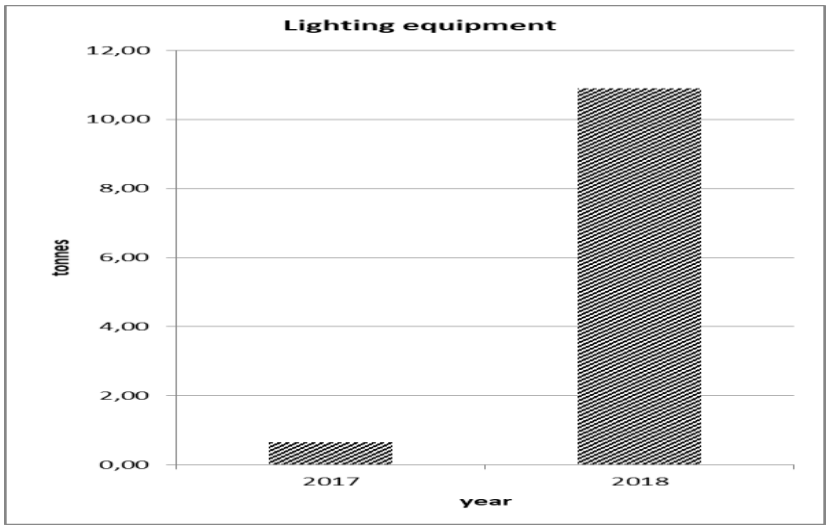


*Fig. 6. Lighting equipment collected during 2017-2018 in Maramures County [16]*

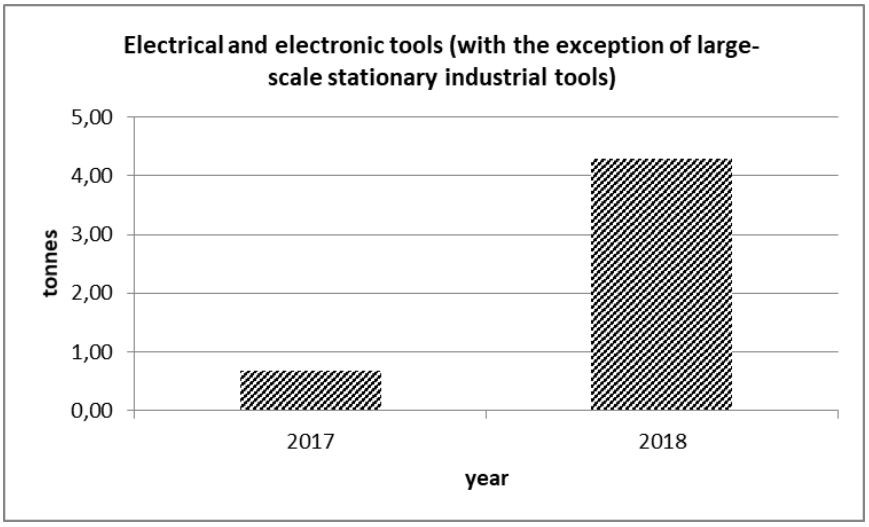


*Fig. 7. Electrical and electronic tools (with the exception of large-scale stationary industrial tools) collected during 2017-2018 in Maramures County [16]*

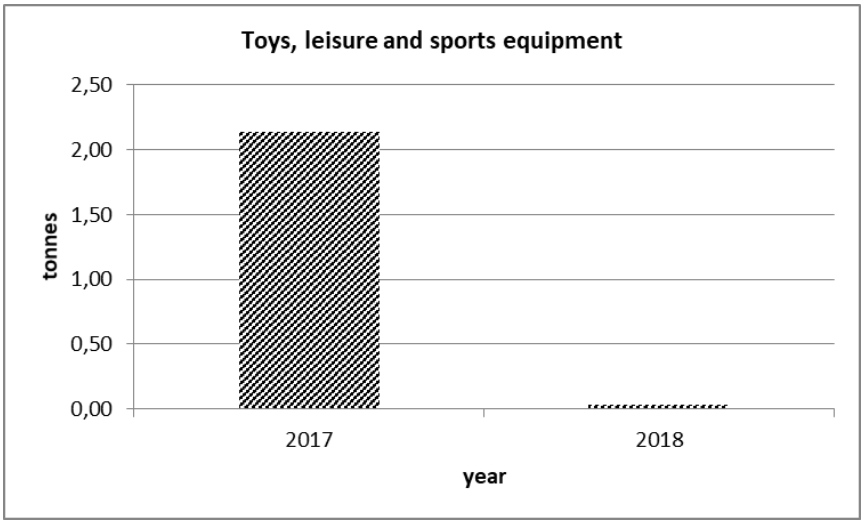


*Fig. 8. Toys, leisure and sports equipment collected during 2017-2018 in Maramures County [16]*

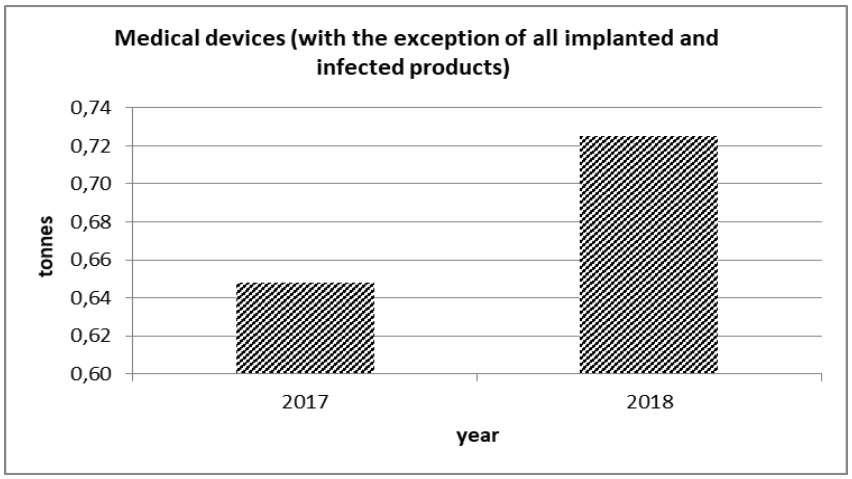


*Fig. 9. Medical devices (with the exception of all implanted and infected products) collected during 2017-2018 in Maramures County [16]*

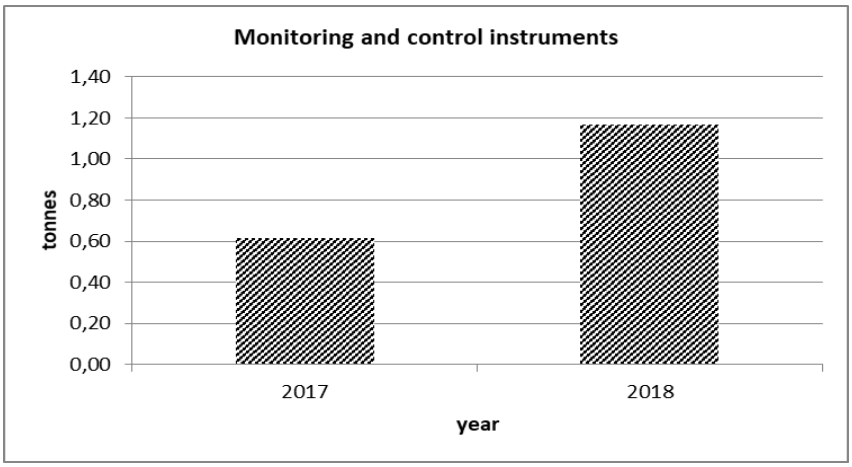


*Fig. 10. Monitoring and control instruments collected during 2017-2018 in Maramures County [16]*

The statistical data presented in the graphs above reveal an increase of about 17 times of the amount collected of Lighting equipment waste in 2018 compared to 2017. A high increase of approx. 6 times are also registered in the case of Electrical and electronic tools (with the exception of large-scale stationary industrial tools) waste and at the opposite side there is a reduction of about 65 times the amount of Toys, leisure and sports equipment waste in 2018 compared to 2017 .

## 5. SWOT ANALYSIS OF WEEE MANAGEMENT IN MARAMUREȘ COUNTY

This method allows the analysis of the global situation, the establishment of key strategic points, as well as the identification of strategic alternatives, helping to make the right decisions, but also to plan strategies. The SWOT analysis of WEEE management in Maramureș County is presented in table 3.

Table 3 The SWOT analysis of WEEE management in Maramureș County

| | |
|---|---|
| **Strengths**<br>• Legislation in the field harmonized with European Union legislation.<br>• The existence of associations that have the role of implementing collection campaigns.<br>• Involvement of producers of electrical and electronic equipment by offering advantages to the purchase of new products provided the delivery of old products such as electrical and electronic equipment.<br>• Introduction of the national program for appliances waste: ”Programul Rabla pentru Electrocasnice” | **Weaknesses**<br>• Lack of waste treatment plants for electrical and electronic equipment (which results in additional costs for transporting waste to treatment plants in neighboring counties).<br>• Reduced number of WEEE collection points.<br>• Lack of state involvement in developing strategies to support the efforts of local authorities.<br>• Lack of legislation to involve more the public authorities in the collection of WEEE. They have direct links with citizens which are the main generators of WEEE |
| **Opportunities**<br>• Potential for developing partnerships with various communities in the European Union.<br>• Increasing investments and increasing associations involved in waste management of electrical and electronic equipment. | **Threats**<br>• The disinterest of the population for respecting and protecting the environment.<br>• Disinterest of both the population and economic agents related to the selective collection of waste electrical and electronic equipment |

## 6. RISKS ON ENVIRONMENT AND HUMAN HEALTH RELATED TO DEEE HAZARDOUS CONTENT.

Over 1000 of the chemicals were identified in e-waste and there is not an exhaustive knowledge about their toxicity and environmental impact [4]. In table 4 some hazardous contents are related to some components of WEEE.

Table 4 Hazardous elements in WEEE [17, 18, 4, 19].

| Hazardous element | WEEE component |
|---|---|
| Mercury | Relays, switches, gas discharge lamps, batteries, Liquid Crystal Display (LCD) |
| Cadmium | Batteries, Printed circuit boards, Chip resistors and semiconductors |
| Lead | Batteries, printed circuit boards, fibre optics, panels and gaskets in computer monitors; as PbO in the Cathode Ray Tubes (CRTs) |

| | |
|---|---|
| Lithium | Batteries, LCD |
| Beryllium | Printed circuit boards, motherboards of computers |
| Antimony | Printed circuit boards, flame retardant, Cathode Ray Tubes (CRTs) |
| Polybrominated diphenyl ethers (PBDEs) used in brominated flame retardants (BFRs) | Plastics, Plastic housing of electronic equipments and circuit boards to reduce f lammabilit |
| Polychlorinated biphenyls | Capacitors |
| Dioxins and furans | PVC in wire insulation when burning |
| Lead | CRTs, Solder of printed circuit boards, glass panels and gaskets in computer monitors |
| Gallium | Silicon chips and LCD, monitors, Integrated circuits, optical electronics, |
| Indium | Silicon chips and LCD, monitors |
| Zinc | LCD, Plating material |
| Fluorine | Fibre optics |
| Yttrium | Fibre optics |
| Zirconium | Fibre optics |
| Arsenic | Transistors |
| Barium | Front panel of Cathode Ray Tubes (CRTs) |
| Chlorofluorocarbons (CFCs); hydrochlorofluorocarbons (HCFCs); hydrofluorocarbons (HFCs) and hydrocarbons (HCs) | In old coolers, refrigerators, air conditionairs |
| Cobalt | Rechargeable batteries and coatings for hard disk drives |
| Copper | Used as a conductor |
| Hexavalent chromium | Used as corrosion protection of untreated and galvanized steel plates and a decorator or hardener for steel housings |
| Asbestos | Used in older appliances such as electric coffee pots, toasters, irons and electric heaters |
| Radioactive substances | Found typically in some medical equipment, certain test instruments, and commonly in smoke detectors |

According to Sepúlveda et al., 2010; Zhao et al., 2010; Wang et al., 2011 [1, 2, 3] the biggest risks for the environment and health are presented by the activities of dismantling and burning WEEE by using rudimentary uncontrolled methods.

The threatness for environment and human health is reprezented by the presence of various hazardous substances in WEEE like: heavy metals (mercury, cadmium, lead, arsenic, zinc, copper, antimony etc), flame retardants (pentabromophenol, polybrominated diphenyl ethers (PBDEs), tetrabromobisphenol-A (TBBPA) etc) [18].

According to Tsydenova&Bengtsson, 2009 [18] even for industrialized/developed countries, there is a concern related to occupational risks of the electronics dismantling workers. They are exposed to contamintion via ingestion, inhalation or dermal contact.

Generally, the most risk is associatd with treatment operation of WEEE because there are involved several processes like: shrreding for components size reduction, grinding, separation by different methods, pyrometallurgical operation etc. From all these result dust composed of plastic, metals, ceramic, glass and silicon, brominated flame retardants (BFRs) and from smelting result fumes of heavy metals, mixed halogenated dioxins and furans etc. The risks associated with landfilling of WEEE is related to leaching and evaporation of hazardous substances [18].

Because of exposure to the WEEE hazardous substances, which might be by ingestion, inhalation, dermal contact, people could get sick of a lot of diseases such as problems of skin, stomach, respiratory tract, tuberculosis, blood diseases, malfunctioning of the kidneys, lung cancer, or congenital ones like birth defects, underdevelopment of the brain of children, damage of nervous and blood systems [4, 5, 6, 17, 20, 21].

In Maramureș County there are no dismantling and recovery centers of some WEEE elements, but only collection [15]. Dismantling and recycling operations are carried out outside the county in authorized installations from the point of view of environmental protection. Therefore, in the absence of facilities and operations for treatment and recycling of WEEE on the territory of our county, the risks of contamination of the environment and the population with hazardous substances contained in WEEE, are relatively low.

## 7. CONCLUSIONS

WEEE management is an activity that can have unpleasant consequences for the environment and human health. The entire flow of WEEE treatment involves a certain risk for environmental factors and the safety of the people involved in the process. Thus, where WEEE is processed with rudimentary techniques and without environmental and munitions protection equipment, there is the possibility of contamination and the generation of diseases associated with different types of hazardous substances.

The present study was carried out for waste management in Maramureș County and it was found that this activity involves only the collection of WEEE, not their treatment, respectively recycling. The treatment and recovery operations, respectively the elimination, as the case may be, are carried out in compliant installations outside the county. Moreover, the activities of economic operators that carry out WEEE collection in Maramureș County are authorized from the point of view of environmental protection. Thus, the risks of environmental contamination and disease of the population associated with WEEE management are relatively low.

To optimize WEEE management it is necessary to improve environmental performance at all levels and apply an environmental management correlated with the principles of circular economy and sustainable development.

## *REFERENCES*


[1] A.Sepúlveda, M. Schluep, F.G. Renaud, M. Streicher, R. Kuehr, C. Hagelüken, A. C. Gerecke, *A review of the environmental fate and effects of hazardous substances released from electrical and electronic equipments during recycling: Examples from China and India*, Environmental Impact Assessment Review, 30, pp. 28–41, 2010

[2] X-R. Zhao, Z-F. Qin, Z-Z. Yang, Q. Zhao, Y-X. Zhao, X-F. Qin, Y-C. Zhang, X-L. Ruan, Y-F. Zhang, X-B. Xu, *Dual body burdens of polychlorinated biphenyls and polybrominated diphenyl ethers among local residents in an e-waste recycling region in Southeast China*, Chemosphere, vol. 78, no. 6, pp. 659–666, 2010.

[3] H. Wang, M. Han, S. Yang, Y. Chen, Q. Liu, S. Ke, *Urinary heavy metal levels and relevant factors among people exposed to e-waste dismantling*, Environment International, vol. 37, no. 1, pp. 80–85, 2011.

[4] K. Lundgren, *The global impact of e-waste: Addressing the challenge*, International Labour Office, Geneva, pp. 72, 2012.

[5] S. Prakash, A. Manhart, *Socio-economic assessment and feasibility study on sustainable e-waste management in Ghana*, Öko-Institut e. V, Freiburg, 2010.

[6] S. Nordbrand, *Out of control: E-waste trade flows from the EU to developing countries*, SwedWatch, 2009.

[7] C. Frazzoli, O.E. Orisakwe, R. Dragone, A. Mantovani, *Diagnostic health risk assessment of electronic waste on the general population on developing countries'scenarios*, Environmental Impact Assessment Review, vol. 30, no. 6, pp. 388–399, 2010.

[8] *** Directive 2012/19/EU of the European Parliament and of the Council of 4 July 2012 on waste electrical and electronic equipment (WEEE).

[9] *** Directive 2011/65/EU of the European Parliament and of the Council of 8 June 2011 on the restriction of the use of certain hazardous substances in electrical and electronic equipment (recast).

[10] GD no. 322 of 29 May 2013 on restrictions on the use of certain hazardous substances in electrical and electronic equipment, published in Of.G. no. 348/13 iun. 2013

[11] GEO no. 5 of April 2, 2015 on waste electrical and electronic equipment, published in Of.G. no. 253/16 apr. 2015

[12] Eurostat, *Waste electrical and electronic equipment (WEEE) by waste management operations*, http://appsso.eurostat.ec.europa.eu/nui/show.do?lang=en&dataset=env_waselee, 2020.

[13] Order no. 269 of March 20, 2019 on the approval of the Procedure for establishing the registration, reporting, frequency of reporting to the National Register of Producers, as well as the way of recording and reporting the information provided in art. 9 para. (4) and to art. 27 para. (6) of the

Government Emergency Ordinance no. 5/2015 on waste electrical and electronic equipment, M.Of. no. 305 of April 19, 2019.

[14] National Environment Protection Agency (NEPA), *Report on the state of the environment in Romania-year 2019, Ministry of Environment, Waters and Forests*, Bucharest, pp. 383-385, http://www-old.anpm.ro/upload/150386_ANPM-PC_RSM%202019.pdf, 2020.

[15] Environmental Protection Agency of Maramures, *County Report on the state of the environment for 2019*, Ministry of Environment, Waters and Forests, pp. 278-281, 2020.

[16] Environmental Protection Agency of Maramures, *Statistical Database*, 2020.

[17] O. Tsydenova, M. Bengtsson, *Chemical hazards associated with treatment of waste electrical and electronic equipment*, Waste Management, vol. 31, no. 1, pp. 45–58, 2011.

[18] O. Tsydenova, M. Bengtsson, *Environmental and Human Health Risks Environmental and Human Health Risks Associated with the End-of-Life Treatment of Electrical and Electronic Equipment*, Institute for Global Environmental Strategies, Japan, 2009.

[19] O.E. Osuagwu, C. Ikerionwu, *E-cycling e-waste: The way forward for Nigeria IT and electro-mechanical industry*, International Journal of Academic Research, vol. 2, no. 1, pp. 142–149, 2010.

[20] K. Grant, F. C. Goldizen, P. D. Sly, M-N. Brune, M. Neira, M. van den Berg, R. E. Norman, *Health consequences of exposure to e-waste: A systematic review*, Lancet Global Health, vol. 1, no. 6, pp. e350-e361, 2013.

[21] M-N. Brune, F. C. Goldizen, M. Neira, M. van den Berg, N. Lewis, M. King, W. A. Suk, D. O. Carpenter, R. G. Arnold, P. D. Sly, *Health effects of exposure to e-waste,* Lancet Global Health 1, no. 2, pp. e70, 2013.

# USING MATLAB-SIMULINK AS TOOL FOR STUDYING INDUCTION MOTOR

Olivian **CHIVER**[1], Paul **LIBOTEAN**[1], Alina **NEAMT**[2], Liviu **NEAMT**[1] and Mircea **HORGOS**[1]

[1] *Technical University of Cluj-Napoca, Faculty of Engineering, Romania,* [2] *"Anghel Saligny" Technical College Baia Mare, Romania*

*olivian.chiver@cunbm.utcluj.ro*

**Keywords: Matlab-Simulink, tool, induction motor, tests**

**Abstract***: The needed models and procedures for simulating induction motor tests are presented in the paper. The induction motor model is one from Simulink library and students can use it in simulation. Measured quantities and necessary relations for parameter determination are shown. In addition to laboratory tests, an attempt is made to find a solution for operation at low load, so that the efficiency is maintained as high as possible. The main purpose is to show students the possibilities of using Simulink in the study of the induction motor and through similarity to the study of any electrical equipment or systems.*

## 1. INTRODUCTION

Matlab-Simulink is well-known as one of the most performant software package used for physical phenomena simulation. The ease of programming, the suggestive logic and easy understandable, the way of working similar to the laboratory one, are just some of the many benefits. The libraries with different models, grouped by specializations, the possibility of coupling models from different library, etc., have imposed the worldwide use of Matlab, both in research work and industry and also in educational activity.

Regarding the field of electrical engineering, this package offers the possibility to model and simulate most of the equipment and systems encountered in practice. In this context, the use in the educational field of electrical engineering is more than justified,

especially considering the attractive possibilities regarding the way of working and those of visualizing the results, very suggestive [1]-[4].

Last but not least, has to be highlighted the open policy of the MathWorks team, which offers free licenses to students and academic staff.

There are mainly two different ways of working in Simulink. First, it is based on the mathematical equations corresponding to the physical model, and the realization of the numerical model is done using mathematical operators (simple but also those of integration and derivation) and mathematical functions predefined or defined by the user. The necessary parameters for solving the integro-differential equations must be known and could be constants or functions of different variable, which in turn are calculated iteratively during the simulation process, in established initial conditions. The quantities of interest can be visualized in different stages, as instantaneous values, or transformed into other values (as RMS) defined by the programmer. The great advantage of this way of working is the fact that it is possible to simulate practically any desired situation, not necessarily ordinary (for example, defects in different equipment or electrical systems can be studied) [5].

The second way involves the use of special libraries, in which we find the necessary models of the desired equipment/system. Thus, modeling in this way is very suggestive and it is close (as a working way) to the practice. For example, if we want to study a power transformer, we find in libraries different models (single-phase or three-phase, with or without saturation), we set the materials, the number of turns, the voltages, etc., then will connect the transformer to a single or three-phase power source whose parameters we can set as needed. Different operation regimes it is possible to study, being able to determine or visualize the quantities of interest in transient or stationary regime [6] - [9].

The paper is addressed mainly to electrical engineering students, but also to those who want to use Simulink in the study of the induction motor. The main contribution of this study is the presentation of some Simulink models, on which the students from electrical engineering specialization can use to model and simulate the different tests that have to perform in the laboratory. A second purpose is showing a way of operating this motor type in the industry. It is desired to highlight a simple method of operation, possible to be used so that the efficiency is maximum, depending on the motor load. Inclusion in a certain efficiency class has also been studied.

## 2. METHODOLOGY

The studied motor is three-phase squirrel cage induction motor. The equivalent one phase diagrams, used in this study, are shown in *fig. 1*. Index 1 is for stator winding parameters, 2 for the rotor, *m* is for magnetizing and σ stand for leakage. The ' index means referred to the stator. *R* and *X* represent resistance and reactance respectively.

The induction motor block has been selected from Simulink Library as shown, *Simscape/ Electrical/ Specielized Power Systems/Fundamental Blocks/ Machines*. In this section are many types of electrical machines.

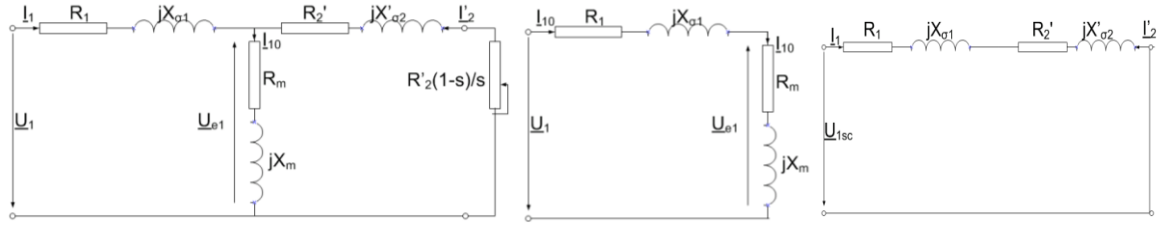


*a)* *b)* *c)*

*Fig. 1. Induction motor equivalent diagrams: a) normal operation; b) no load; c) locked rotor*

Different types of electrical machines there are also in *Simscape/ Electrical/ Electromechanical* library. The models from *.../Machines* are different by models from *.../Electromechanical*, the latter can be coupled with a model corresponding to a mechanical equipment, while the former allow the definition of the input quantity, torque [Nm] or speed [rad/s], as a function. We worked with the model from the library, but also it can be done based on motor's equations [10], [11].

Of course, once a motor of a certain power is chosen, it has all the characteristic parameters defined, both the electrical ones consisting of a number of poles, resistances and inductances, but also the mechanical ones as inertia and friction factor, just like a real motor. In addition, the initial conditions regarding the values of some parameters at the time of starting simulation can also be defined. The problem that we want to resolve is to determine these parameters by simulating tests, just like in the laboratory. This is what we achieved next. The data that were taken into account are the rated ones such as line voltage and phases connection (Y / D 400 / 230V), frequency (50Hz), rotor speed (1430 rpm), mechanical power (4 kW), stator current (7.9 A) and stator winding resistance (1.405 Ω), which is relatively easy to measure in the laboratory. Among the mechanical parameters, friction factor (0.002985 Nms) has been used. The other electrical parameters have to be identified by tests: the no-load operation and locked rotor. Operation curves have been obtained from the load operation test.

### 2.1. No-load test

For no-load test, the chosen input mechanical quantity has been the load torque, and zero value was imposed. In *fig*. 1 the carried out model and the measured quantities are shown. The motor is connected to a three phase power source through a measuring kit. The instant currents and voltages are measured, and also active and reactive power. The rms values are

determined and displayed. From the motor model, all electrical and mechanical instant quantities and also electromagnetic torque are obtained.

The friction factor (*F)* and the pole pairs number (*p*), have been used in order to obtain the mechanical losses in the no-load regime (negligible) knowing that,

$$p_m = F\Omega^2 = F\left(\frac{2\pi n}{60}\right)^2 \tag{1}$$

Magnetising resistance, in terms of the measured power, *P*, and average value of the stator currents, $I_1$, is,

$$R_m = \frac{P - p_m}{3I_1^2} - R_1 \tag{2}$$

No-load reactance also can be determined,

$$X_0 = X_m + X_{\sigma 1} = \frac{Q}{3I_1^2} \tag{3}$$

No-load power factor is,

$$cos\varphi_0 = \frac{P}{\sqrt{3}U_1 I_1} \tag{4}$$

Obtained values in no-load operation: Ω=156.97rad/s; $p_m$=0.468W; $R_m$=1.44Ω; $X_{10}$=55.9Ω; $cos\varphi_0$=0.051.

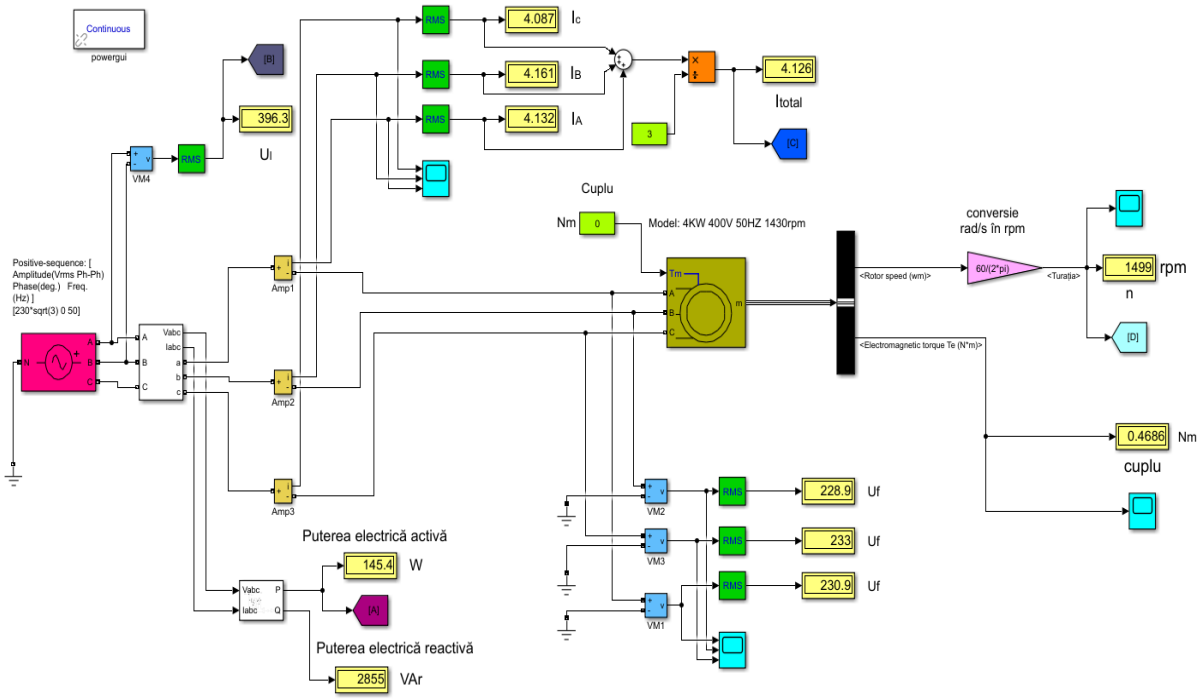


*Fig. 2. Carried out model for the no-load test*

## 2.2. Locked rotor test

The realized model and the measurements are shown in *fig*. 3. In this case, the mechanical input has been set the speed, and the imposed value was zero.

The rotor resistance referred to the stator is,

$$R_2' = \frac{P}{3I_1^2} - R_1 \tag{5}$$

The stator leakage reactance and rotor leakage reactance referred to the stator have been considered equals, and they are half of the short circuit reactance,

$$X_{\sigma 1} = X_{\sigma 2}' = \frac{X_{sc}}{2} = \frac{1}{2}\frac{Q}{3I_1^2} \tag{6}$$

Short circuit power factor is determined with the same formula as in no-load regime. Obtained values are: $R_2' = 1.29\Omega$; $X_{\sigma 1} = X_{\sigma 2}' = 1.81\Omega$; $cos\varphi_{sc}$=0.595.

Now, having the stator leakage reactance, the magnetizing reactance can be obtained, and the value is $X_m$=54.1Ω.

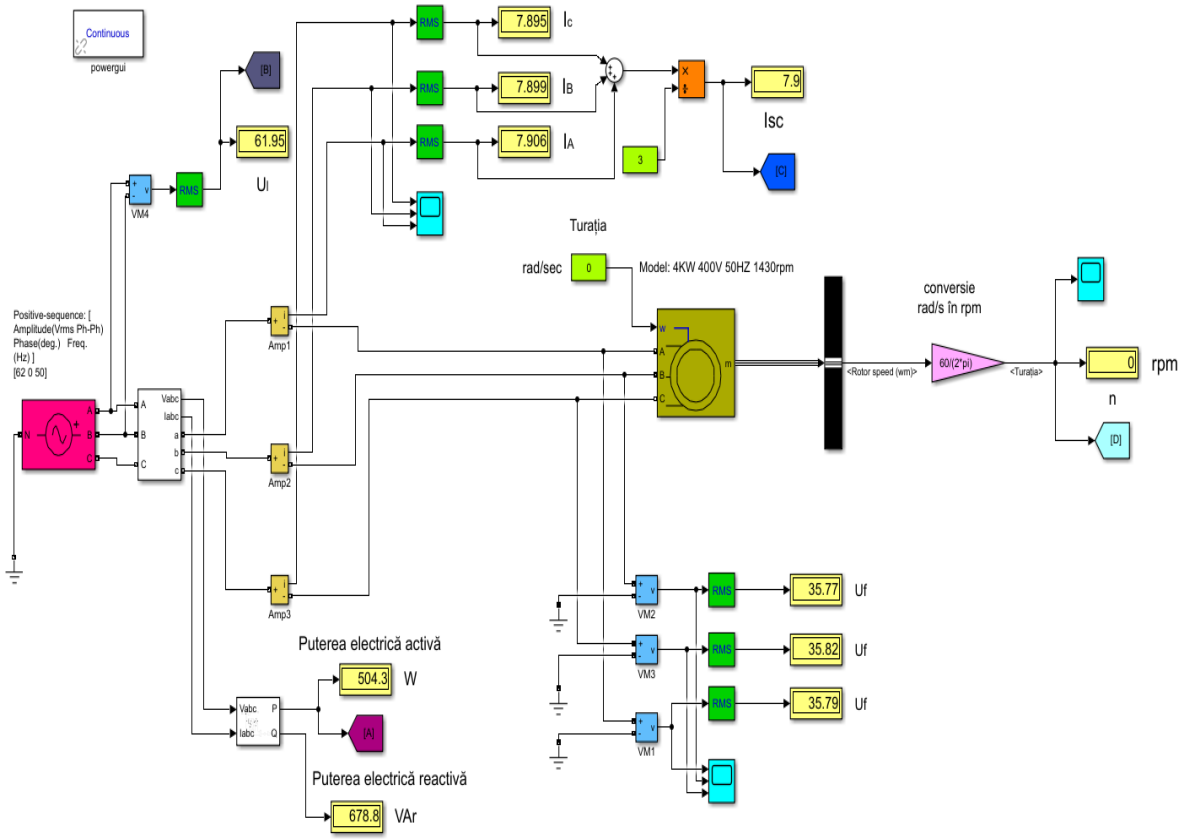


*Fig. 3. Model for the locked rotor test test*

### 2.3. Load operation

For testing the motor with load, the model from *fig*. 2 has been used, but the imposed torque values was set from very low to more than 150% load. All operation characteristics are obtained, as: $I$=f($s$), η=f($P_2/P_n$), *fig*. 4 and $\Omega$=f($M$), *fig. 5*.

Were noted: $s$ for slip, $P_2$ for motor mechanical power and $P_n$ for motor rated power, $I$ for stator current and $M$ for electromagnetic torque.

### 2.4. Mechanical charateristics

In order to obtain the entire natural characteristic $M$=f($s$) (or $\Omega$=f($M$)) , the model from *fig*. 3 has to be used, imposing rotor speed so that the slip is in 0…1 range.

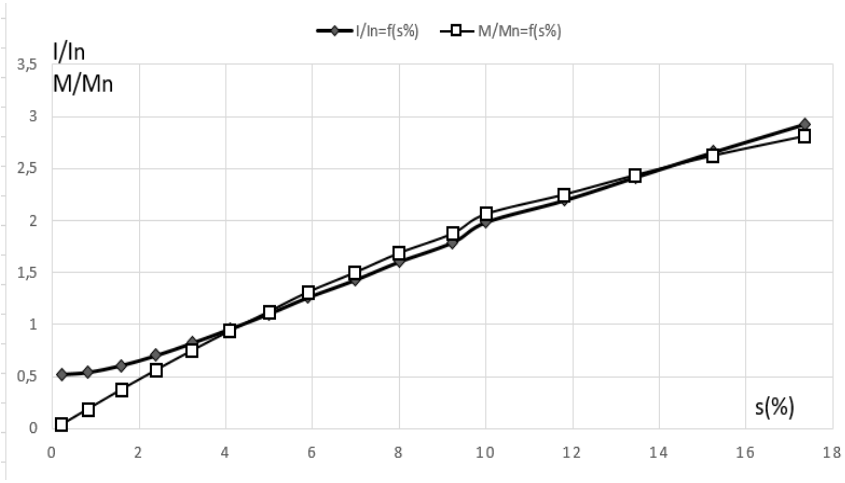


*a) $I/I_n$ and $M/M_n$*

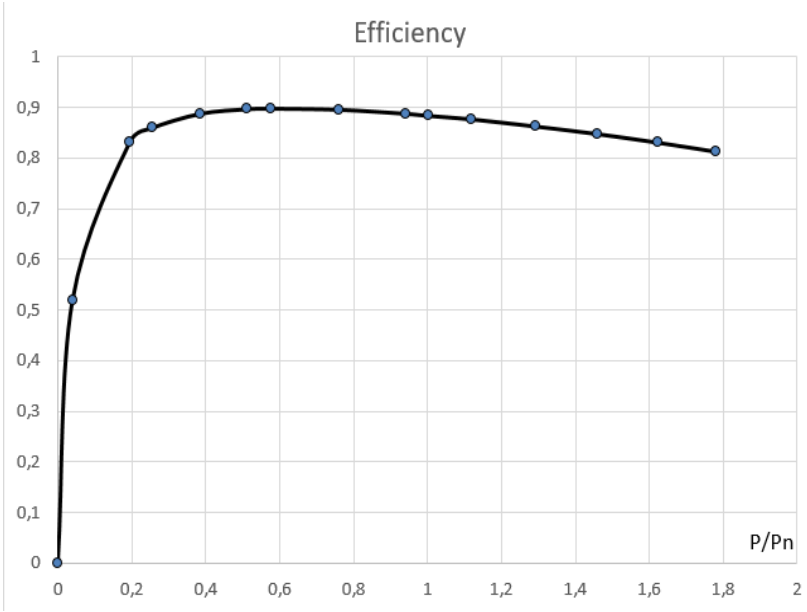


*b) Efficiency*

*Fig. 4. Load operation characteristics*

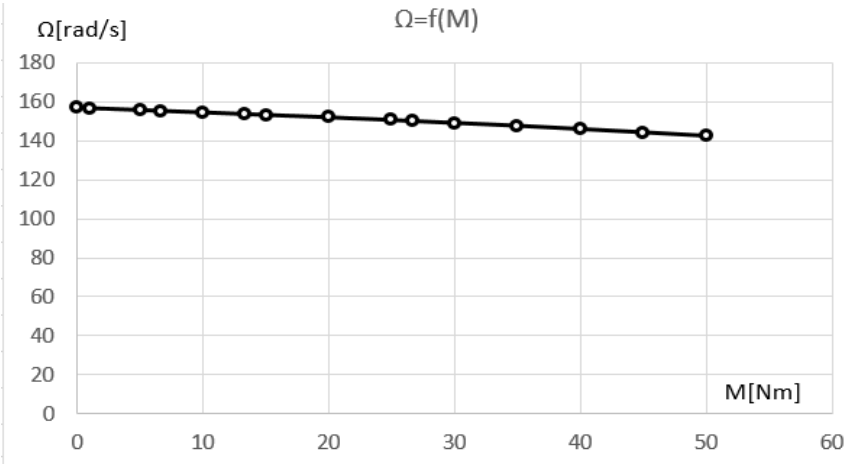


*Fig. 5. Natural characteristic Ω=f(M)*

The voltage and frequency characteristics are obtained also, varying the voltage amplitude (the frequency being constant) and the voltage frequency (the amplitude kept constant) respectively. *Fig*. 6 shows these characteristics.

## 2.5. Optimal operation

Looking to the *fig*. 5, b), it is observed that the rated motor efficiency is 88.4%, so it is in IE3 efficiency class (premium) according to the standard IEC 60034-30-1. But this efficiency is the rated one, so when the motor is underload (lower than 20%), the efficiency decrease rapidly. In order to improve the efficiency when the motor is low loaded, a simple possible solution have been studied, consisting in changing phases connection (from D to Y), resulting a lower phase voltage. This is easy to apply, changing connection in relation with the stator current. So, for D and Y connection, for reduced load torque, the efficiency has been compared, *fig*. 7.

For the studied motor, when the load torque is lower than 22.5% by rated torque, the efficiency is greater when Y connection is chosen. This is generally true for all induction motors, of course the torque percentage may be different.

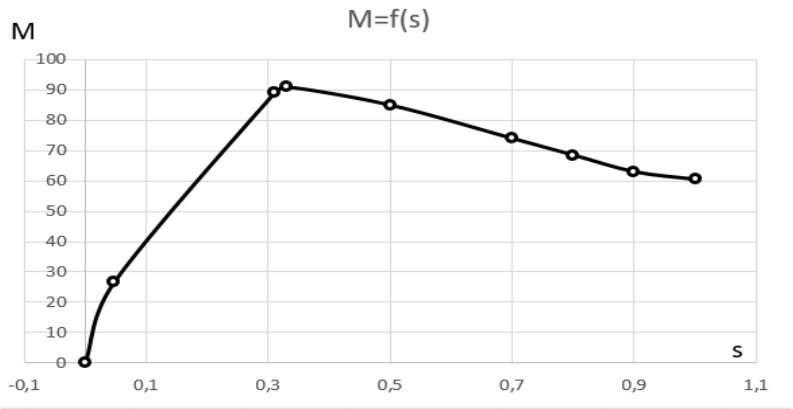


*a)Natural characteristic M=f(s)*

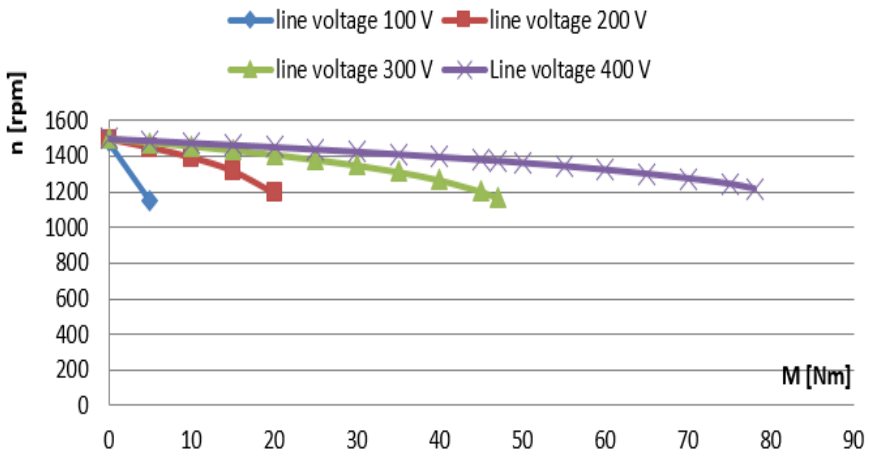


*b) Voltage characteristics*

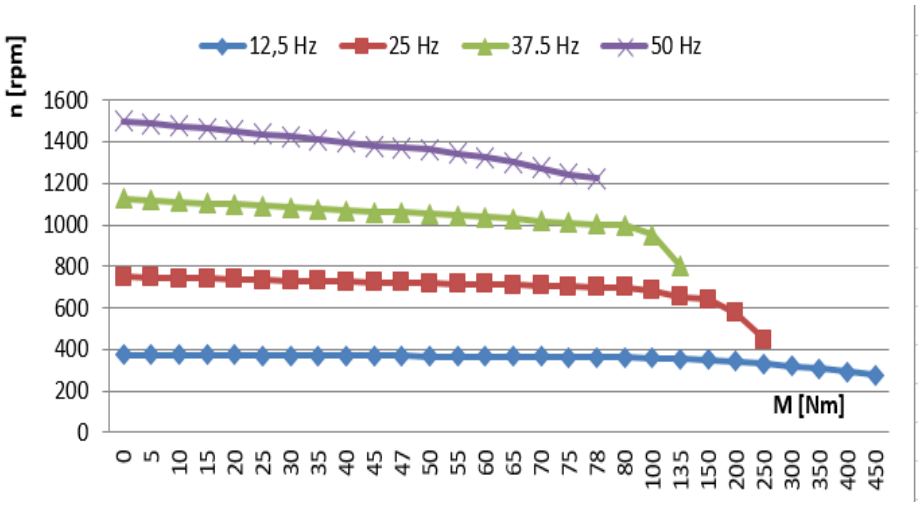


*c) Frequency characteristics*

*Fig. 6. Mechanical characteristics*

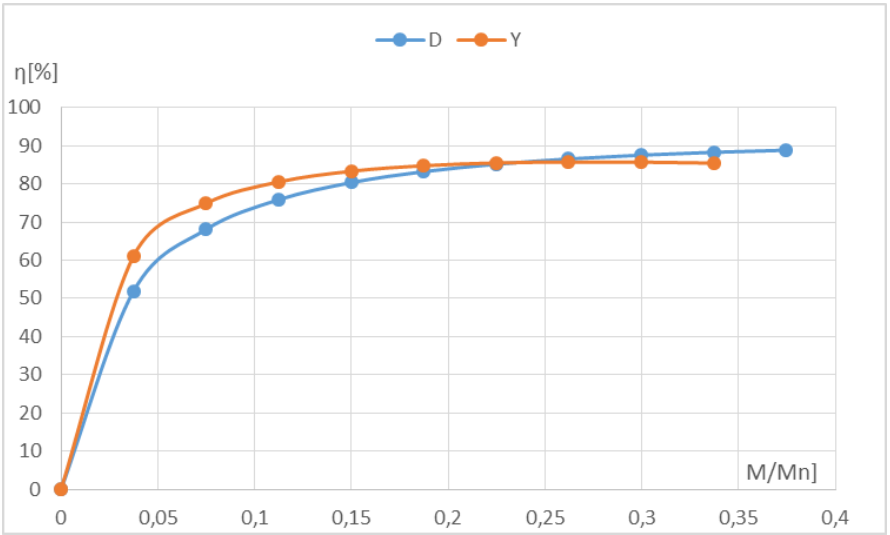


*Fig. 7. Efficiency as function of the load torque for D and Y connection*

But unlike laboratory tests, where special equipment is needed, in the case of simulations, it is very easy to record transient quantities. In fact, Simulink always works with instant quantities. For example, the variations of some quantities during the starting process of induction motor, are show in *fig*. 8.

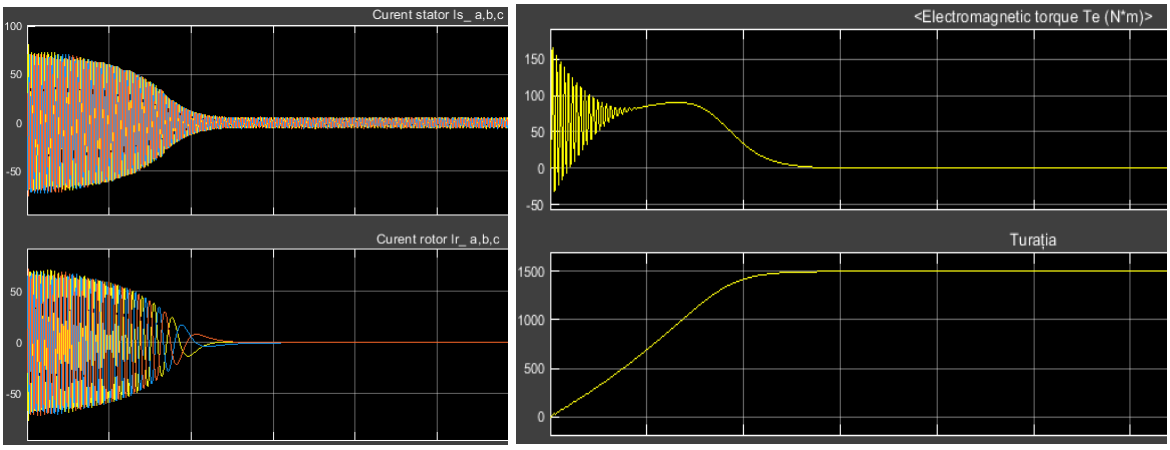


*a) Stator and rotor currents;* *b) Torque and rotor speed (rpm)*

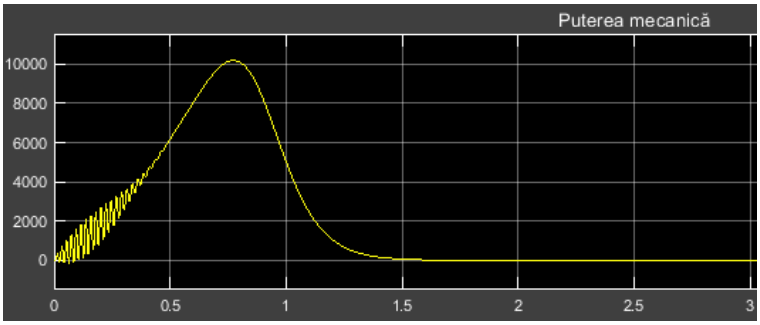


*c) Mechanical power*

*Fig. 8. The strating process*

## 3. CONCLUSION

Utilization of Matlab-Simulink for simulation of laboratory tests of induction motor has been presented in this paper. The corresponding models are shown including the measured quantities, and the used formulas are presented. Also, the measured quantities correspond to those from the laboratory tests.

Given that the possibilities of working in the laboratory with the students, considering the global pandemic situation, are very difficult to achieve, we believe that such an approach is very necessary. We are aware that practice cannot be replaced, but in its absence, theory, tests, working methods, and results can be more easily understood by modeling. And the Simulink environment offers unlimited possibilities for modeling and simulating electrical equipment and systems.

## *REFERENCES*


[1] A. V. Kupova, E. V. Lanovenko and E. B. Solovyeva, *Modeling of Three-Phase Circuits by Means of MatLab in Electrical Engineering Course*, 2019 International Conference "Quality Management, Transport and Information Security, Information Technologies" (IT&QM&IS), Sochi, Russia, pp. 526-530, 2019.

[2] N. F. Naim, N. Syahida Mat Nusi, S. S. Sarnin and N. Yaa'cob, *Development of Educational Software for Electrical Engineering Subjects using MATLAB*, 2019 International Conference on Information and Communications Technology (ICOIACT), Yogyakarta, Indonesia, pp. 884-888, 2019.

[3] W. Hao, H. Liu, Y. Wang and Y. Gou, *The design and simulation of a teachingvirtual platform by combining LabVIEW and Simulink for undergraduates of electrical engineering*, 2017 20th International Conference on Electrical Machines and Systems (ICEMS), Sydney, NSW, pp. 1-4, 2017.

[4] Z. Zhiling, Y. Shulian and F. Xiang, *Using Powergui Capabilities of Matlab in Teaching of Electric Power Engineering*, 2007 8th International Conference on Electronic Measurement and Instruments, Xi'an, pp. 3-683-3-686 2007.

[5] D. I. Ivanchenko and A. I. Smirnov, *Simulation of Interwire Short Circuits in Transformer Windings by Means of Simulink MATLAB*, 2019 IEEE Conference of Russian Young Researchers in Electrical and Electronic Engineering (EIConRus), Saint Petersburg and Moscow, Russia, pp. 977-980, 2019.

[6] K. Bhuyan and S. Chatterjee, Study of effects of standard and non-standard impulse waves on power transformer, 2010 Joint International Conference on Power Electronics, Drives and Energy Systems & 2010 Power India, New Delhi, pp. 1-4, 2010.

[7] R. Perez Pineda, R. Rodrigues and A. Aguila Tellez, *Analysis and Simulation of Ferroresonance in Power Transformers using Simulink*, in IEEE Latin America Transactions, vol. 16, no. 2, pp. 460-466, Feb. 2018.

[8] R. H. G. Tan and V. K. Ramachandaramurthy, *Simulation of power quality events using simulink model*, 2013 IEEE 7th International Power Engineering and Optimization Conference (PEOCO), Langkawi, pp. 277-281, 2013.

[9] A. H. M. Nordin, R. F. Mustapa, M. E. Mahadan, N. H. Ahmad and N. Y. Dahlan, *Transformer interactive learning tool based on MATLAB Simulink and GUI*, 2017 IEEE 9th International Conference on Engineering Education (ICEED), Kanazawa, pp. 42-47, 2017.

[10] G. Renukadevi and K. Rajambal, *Generalized model of multi-phase induction motor drive using matlab/simulink*, ISGT2011-India, Kollam, Kerala, pp. 114-119, 2011.

[11] A. W. Leedy, *Simulink/MATLAB dynamic induction motor model for use in undergraduate electric machines and power electronics courses*, 2013 Proceedings of IEEE Southeastcon, Jacksonville, FL, pp. 1-6, 2013.

# THE MANAGEMENT OF A HYBRID RENEWABLE ENERGY PRODUCTION SYSTEM

Radu **JOIAN**, Claudiu **LUNG,** Mircea **HORGOȘ**
*Electric, Electronic and Computer Engineering Department, Technical University of Cluj-Napoca, North University Center Baia Mare, Romania*
*yo5pcw@yahoo.com*

**Keywords: Energy management, Homer software, hybrid system**

**Abstract***: The paper focuses on the use of the Homer software on an autonomous hybrid system. The dedicated Homer software is intended for the energy management analysis of renewable electricity sources. The program simulates the operation of the systems, performing calculations on energy variations for each of the 8760 hours (specific to one year).*

## 1. INTRODUCTION

The best known software product specific to the design and evaluation of renewable hybrid systems is Homer software. The optimizations and the algorithms of sensitivity analysis make it easier the evaluation of many power supply system configurations.

The Homer software can also answer at the various questions about the configuration of low-capacity energy systems, questions that address various issues, including: the effectiveness of introducing an electric turbine in a system with diesel generator and batteries; the economic efficiency when using the wind turbines for the supply of electricity and heat for a system with possibility for connection at the network; how much the price of fuel must increase to make it economical the use of renewable sources etc.

For using the Homer software environment, the user must provide ton the program the input data describing the tasks, the technological options (in principle the components of the system to be simulated and analyzed), the component prices and the availability of renewable and diesel resources.

The program uses these inputs to simulate different system configurations or combinations components and it generates the results that can be viewed as a list of reliable systems, sorted by net present cost. Homer will also display the simulation results in a wide variety of tables and graphs which compare the configurations and evaluate them based on economic and technical merit.

The functions of the Homer system are:

- Simulation: for each hour specific to a year, the software compares the electricity and the heat demand for that hour with the energy that the system can deliver at that time and calculates the energy input to and from, each component of the system . The program also calculates the energy variations for each system configuration that can be considered. In this way it determines if a system is reliable, if it can cover the demand for electricity under the specified conditions and, at the same time, it estimates the cost of installing and operating a system over the entire life of the project, considering the following costs: the initial capital, the capital for replacements, the cost of operation and maintenance, the cost of fuel and the interest:
- Optimization: after simulating all possible configurations, the program displays a list of possible configurations, sorted by current net cost, which can be used to compare different constructive variants of systems. It can view all possible configurations or the Homer program, it can be left to choose only one option, the most economical, for each system.
- Sensitivity analysis: if we enter in the program, as primary data, the sensitivity variables such as the wind speed, the fuel price, etc., it will repeat the optimization process for each variable entered.

## 2. HYBRID ELECTRICITY PRODUCTION SYSTEM

The North University Center of Baia Mare has installed a hybrid system, photovoltaic and wind, for electricity production composed of the following equipment:

- Wind turbine AirXLand regulator included 24V - 400W;
- Current shunts;
- Battery PS PNGB 121400 - 140 Ah;
- Inverter Xantrex 3300 W with 220 V charge controller;
- 150 W photovoltaic panels;
- 30 A solar regulator;
- Digital control and acquisition devices;
- Electrical fuses;
- Cables and installation materials

The principle scheme of the system is shown in *figure 1*.

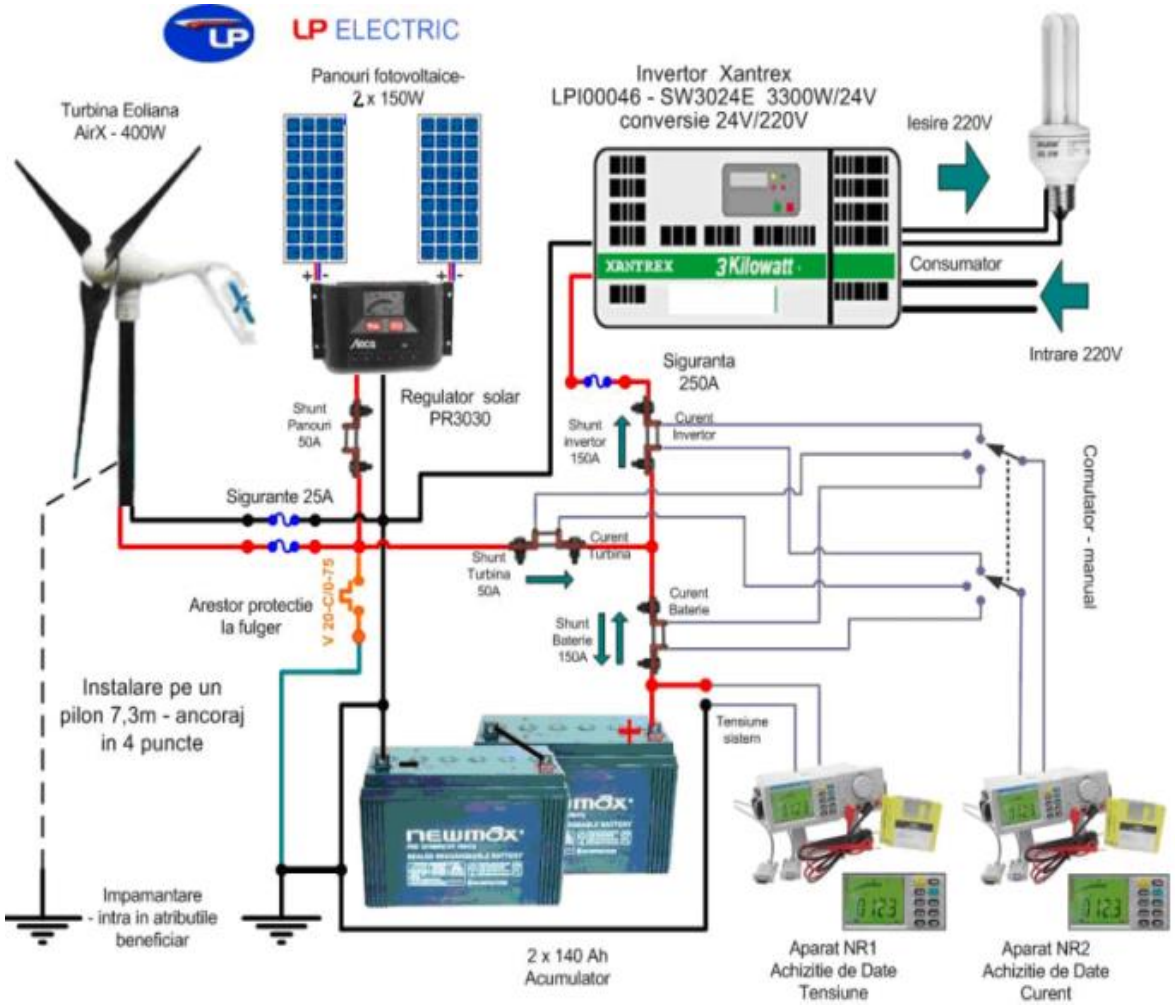


*Fig. 1. The hybrid, photovoltaic and wind system for electricity production at CUNBM*

The system is equipped with two meters, one for the energy produced from renewable sources and the other for the power supply option from the electricity supplier's network, in case that the discharge of the batteries cannot be compensated by the renewable sources.

The system is also connected to the Weather Station of the North University Center in Baia Mare (*fig. 2,3,4*) which was installed in 2008 and is of the Oregon Scientific Weather Station WMR 100 type. It has ten external sensors (without the internal of the console) which are grouped in the following functional units: anemometer, rain gauge and barometer. The console includes an atomic clock with autonomous and automatic adjustment.

The recorded meteorological quantities are: the indoor and outdoor temperature, the indoor and outdoor humidity, the wind speed and direction, the monthly precipitation amount, the daily and annual atmospheric pressure, the dew point temperature, the wind cooling, the temperature index etc.

The software used for data management is Weather Display.

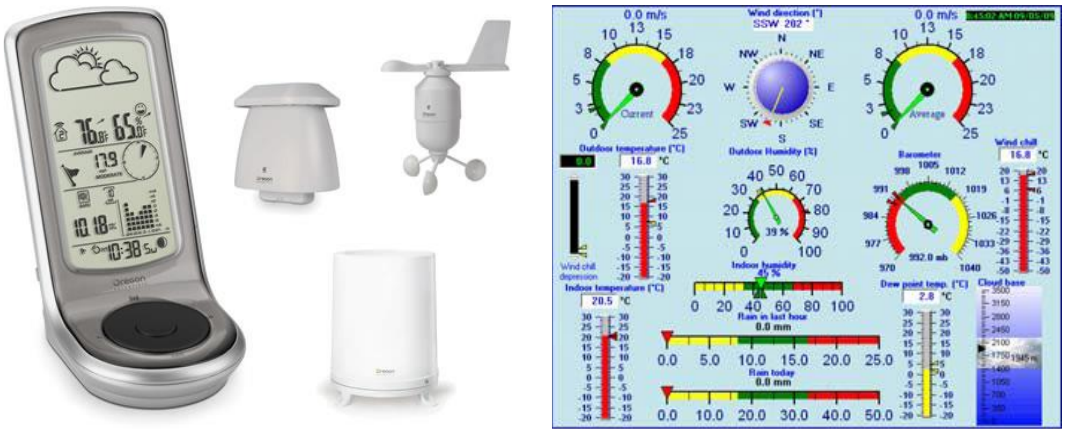

*Fig. 2. Oregon Scientific WMR weather station and weather display interface*

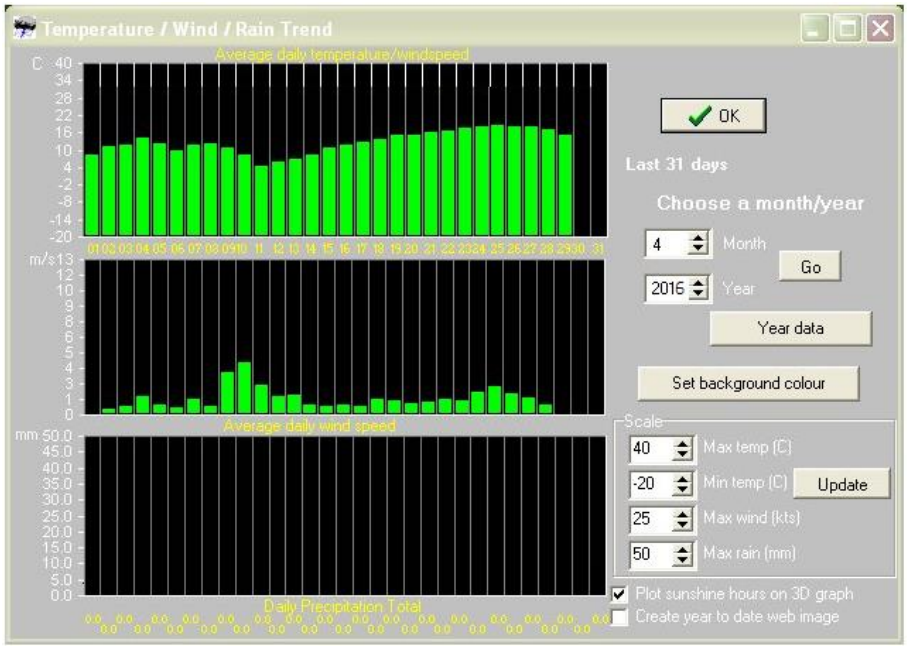


*Fig. 3. The variation temperature and the wind speed in April 2016*

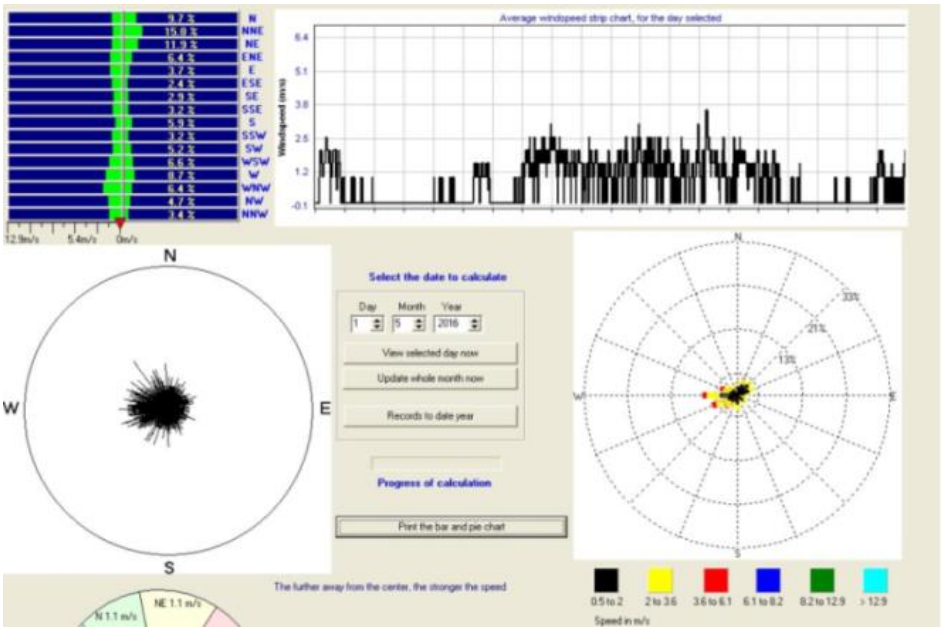


*Fig. 4. Graphic report in CUNBM weather station, May 2016*

## 3. EXPERIMENTAL DETERMINATIONS

The 400W wind turbine and the 300W solar module, component parts of the hybrid system within the CUNBM are installed on the roof of the Faculty of Engineering.

The equipments considered for optimization is shown in *figure 5*.

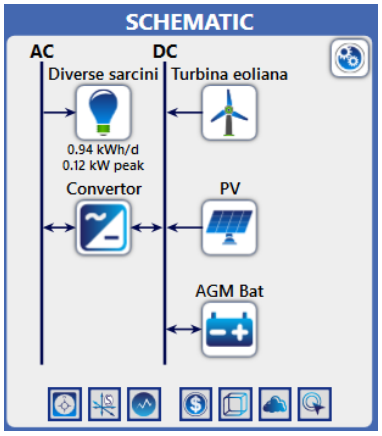


*Fig. 5. The equipment considered in optimization*

The profile of solar radiation is presented in *figure 6*. According to the Maramureș Energy Management Agency, the solar radiation corresponding in Baia Mare is 1450 kWh /m2/year. Thus, the coordinates corresponding to the location were entered, as well as the annual average of the local temperatures. *Figure 7* shows the profile of the solar panels.


*a) The solar radiation profile*


*a) The temperature variations*

*Fig. 6. The solar radiation profile and the temperature variation*

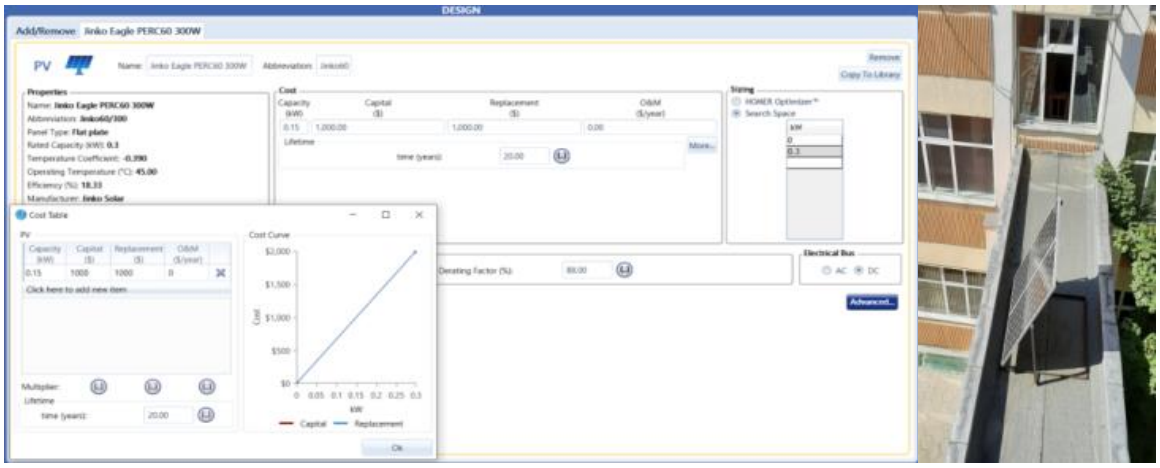


*Fig. 7. The photovoltaic panels properties and mounting location*

Based on the data obtained from the weather station, *figure 8* shows the profile of the wind speed during 2016. The average daily speed is 2.2 m/s, measured with the help of the weather station located at a height of 17.2 meters above the soil. In *figure 9* it can see the profile of the wind system for which we used the results obtained from the experimental measurements.


*Fig. 8. The wind speed profile*

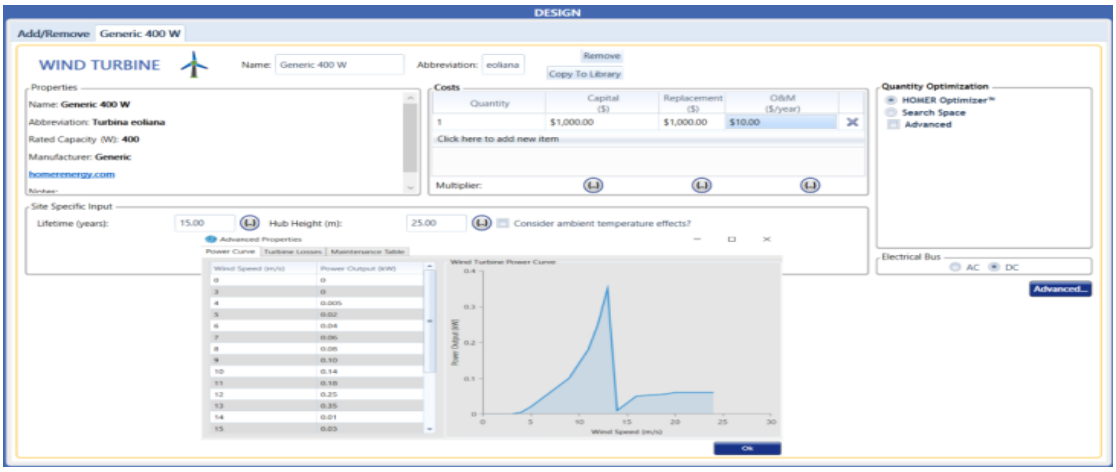


*Fig. 9. The profile of wind system*

The battery is a 6FM200D model. It has a rated voltage of 12 volts and a rated capacity of 200Ah (2.4 kWh). In the simulation, 2 batteries were considering, the profile of the batteries being the one in *figure 10*.

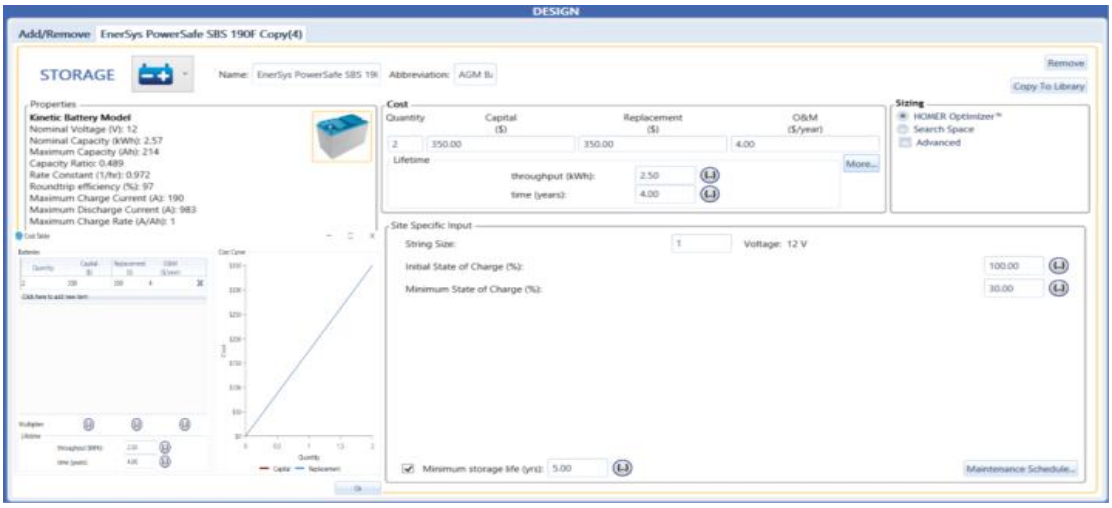


*Figure 10. The battery profile*

The conversion system is shown in *figure 11*.

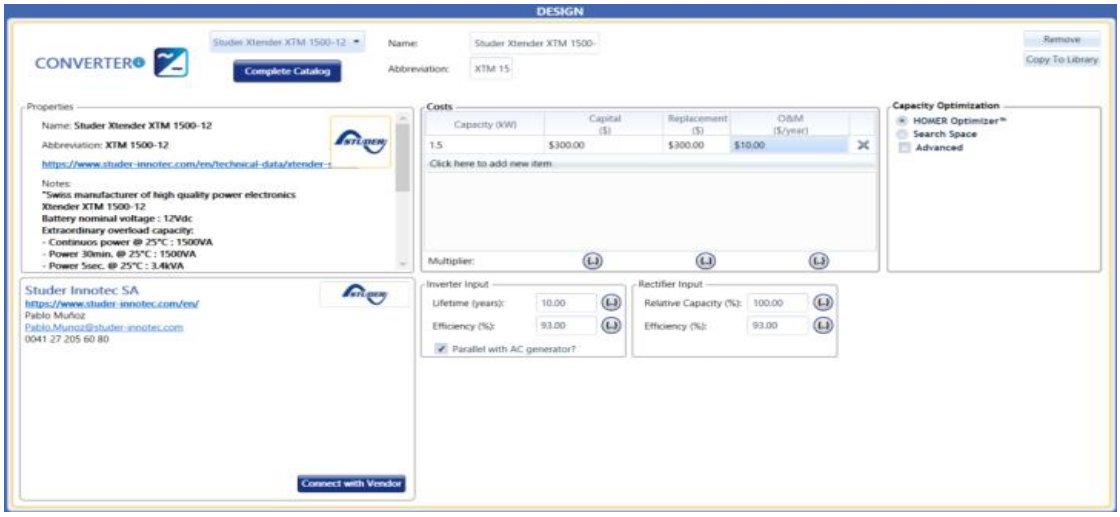


*Fig.11. The profile of converter and inverter*

We considered a task composed of several components such as: workbenches, projectors, PC stations etc. as in *figure 12.*


*Fig. 12. The task of the considered system*

The result obtained from the optimization (*figure 13*) gives the initial capital cost of $ 3,425 while the operating cost is $ 69 / year. The total net cost is $ 4259 and the energy cost (COE) is $ 1.74 / kWh.

The cost-benefit analysis of the hybrid system, compared to the tariff of energy supplied from the national grid, showed that the hybrid system is not economically cheap and must have a payback period of thirty-five years.

A hybrid energy system with solar cells, wind turbines would be cost effective if there were a reduction in component costs by installing more components, thus reducing the cost of investment per kW, the availability and the sustainability.


*Fig. 13. The System Optimization*

## 4. CONCLUSION

The use of this software is very useful, because you can analyze some constructive types of systems and their operation in conditions imposed by the user.

Simulating the variants of the energy system with such a program, can be useful in establishing the possibility of placing a hybrid system for converting the wind energy, in a place about which the data on average wind speed are known.

The program can also answer at the various questions related to the configuration of the low-capacity of energy systems, questions that address various issues, such as the economic efficiency of using the wind turbines for providing electricity for a system with the possibility of connection to the grid. After the simulation, the user can view detailed information about the chosen system and can analyze the system for several reasons: cost, electrical and components.

The program uses a relatively poor initial information on the wind potential of the area: monthly average wind speed values, possibly Weibull distribution parameters. Some problems that the Homer software has are related to the consideration of energy transfer through the battery, in the case of relatively short periods of the excess wind energy or considerating the situation when the charging controller works on *dump load* etc.

## *REFERENCES*

[1] A. I. Goveas, *Simulation of a Wind Powered Freshwater and Electricity Production System: Numerical Modeling and Optimization*, Delft University of Technology, 2020.

[2] C. Zhang, *Modelling and Simulation of Energy Storage System for Frequency Stability Studies*, Delft University of Technology, 2020.

[3] I. Ciocan, *Theoretical and experimental researches regarding the methods of energy production and storage in photovoltaic systems*, Doctoral thesis elaborated within the UT Doctoral School Cluj-Napoca, 2015.

[4] A. Leca, V. Mușatescu, ș.a., *Energy management. Principles, concepts, policies, tools*, Agir publishing house, Bucharest, 2008.

[5] E. Lazar, *Software development for the design and control of microgrids with renewable energies*, Doctoral thesis, Cluj – Napoca, 2018.

[6] A. B. T. Attya, *Wind energy penetration impact on grid frequency during normal operation on frequency deviations*, Doctoral thesis, Darmstadt, 2014.

[7] N. Bizon, *Optimized systems for clean energy conversion*, MatrixRom, Bucharest, 2008.

# A SURVEY ABOUT POWER CONSUMPTION FOR ARDUINO

Sabou **SEBASTIAN**
*Techical University of Cluj Napoca*
*sebastian.sabou@cunbm.utcluj.ro*

**Keywords: Survey, power, Arduino, low-power**

**Abstract***: The choice of a hardware platform for the implementation of a project is very important also from the perspective of the electricity consumption that it implies. For example, systems that will operate on the basis of energy stored in batteries, or those powered by renewable sources, whose availability is difficult to predict and also monitoring and control systems that are located in hard to reach areas or that are rarely physically checked require increased attention in the selection of the platform to be used. This study aims to provide a comparison, in terms of energy consumption, of the most used Arduino systems, as well as some possible solutions to further reduce their consumption.*

## 1. INTRODUCTION

Lately, there is a growing need to design and build systems that can be powered by batteries or that can use renewable electricity. This fact implies the use of systems that have a low electricity consumption but on the other hand to be available in large quantities and at the lowest possible price. Some of the most common microcontroller systems are those in the Arduino family.

The purpose of this study is to make a comparative analysis of electricity consumption among the most common models of Arduino development systems: Uno, Nano, Pro Mini and Mega. Most of them use the same microcontroller but are in different formats and some different components. Also, there are presented some hardware and software solutions to reduce the power consumed by these systems.

Being a study, measurements and results obtained by the author are presented, as well as data taken from bibliographic materials.

### 1.1. Arduino

The Arduino family of development systems contains a wide variety of platforms, using many types of microcontrollers or microprocessors. In this case we will focus on systems that use 8-bit microcontrollers, being among the most used, from CNC or 3D printers to automation systems, to develop intelligent sensors, systems for measuring and monitoring various parameters, having available for use a very large number of sensors, there are an impressive number of implemented projects whose documentation is available free of charge on the Internet.

Table 1. Characteristic of the studied Arduino systems [1-5]

| **Board** | **Arduino Mega** | **Arduino Uno** | **Arduino Nano** | **Arduino Pro Mini 5V** | **Arduino Pro Mini 3.3V** |
|---|---|---|---|---|---|
| Processor | ATmega2560 | ATmega328P | ATmega328 | ATmega328P | Atmega328P |
| Clock speed | 16MHz | 16MHz | 16Mhz | 16MHz | 8MHz |
| SRAM | 8kB | 2kB | 2kB | 2kB | 2kB |
| Flash Memory | 256kB | 32kB | 32kB | 32kB | 32kB |
| EEPROM | 4kB | 1kB | 1kB | 1kB | 1kB |
| Digital I/O pins | 54 | 14 | 22 | 14 | 14 |
| Analog I/O pins | 16 | 6 | 8 | 6 | 6 |
| Operating voltage | 5V | 5V | 5V | 5V | 3.3V |
| Input voltage | 7-12V | 7-12V | 7-12V | 5-12V | 3.35-12V |

## 2. RESEARCH AND MEASUREMENTS

Table 2 shows the measurements performed on several Arduino systems, compared to those taken from [6]. No measurements were performed with USB powered systems because in this case it depends a lot on the USB interface circuit and on the other hand the stand-alone systems are not permanently powered via USB.

Table 2. Power consumption ([6] and personal measure)

| **Board/VCC** | **Arduino Mega** | **Arduino Uno** | **Arduino Nano** | **Arduino Pro Mini 5V** | **Arduino Pro Mini 3.3V** |
|---|---|---|---|---|---|
| **Reference** | | | | | |
| 9V | 73.2mA [6]<br>71.2mA | 98.4mA[6]<br>94.2mA | 22.1mA[6]<br>22.0mA | 14.6mA[6]<br>14.3mA | 5.1mA[6]<br>5.2mA |
| **Reduce clock** | | | | | |
| 9V | 61.8mA[6]<br>62.0mA | 42.8mA[6]<br>42.3mA | 18.5mA[6]<br>18.6mA | 10.0mA[6]<br>10.1mA | 3.8mA[6]<br>3.9mA |
| **Enable Low Power** | | | | | |
| 9V | 26.9mA[6]<br>27.1mA | 27.9mA[6]<br>28.1mA | 4.8mA[6]<br>4.9mA | 3.2mA[6]<br>3.2mA | 3.2mA[6]<br>3.2mA |

The measurements were performed after programming an empty program, so that the systems do not use any peripheral device.

The differences between the measurements can also be explained by the fact that there may have been different versions of Arduino systems or even by different manufacturers. Also, the stabilizer circuit and the USB interface circuit may be different.

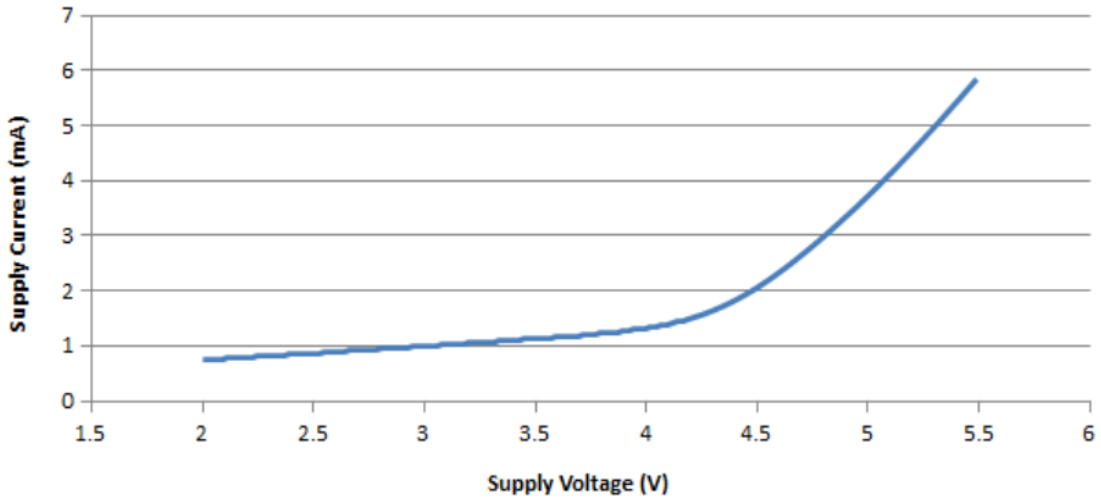


*Fig 1. Atmega328P Vcc vs Supply Current (at 1MHz clock)[datasheet]*

A series of useful information can also be obtained from the datasheets, thus, in *figure 1* you can see the change in consumption compared to the supply voltage, at a certain clock frequency, and in *figure 2* the variation of the electric current depending on the clock frequency at a constant supply voltage of 5V

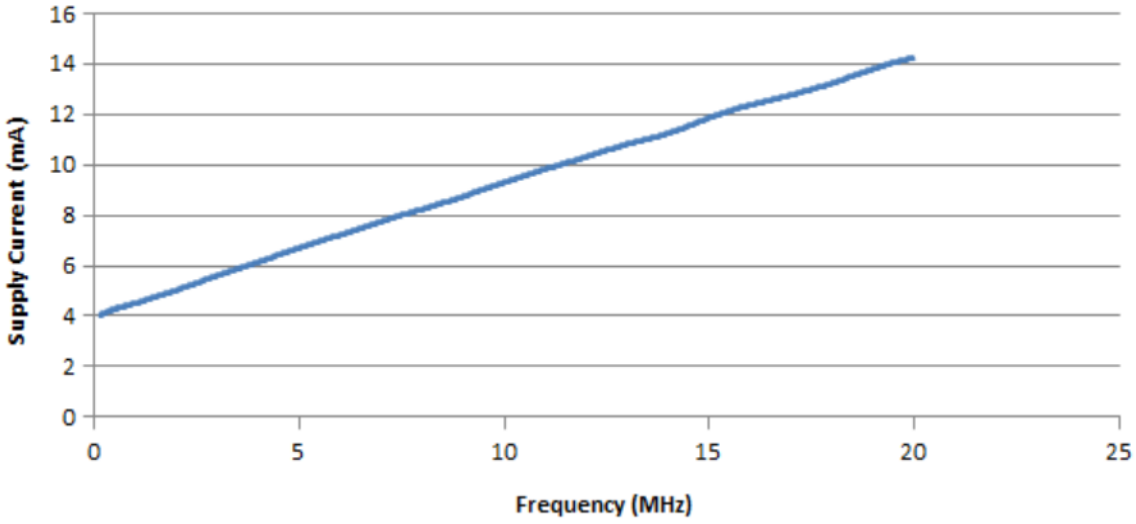


*Fig. 2 Atmega328P Frequency vs Supply Current (5V) [datasheet]*

Reducing the frequency of the clock signal is another method of reducing power consumption, software can be implemented, reducing the frequency from 16MHz to 8MHz can reduce the current from 12mA to 8.5mA, over an extended period of time can mean greater autonomy. Reducing the clock frequency means even fewer calculations performed over a period of time, often not the best method, being preferred methods to put the system into deep sleep, for example, being more efficient that way.

On the other hand changing clock speed can cause boot loader issues and your Arduino may get damaged.

In certain situations, hardware changes can be made that allow a significant reduction in consumption, as in [7] where some changes that require certain knowledge of electronics, such as modifying the circuit to power the USB interface circuit from this USB interface. , resulting in a reduction of 44.7%, the reduction by 7mA of the current by disconnecting the power led and a major change is the use of a switching voltage stabilizer instead of the linear voltage stabilizer. All these involve quite important changes on the system, changes that are not the subject of this study but are mentioned as a possible way to reduce consumption.

There is also another way to reduce electricity consumption, namely by using the library of low power functions [8]. The advantage of this method is that it does not require hardware changes, it requires only a more detailed knowledge of the programming process and microcontroller architecture, the reduction of consumption can be significant (according to Table 2) depending very much on the requirements to implement software.

## 3. CONCLUSIONS

There are several solutions to use an Arduino system that is best suited to the requirements of low power consumption. The first and easiest solution is to choose a system that is as close to the design requirements as possible, so if you need a circuit that requires only a few digital inputs or outputs and a few analog inputs, you can opt for an Arduino Nano (22mA) or Arduino Pro Mini (15mA) compared to an Arduino Uno (98mA). A second solution, which requires only the use in the programming of function libraries that allow the use of low power facilities, involves the development of programs that are designed to make the most of these functions. A third option, with more effort, is one that involves hardware changes, eliminating any consumers that are not needed but are present on these systems.

## *REFERENCES*

[1] https://store.arduino.cc/arduino-mega-2560-rev3.

[2] https://store.arduino.cc/arduino-uno-rev3.

[3] https://store.arduino.cc/arduino-nano.
[4] https://store.arduino.cc/arduino-pro-mini.
[5] https://learn.sparkfun.com/tutorials/reducing-arduino-power-consumption/all.
[6] https://diyi0t.com/arduino-reduce-power-consumption/.
[7] https://www.defproc.co.uk/tutorial/how-to-reduce-arduino-uno-power-usage-by-95/.
[8] https://www.arduino.cc/en/Reference/ArduinoLowPower.
[9] E. White, *Making Embedded Systems*, O'Reilly Media; Inc. USA, 2011.
[10] J. Henkel, S. Parameswaran, *Designing Embedded Processors. A Low Power Perspective*, Springer Netherlands, 2007.

# INSTRUCTIONS FOR AUTHORS

Name **SURNAME**[1], Name **SURNAME**[2], **...**

[1] *Affiliation of 1st author,* [2] *Affiliation of 2nd author, ...*

*Email of 1st author, Email of 2nd author, ...(it is compulsory only for the first author)*

**Keywords: List 3-4 keywords** *(aligned to the left, 10 pt. bold, separated by commas; please choose keywords from IEEE Approved Indexing Keyword List)*

**Abstract:** *Abstract of max. 200 words, justify, 10 pt. italic.*

## 1. INTRODUCTION

The paper must be written in English. It shall contain at least the following chapters: introduction, research course (mathematical algorithm); method used; results and conclusions, references.

### 1.1. Fonts

Use DIN A4 Format (297 x 210 mm) MSWord format. Margins: top, bottom, left and right 2.5 mm each. The text should be written on one side of the page only. Use Times New Roman fonts, line spacing 1.3. The font formats are: paper title: 14 pt, bold, italic, capital letters, author's name(s): 12 pt, regular for name and 12 pt., bold, for surname; Affiliation: 11 pt., italic; key words: 10 pt., bold; Abstract: 10 pt., italic, word Abstract in 10 pt., bold; chapter titles (do not use automatic numbering): 12 pt., bold, capital letters; subtitles: 12 pt., bold, lower case letters; subsubtitles: 12 pt., italic, lower case letters; body text: 12 pt., regular; tables and figures caption: 11 pt.; italic; references: author 11 pt.; regular, title 11 pt. italic, year, pages, ... in regular.

#### *1.1.1. Number of pages*

The number of pages is not restricted.

## 2. FIGURES AND TABLES

Figures have to be made in high quality, which is suitable for reproduction and printing. Don't include photos or color prints if there are not clearly intelligible in gray scale option. Place figures and tables at the top or bottom of a page wherever possible, as close as possible to the first reference to them in the paper. Use either *fig. 1* or *figure 1* when necessarily.

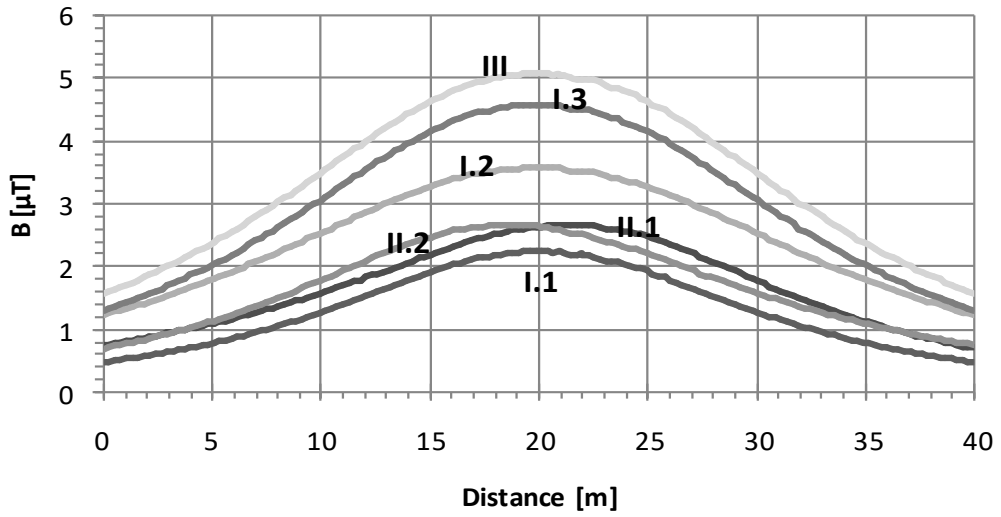


*Fig. 1. Magnetic flux density at 1 m above the ground*

Table 1. Transposing principle

| | *Circuit* | | | | | | | | | | | |
|---|---|---|---|---|---|---|---|---|---|---|---|---|
| | *1* | *2* | *1* | *2* | *1* | *2* | *1* | *2* | *1* | *2* | ***1*** | ***2*** |
| *1/3* | *R* | *T* | ***R*** | ***R*** | *R* | *S* | *R* | *T* | *R* | *S* | ***R*** | ***R*** |
| *line* | ***S*** | ***S*** | *S* | *T* | *S* | *R* | *S* | *R* | *S* | *T* | ***S*** | ***S*** |
| *length* | *T* | *R* | *T* | *S* | ***T*** | ***T*** | *T* | *S* | *T* | *R* | ***T*** | ***T*** |
| *1/3* | *T* | *S* | ***T*** | ***T*** | *T* | *R* | *T* | *S* | *T* | *R* | ***T*** | ***T*** |
| *line* | ***R*** | ***R*** | *R* | *S* | *R* | *T* | *R* | *T* | *R* | *S* | ***R*** | ***R*** |
| *length* | *S* | *T* | *S* | *R* | ***S*** | ***S*** | *S* | *R* | *S* | *T* | ***S*** | ***S*** |
| *1/3* | *S* | *R* | ***S*** | ***S*** | *S* | *T* | *S* | *R* | *S* | *T* | ***S*** | ***S*** |
| *line* | ***T*** | ***T*** | *T* | *S* | *T* | *S* | *T* | *S* | *T* | *R* | ***T*** | ***T*** |
| *length* | *R* | *S* | *R* | *T* | ***R*** | ***R*** | *R* | *T* | *R* | *S* | ***R*** | ***R*** |
| *Name* | ***I.1*** | | ***I.2*** | | ***I.3*** | | ***II.1*** | | ***II.2*** | | ***III*** | |

## 3. EQUATIONS

Equations are centred on page and are numbered in round parentheses, flush to right margin.

$$a = b + c \tag{1}$$

Between equations, not interfered by text, there is only one empty line:

$$a = b + c \tag{2}$$

$$a = b + c \tag{3}$$

In text respect the following rules: all variables are italic, constants are regular; the references are cited in the text between right parentheses [1], the list of references has to be arranged in order of citation.

*REFERENCES*

[1] International Commission on Non-ionizing Radiation Protection, *Guidelines for limiting exposure to time-varying electric, magnetic and electromagnetic fields (Up to 300 GHz)*, Health Physics, vol. 74, no. 1, pp. 494-522, 1998.

[2] A. Marincu, M. Greconici, *The electromagnetic field around a high voltage 110 KV electrical overhead lines and the influence on the biological systems*, Proceedings of the 5th International Power Systems Conference, pp. 357-362, Timisoara, 2003.

[3] Gh. Hortopan, *Compatibilitate electromagnetică*, Ed. Tehnică, 2005.